Aus der Medizinischen Klinik und Poliklinik IV

der Ludwig-Maximilians-Universität München

Direktor: Prof. Dr. med. Martin Reincke

Role of SDF-1/CXCL12 in Glomerular Disease and Regeneration

Dissertation

zum Erwerb des Doktorgrades der Humanbiologie

an der Medizinischen Fakultät der

Ludwig-Maximilians-Universität München

vorgelegt von

Hr. Simone Romoli

aus Florenz, Italien

2016

Mit Genehmigung der Medizinischen Fakultät

der Ludwig-Maximilians-Universität München

Berichterstatter	: Prof. Dr. med. Hans-Joachim Anders
Mitberichterstatter:	: Prof. Dr. Jürgen E. Scherbevich
Mitberichterstatter:	: Prof. Dr. Christian Weber
Mitberichterstatter:	: Priv. Doz. Dr. Bärbel Lange-Sperandio
Mitberichterstatter:	

Dekan	: Prof. Dr.med.dent Reinhard Hickel

Tag der mündlichen Prüfung	: 14.9.16

This work is dedicated to my beloved Family

Table of contents

Declaration

I hereby declare that all of the present work embodied in this thesis was carried out by me from 01/2012 until 01/2015 under the supervision of Prof. Dr. Hans Joachim Anders, Nephrologisches Zentrum, Medizinische Klinik und Poliklinik IV, Innenstadt Klinikum der Universität München. This work has not been submitted in part or full to any other university or institute for any degree or diploma.

Part of the work was supported by others, as mentioned below:

Parts of the work were performed by me at the University of Florence, in the laboratory of Prof. Paola Romagnani, as mentioned below (In-vitro experiment using human renal progenitors, in-vivo studies using Pax2 mT/mG.

Parts of the work are in submission.

Date: 15.09.16 Signature: ***Simone Romoli***

Place: Munich, Germany (Simone Romoli)

Zusammenfassung

Stromal-derived factor (SDF)-1/CXCL12 ist ein homöostatisches Chemokin, welches das Homing und die Aktivierung von Stammzellen fördert. Bisher ist unklar, warum Podozyten CXCL12 konstitutiv freisetzen und warum die Inhibierung von CXCL12 zur Verminderung progressiver Glomerulosklerose beiträgt. Es ist anzunehmen, dass CXCL12 im Wesentlichen das Überleben und die Regenerierung von Podozyten reguliert. *In-vitro* konnte gezeigt werden, dass CXCL12 humane Podozyten vom toxischen Schaden schützt und eine *in-vivo* Blockade von CXCL12 zu einer verstärkten Proteinurie und einem Podozytenverlust in zwei unterschiedlichen Mausmodellen des toxischen Podozytenschadens führte. Stattdessen verhinderte die fortgesetzte Blockade von CXCL12 signifikant den Verlust von Podozyten, die Proteinurie und Glomerulosklerose als Folge einer Adiamycin (ADR)-Nephropathie nach 14 Tagen- In der frühen Schadensphase führte CXCL12 Blockade zu einem signifikanten Anstieg der Podozytenanzahl im Vergleich zur Vehiculum-behandelten Gruppe auslöste, dies bedeutet, dass CXCL12 die Regeneration von Podozyten beeinträchtigt. Humane Nierenprogenitorzellen haben die Fähigkeit in reife Podozyten zu differenzieren. In Gegenwart von CXCL12 wurde das Wachstum der humanen Nierenprogenitorzellen und ihre Differenzierung in Podozyten unterdrückt, was durch CXCL12 Inhibierung aufgehoben und somit das Outcome in Mäusen verbessert werden konnte. Dieser Effekt war abhängig von der Unterdrückung des Notch-Signalwegs in Podozytenprogenitorzellen, ausgelöst durch freigesetztes CXCL12 von nekrotischen Podozyten. Um dieses Phänomen genauer zu untersuchen, wurde eine ADR-Nephropathie in Mäusen induziert, welche eine *in-vivo* Verfolgung der Abstammung von Pax2+ Podozytenprogenitorzellen in der Bowman's Kapsel ermöglichen. Die pharmakologische Inhibierung von CXCL12 erhöhte die Anzahl von Pax2+ Podozyten, was zur verminderten Proteinurie und Glomerulosklerose in beiden Tiermodellen der ADR-Nephropathie führte. Schlussfolgernd kann man sagen, dass von Podozyten freigesetztes CXCL12 unterschiedliche biologische Funktionen bei einem Podozytenschaden hat. Zum Einen, dient CXCL12 als Überlebensfaktor für Podozyten, um Notch-vermittelte mitotische Katastrophe von Podozyten zu verhindern. Zum Anderen, kann CXCL12 den Arrest von Podozytenprogenitorzellen fördern, und dessen Blockade die Pax2+ Podozytenprogenitor-vermittelte Podozytenregeneration beschleunigen.

Summary

Stromal-derived factor (SDF)-1/CXCL12 is a homeostatic chemokine facilitating the homing and activation of stem cells. It is unclear, why podocytes constitutively secrete CXCL12 and why CXCL12 blockade can attenuate progressive glomerulosclerosis. It can be assumed that CXCL12 plays a regulatory role on podocyte survival and podocyte regeneration. *In-vitro* CXCL12 protected human podocytes from toxic injury and *in-vivo* blocking intrinsic CXCL12 aggravated proteinuria and podocyte loss in two different mouse models of toxic podocyte injury. However, continued the blockade of intrinsic CXCL12 during the course of Adriamycin (ADR) nephropathy significantly attenuated podocyte loss, proteinuria, and glomerulosclerosis. Indeed, CXCL12 blockade significantly increased podocyte numbers not only as compared to vehicle-treated controls but also versus the earlier time point of injury, implying that intrinsic CXCL12 suppresses podocyte regeneration. To study this aspect, RPCs were used that have the capacity to differentiate into mature podocytes. CXCL12 suppressed progenitor growth and their induced differentiation into podocytes, which could be reversed by the same CXCL12 inhibitor that improved outcomes in mice. This effect depended on the suppression of Notch signaling in podocyte progenitors as being triggered by necrotic podocytes releases. To study this phenomenon *in-vivo* ADR nephropathy was induced in mice that allow lineage tracing of Pax2+ podocyte progenitor cells of the Bowman`s capsule. A delayed onset of pharmacological CXCL12 inhibition increased the number of Pax2 positive podocytes, an effect associated with less proteinuria and glomerulosclerosis in two different versions of the ADR nephropathy model. In conclusion, podocyte-derived CXCL12 has different biological functions during podocyte injury. First, CXCL12 serves as a podocyte survival factor, by preventing Notch-mediated mitotic catastrophe of podocytes. Second, CXCL12 promotes podocyte progenitor quiescence, vice-versa, CXCL12 inhibition can accelerate Pax2+ podocyte progenitor-mediated podocyte regeneration.

1. Introduction

1.1. Chronic Kidney Disease

Chronic kidney disease (CKD) is defined as an irreversible and progressive decline of kidney function leading to kidney failure, known as end-stage renal disease (ESRD). It has been estimated that 14-15% of the adult population in the United States is affected by CKD and its prevalence has been estimated to increase by 50% over the next two decades (1, 2). CKD is defined by structural and functional abnormality of the kidney: albuminuria more then 3mg/mmol and glomerular filtration rate less than 60ml/min/1.73m^2 present for 3 months, with implications for health. CKD is mostly a consequence of podocyte loss-related glomerulosclerosis, e.g. in aging, diabetes, hypertension, and glomerulonephritis (3, 4).

1.2. Podocytes and the glomerular filtration barrier

The glomerular filtration barrier is a highly specialized blood filtration interface that displays permeability to small- and midsized solutes in the plasma but restricts the flow of larger plasma proteins into the urinary space (Figure 1). The glomerular filtration barrier is a three-layered structure consisting of endothelial cells, glomerular basal membrane (GBM), and podocytes (5, 6). Podocytes, located outside the glomerular capillary loop, play a crucial role in the formation and maintenance of the glomerular filtration barrier. They have a complex cellular organization consisting of a large cell body leaning out of the urinary space and long cellular extensions (foot processes) that interdigitate with those of neighboring podocytes to cover the outer part of the GBM (5). Podocyte foot processes are anchored to the GBM through α3-β-integrins and β-dystroglycans (7). These characteristics, interdigitating patterns between foot processes of neighboring podocytes, are bridged by a 40nm wide zipper-like slit diaphragm (8). Podocyte foot processes and the interposed slit diaphragm cover the outer part of the GBM and play a major role in establishing the selective permeability of the glomerular filtration barrier (9). The glomerular filtration barrier is highly permeable to water and small solutes, but the small pore size (5-15nm) of the slit diaphragm limits the passage of larger proteins, for example, albumin (10).

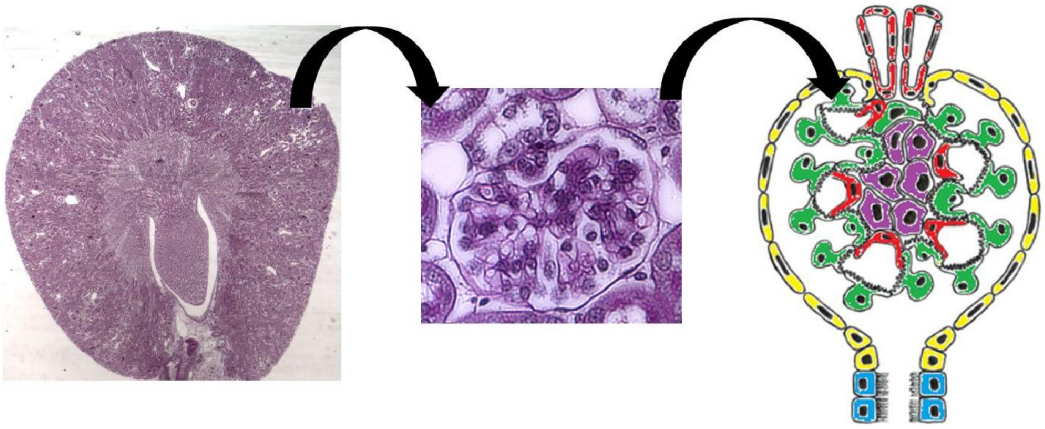

Figure 1. The structure of the glomerulus and the cellular components. The GBM comprised of fenestrated glomerular endothelial cells (red cells), glomerular basement membrane and podocytes (dark green cells). The parietal epithelial cells (PECs) along the Bowman 's capsule (yellow cells). Tubular cells in the urinary pole of the glomerulus (blue cells), PAS panoramic 1x, glomerulus magnification 40x) The image was adapted and used with the agreement of the copyright owner Duccio Lombardi and Laura Lasagni (see last page agreement), from *Lombardi and Lasagni et al(11)*,

1.3. Focal Segmental Glomerulosclerosis

Focal segmental glomerulosclerosis (FSGS) is not a single disease but rather a group of clinical-pathologic syndromes sharing a common glomerular lesion and mediated by different types of insults within podocytes (12). FSGS is characterized by the presence of focal (in some isolated glomeruli) and segmental (in some part of a single glomerulus) lesions with obliteration of glomerular capillaries, adhesion with the glomerular tuft and BC and podocyte hypertrophy (13). More than 80% of FSGS cases are classified as idiopathic if the cause is unknown. A genetic mutation affecting podocytes proteins have been identified as the primary cause of sporadic types of FSGS, often these mutations correlate with the nephrotic syndrome and they have a familiar genetic outcome (14). in particularly the mutations have been found in the podocyte protein of the slit diaphragm as Nephrin, Podocin and CD2-associated protein (CD2AP) (15-17) or inside the podocyte nucleus as Wilms-tumor protein 1 (WT-1) (18, 19). Sclerosis of the glomerulus occurs as a response to injury. The functional kidney is then replaced by scarring tissue, leading to progressive and irreversible loss of function. The glomerular structure consists of an endo-capillary compartment containing mesangial cells and capillaries, and an extra-capillary compartment containing podocytes and the parietal epithelial cells (PECs) lying on the Bowman´s capsule (20). The "spine cord" of this structure is maintained by podocytes, are terminally differentiated epithelial cells that are specialized to their architecture, and are responsible for the maintenance of the GBM and the GFB

as shown in Figure 1. A recent study was able to show that all forms of glomerulosclerosis start with either a lesion or a dysfunction of podocytes (21). This is true for many kidney diseases, with particularly important in that disease that give a late onset like diabetic nephropathy or FSGS feature of many kidney diseases with late onset like diabetic disease (22), FSGS (23, 24). High cytoskeleton complexity and physiological-complex structure of podocyte is the reason for the limited capacity for cell cycle re-entry and proliferation for replacing podocyte loss (25). When podocytes are lost during glomerular injury how can the glomerulus maintain the structure and part of its functionality? Till today, this question is not completely undertaken and many hypotheses have been formulated: podocyte hypertrophy that rescued and increased glomerular workload (26) and podocyte replacement by activated renal stem cell progenitors (RPCs) recruitment (27, 28). However, podocyte hypertrophy or RPCs replacement occurs slowly and can lead to d loss of GBM integrity (29). Loss of podocytes will end in a formation of "uncover" GBM and the loss of distance between the capillary tuft and the BC allow PECs of the Bowman´s capsule to start to form the multi-layer formation, that cover the tuft and create a fibrotic scar as known as crescent formation (30, 31). Crescent formation may stop the entire afflicted glomerulus, this process compromises the other lobules leading to a segmental or later global sclerosis (32). There are several studies with transgenic animal models that showed a correlation between the severity and progression of sclerotic lesions and the amount of podocyte loss (29, 33). When mild podocyte loss is occurring (20% or less) the effects on the glomerular architecture can be just transient with low proteinuria and no real change in renal function (34). If the loss is more than 40%, the remaining podocytes cannot compensate, which is associated with the crescent formation, FSGS and mild proteinuria in the absence of changes in renal function. However, scar formation can be detected and seen as a result of an excessive repair mechanism (35). Over 40% of podocyte loss, a considerable proportion of glomeruli with adhesions and high proteinuria can be observed.

1.4. Adriamycin-induced focal segmental glomerulosclerosis

ADR nephropathy is a highly reproducible and robust model of proteinuric renal disease, resulting from selective podocyte injury (36). In rodents, like in the Balb/c mouse strain, a single injection of ADR also knows as doxorubicin, induces kidney damage that mimics human FSGS(37). ADR is an anthracycline antibiotic with pleiotropic cytotoxic effects used for the treatment of a wide spectrum of human cancers. It is a DNA intercalating agent, which inhibits the enzyme topoisomerase II and thereby generates free radicals, which induce DNA damage and subsequent cell death (38). Balb/cmice have shown a high susceptibility to ADR injection compared to C57BL/c mice that are highly resistant and multiple ADR injections were required to develop a

glomerulosclerosis. 1-2 weeks after ADR administration, altered renal function and induced thinning of the glomerular endothelium together with altered podocytes structure, in particular inside the SD. Loss of podocyte from the GBM is the normal epilog (39). Importantly, it was proved on severe combined immunodeficiency (SCID) mice that the structural and functional injury induced by ADR was not involving immune cell activation (40).

1.5. Podocyte regeneration from glomerular progenitors

The kidneys have been classically considered as organs with low capacity for regeneration. Mesangial and endothelial cells have been reported to have the capacity to proliferate and replace the loss of neighboring cells upon insult, but this does not apply to podocytes(41). Podocytes are terminally differentiated cells and are unable to proliferate (42). The loss of these specialized cells is a common cause of FSGS and progressive CKD (35).

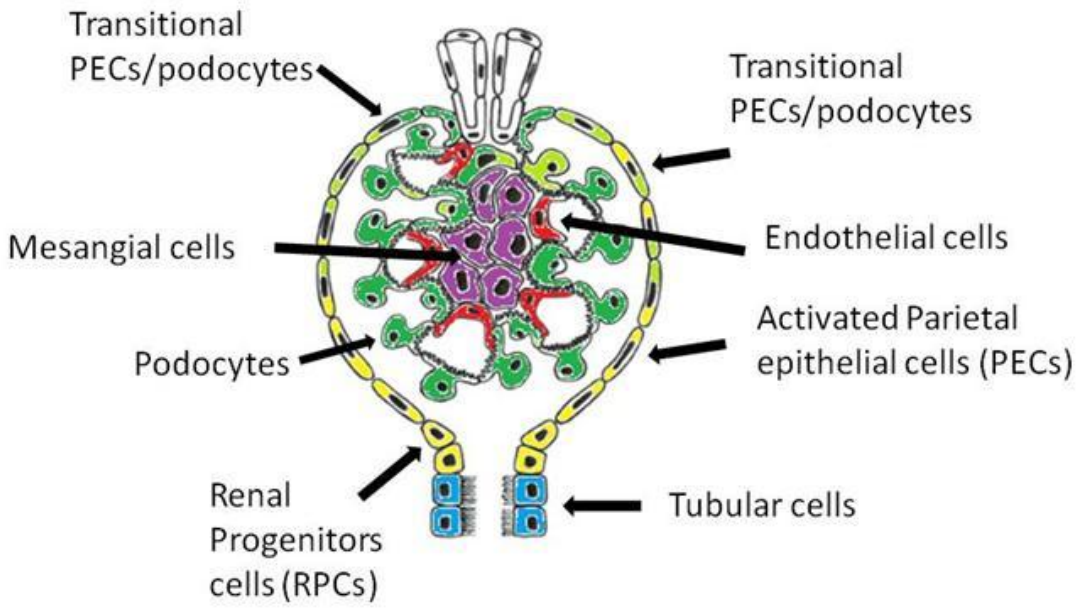

Figure 2. Representation of the glomerulus structure and cells components. The GBM comprised of fenestrated glomerular endothelial cells (red cells), glomerular basement membrane and podocytes (dark green cells). The parietal epithelial cells (PECs) along are present along the Bowman´s basement membrane during RPCs differentiation toward podocyte lineage after RPCs activation from the renal stem cell niche. (The image was adapted and used with the agreement of the copyright owners Duccio Lombardi and Laura Lasagni (see last page agreement), from *Lombardi and Lasagni et a(11)l*).

Recently, it has been proved that adult human glomeruli contain resident stem cell populations in a stem cell niche localized at the urinary pole of the Bowman´s capsule. This population is identified by the presence of cluster of differentiation 24 (CD24) and prominin-1 (CD133) (43-45) and has self-renewal properties and the capacity to differentiate into podocytes or

into tubular cells, *in-vitro* and *in-vivo* (35, 46). This double positive population demonstrated their capacity to proliferate and differentiate along the Bowman´s capsule, move to the vascular stalk and generating neo-podocytes. However, in glomerular disorders, characterized by acute or severe podocyte loss, the regenerative capacity of epithelial glomerular stem cells is inadequate because of an imbalance between the proliferative response and the degree of damage (47, 48). In addition, crescentic glomerulonephritis or collapsing glomerulopathy shows excessive proliferative response by RPCs (31, 49-51). This reflects the inability to restore lost podocytes, contributing to the crescent formation and glomerulosclerosis (31, 52, 53). Glomerular renal progenitors display different regenerative potentials throughout distinct disease stages and are modulated by the surrounding environment (54, 55). In a recent article by *Peired et al.*, one of the environmental factors that deregulated the RPC-induced regeneration and the amount of albumin in the urinary proteinuria was described (56). This study demonstrated that albumin impaired the RPC capacity to differentiate into podocytes. Albumin has the dose-dependent capacity and the affinity to sequestering the retinoic acid (RA). After GBM damage, the retinol passed in the Bowman's space was transformed in RA by the podocyte retinaldehyde dehydrogenases (Aldh1) enzyme. RPCs differentiation was a direct consequence of RA accumulation in the Bowman´s space. Retinoic acid-induced PECs differentiation toward podocytes lineage by the retinoic acid response element (RARE) is shown in Figure 3 (56).

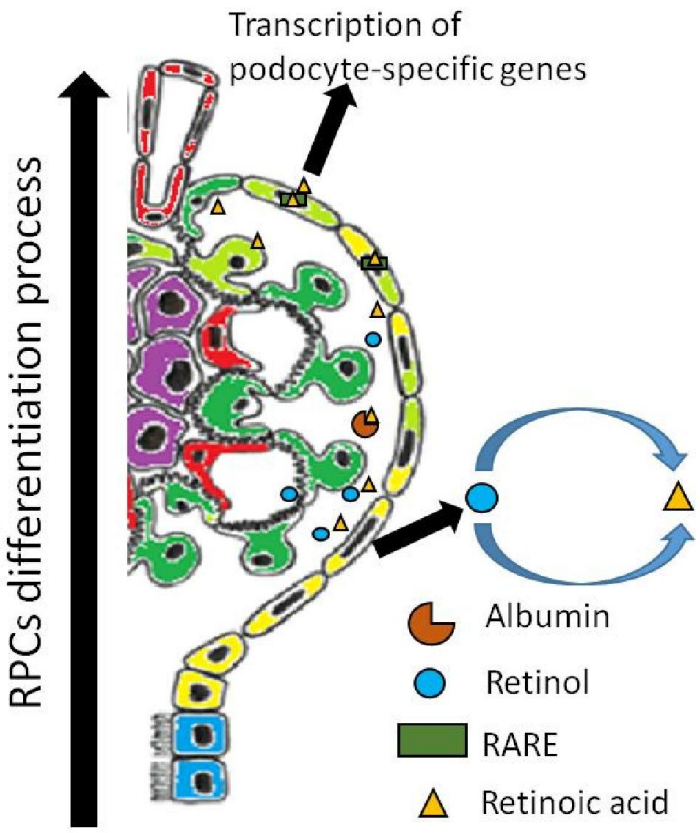

Figure 3. Renal progenitor cell differentiation toward podocyte lineage in mild proteinuria status. In a mild glomerular proteinuria disease, the podocytes can derivate (green and red/green cells) RA from the blood retinol and activates RPCs (red cells) can fully differentiate to podocyte. (right part). When proteinuria levels are too high in the BS, the RA is sequester by the albumin and the RPCs proliferation is not stopped by the differentiation toward podocyte lineage. RPCs uncontrolled proliferation can generate crescent formations (red cells) and consequently glomerular sclerosis and degeneration is established. (The image was adapted and used with the agreement of the copyright owners Duccio Lombardi e Laura Lasagni, from *Lombardi and Lasagni et al*,(11)).

Albumin is a high-affinity carrier of RA in the blood stream, which explains why a reduced quantity of albumin in the glomerular space was able to bind all RA, reducing drastically the major RPC differentiation factor and impairment of glomerular regeneration (56). As a result of this prolonged albumin lack, the activated and proliferating RPCs were not able to finalize the differentiation program toward podocytes leading to an accumulation of PECs in the BC and BS, that can degenerate to crescent formations, and finally to FSGS disease (30, 35, 56), as shown in Figure 4. However, further studies needs to be done to be able to fully understand the complex plethora of stimuli, which induce RPC regeneration.

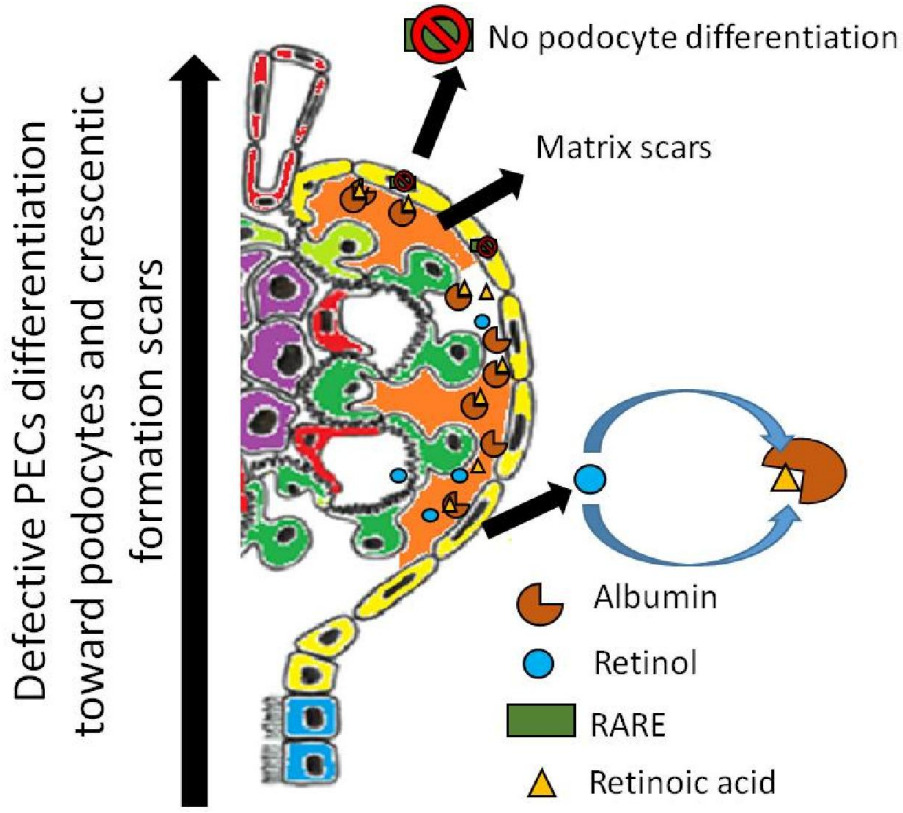

Figure 4. RPC over proliferation can generate crescents formations in high proteinuria status. When proteinuria levels are too high in the BS, the RA (orange triangle) is sequester by the albumin (brown half dot) and the RPCs proliferation (yellow cells) is not stopped by the differentiation toward podocyte lineage. RPCs uncontrolled proliferation can generate crescent formations (orange areas) and consequently glomerular sclerosis and degeneration is established. (The image was adapted and used with the agreement of the copyright owners Duccio Lombardi e Laura Lasagni, from *Lombardi and Lasagni et al*,(11))

1.6. Notch pathway

The Notch (neurogenic locus notch homolog protein) pathway was discovered in *Drosophila melanogaster* in 1917 by T.H. Morgan (57). At the beginning of the '80s, the Notch gene was found to encode a 300kDa single-pass transmembrane receptor (58). It was established that Notch was involved in cellular signaling and contains multiple conserved protein domains. In mammals, four Notch receptors (Notch 1-2-3-4) and five trans-membrane ligands Jagged-1-2 (Jag-1-2), Delta-like1-3-4 (Dll-1-2-3-4) have been identified (59). The Notch signaling cascade appears simple with few or no second messengers involved as shown in Figure 5.

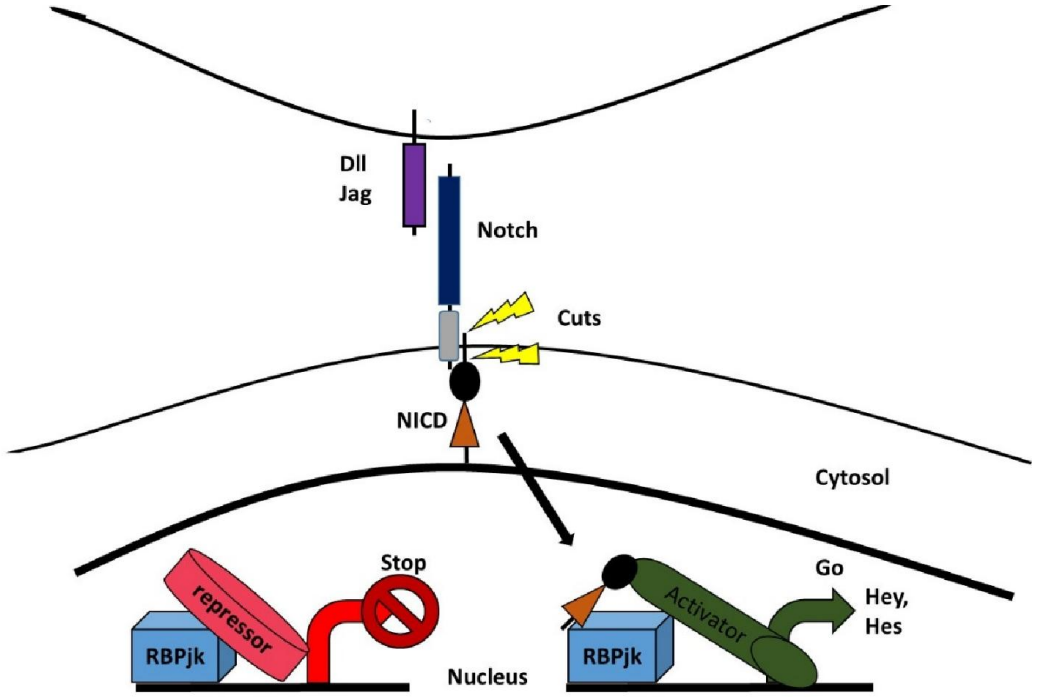

Figure 5. Notch pathway, ligands, receptors, and downstream genes. After the cuts from the proteases ADAM and gamma-secretase, the NICD entered in the nucleus and makes the complex with recombination signal sequence-binding protein-jk (RBP-jk) and the activator to starts Hey and Hes, Notch downstream genes activation.

However, the role of Notch signaling and the activation of downstream genes in many tissues remain complex and in many cases, unpredictable (59). The Notch signaling cascade is activated upon cell-to-cell contact as a result of interactions between Notch receptors and their ligands (60). At the molecular level Notch activation promotes two cleavage events on the Notch receptor (Figure 5). The first cleavage is catalyzed by the A-Disintegrin-And-Metalloproteinase (ADAM)-family-metalloproteases, whereas the second cleavage is mediated by gamma-secretase, a complex enzyme that contains presenilin and nicastrin (60). The second cleavage releases the Notch intracellular domain (NICD), which then translocates to the nucleus and acts as a transcriptional factor. NICD is a co-factor DNA binding protein RBP-jk and can activate the transcription of genes containing RBP-Jk binding sites. NICD binding to RBP-J is crucial for the switch from a repressed to an activated state. Notch receptors have diverse outcomes, only a fairly limited set of Notch target genes have been identified in various cellular and developmental contexts (60, 61). Therefore, in mammals, the best-described Notch target genes are the transcription factors Hey-1 and Hes-1-5-7 (62, 63). Hes and Hey proteins are helix-loop-helix transcription factors that function as transcriptional repressors. *Hes-1* deficient mice are not viable and display multiple developmental defects (61). Signaling mediated by Notch receptors and ligands is involved in regulation of many

biological functions including cell proliferation and differentiation (64), and homeostasis of adult self-renewing organs (65).

Notch signaling can also drive a terminal differentiation program by inducing cell cycle arrest like it is observed in keratinocytes in the skin. Notch regulates binary cell fate decisions and stem cells maintenance. A second general role of Notch is to promote the development of a given cell type or body region, often by inducing the expression of positively acting regulatory molecules. For example, in mammals, Notch signaling induces a terminal differentiation program in human skin (65, 66). In the kidney, it is known from the literature, that the Notch pathway is very important during the nephrogenesis of fetal kidney development (67). However, a very delicate equilibrium is set inside the glomerulus between Notch activation and its suppression. *Lasagni, et al*. (64) have demonstrated a double role of the Notch pathway during the endogenous podocyte-RPCs-driven regeneration after ADR nephropathy. In the context of glomerular ADR disease using SCID mice, the Notch pathway activation was negative for podocytes. Podocytes can start DNA synthesis for the cell cycle, but they cannot complete the cytokinesis. The principal reason was the very end-differentiated podocyte structure. Indeed, when podocytes re-enter the cell cycle, they would literally "destroy" the specific and characteristic cytoskeleton structure, in particular, the actin system (68, 69). In a disease condition, where many podocytes are lost or in a critical status, Notch activation of the Notch 1 receptor is the primarily induced signal (27) and can finally trigger GBM detachment or cell death. A recent study reported that if podocytes were forced to entry in mitosis, mitotic catastrophe (CM) can be established (42). DNA synthesis and chromosome segregation cannot complete cytokinesis due to poor expression of Aurora Kinase B, which is essential for this process (64, 70, 71) (Figure 6). Abnormal mitotic podocytes expressing histone H3 were observed in ADR-induced FSGS models and podocyte death through catastrophic mitosis was prevented by treatment with Notch inhibitors. This Notch activation mediated the down-regulation of cell cycle inhibitors that force podocytes to progress toward mitosis (64).

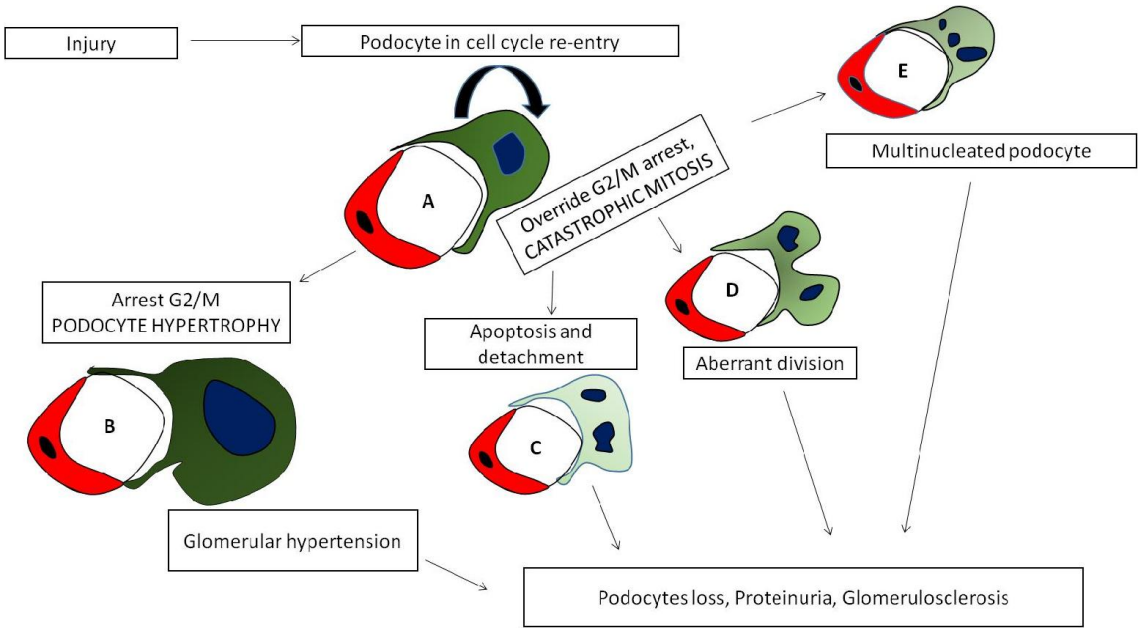

Figure 6. Destinies of a re-entry cell cycle podocyte after injury. Podocytes complete the DNA synthesis but cannot proceed through the M phase (**A**) owing to the activation of mitotic catastrophe. (**B**) increase their size thus becoming hypertrophic. When division cannot be complete and cytokinesis fails, cells with gross nuclear alterations are generated which quickly undergo "mitotic death" program; **D**) cells can exit mitosis containing a variable number of nuclei or micronuclei; these cells are viable because lethal pathway is not executed until cells reach interphase of the next cell cycle, but are unstable and detach from the GBM (**C**); in this case, cell death can occur in a delayed fashion even after years; **E**) when the aberrant division is productive aneuploidy cells form; most of these are unviable, owing to chromosomal rearrangements that result in progressive detachment to eliminate genomically unstable cells.

RPCs are highly activated by the Notch pathway, in particularly the Notch-3 receptor that leads RPCs to proliferate during AN, even after 21 days after the model induction, where Notch-3 was still strongly expressed in RPCs compared to the Notch-1 receptor (64). This positive PRC activation via the Notch pathway in an *in-vivo* model was further proven when a Notch inhibitor was injected in the FGSG model. The urine proteinuria was reduced at the beginning of the model on day 7 when Notch blockade dues to reduced podocyte' CM induction and less podocyte loss ratio. Nevertheless, the final outcome of the disease during the regenerative phase was compromised by the Notch inhibition effects on RPC proliferation and differentiation toward podocytes. The final number of podocytes in the glomeruli after inhibition was assessed and reduced in the treated group compared to the control (64). Also*, Lasagni, et al.* demonstrated the differential role of Notch signaling in several *in-vitro* experiments with RPCs and Notch inhibitors (64).

1.7. Stromal-derived factor 1 (SDF-1)/CXCL12

CXCL12, previously named stromal-derived factor 1 (SDF-1), was first described as a growth factor for pre-B cells but turned out to be also expressed in numerous hematopoietic and non-hematopoietic tissues (72) (Table.1). Nowadays, CXCL12 is known to be an essential regulator of progenitor cell homing and recruitment (73, 74), which includes bone marrow progenitors of the hematopoietic system as well as committed progenitors in peripheral tissues (75, 76). In addition, like pro-inflammatory chemokines, CXCL12 is induced following tissue injury and mediates the recruitment of progenitor and effector cells, which further contribute to tissue injury as well as wound healing (76, 77). CXCL12 mediates its biological effects via the receptors CXCR-4 and CXCR-7, which can form hetero- or homodimers and exert a variety of different biological effects. The CXCL12/CXCR4/7 axis can be modulated by pharmacological intervention in various diseases (78-80) including abdominal aortic aneurysm and diabetic nephropathy (81-83). In breast and colon cancer as well as renal cell carcinoma (RCC), blockade of the CXCL12/CXCR-4 interaction has been shown to reduce the ability to make metastasis due to CXCL12-dependent invasion and migration mechanisms (84-87).

Table 1. CXCL12/CXCR-4/CXCR-7 positive cells

Cell type	CXCL12	CXCR-4	CXCR-7
Podocytes (82, 83)	+	+	+
RPCs (88)	-	+	+
TECs (89)	+	+	+
HPSCs (90, 91)	-	+	+
BMSCs (92, 93)	+	+	-
Neutrophils (94, 95)	-	+	+
RCC (96, 97)	+	+	+
EPCs (98, 99)	-	+	+

List of abbreviations: Renal Progenitors cell; RPCs, Tubular endothelial cell; TECs, Hematopoietic stem cells; HPSC, Bone marrow mesenchymal stem cell; BMSCs, Endothelial Progenitor cells; EPCs.

1.8. CXCL12 in kidney development

Embryonic development requires directed progenitor cell migration (100). For example, the fetal bone marrow expresses high levels of CXCL12, which promotes the migration and homing of myeloid cells from the fetal liver (72). However, CXCR-7 seems redundant in mice because CXCR-7-deficient mice do not show abnormal hematopoietic tissue or hematopoiesis (101, 102). CXCR-7 is a critical regulator of CXCR-4-mediated migration of primordial germ cells and one of the main fine regulators of the signaling between podocytes and glomerular capillaries (103). Self-generated CXCL12 gradients by polarized CXCR-7 internalization support a self-directed stem cell migration in the capillary tuft (103, 104). The developing kidney expresses CXCL12 and CXCR-4 in the comma and S-shaped body, the mesangium, and the collecting ducts (105, 106). Inside the glomerulus, CXCL12-expressing podocytes are in close touch to CXCR-4^{+} endothelial cells located in the vascular cleft in the S-phase of forming glomerulus (106). Targeted deletion of CXCL12 or CXCR-4 resulted in defective blood vessel formation with a highly disorganized vasculature in the glomerular tufts (106). Deleting CXCR-4 selectively in endothelial cells gave a similar phenotype (106). Interestingly, no defects were found in mice with *Cxcr-4*-deficient podocytes suggesting that podocyte-derived CXCL12 is a paracrine signal for endothelial cells (106), conceptually similar to the glomerular vascular endothelial growth factor (VEGF) system (107). *Doná et al.* clarified several aspects of such CXCL12 gradients during kidney development, they showed an important impact for the CXCL12 atypical receptor CXCR-7 during the generation of the migration gradient (104).

1.9. CXCL12 in stem cell homing and homeostasis outside and inside the kidney

Hematopoietic stem and progenitor cells (HSCs) and their niches in the bone marrow (BM) are one of the most studied stem cell systems. CXCL12 is the predominant signal that maintains CXCR-4^{+ve} HSCs quiescent inside the bone marrow stem cells niche (108, 109). In the perivascular niche, CXCL12-abundant reticular cells (CAR) as shown in Figure 7, constitutively express CXCL12 to facilitate the homing of CXCR-4^{+} blood cell progenitors and endothelial progenitor cells (EPCs) (108). In contrast, osteoblasts along the inner bone surface home more immature and quiescent HSCs to the endosteum niche (108). CXCL12 also induces the production of matrix metalloprotease 9 (MMP-9) and the shedding of the CD117 ligand to mobilize quiescent HSCs from the vascular niche to expand before mature granulocytes and monocytes egress into the blood (102). Consistent with this, genetic variants that increase CXCR-4 signaling can cause a hypercellular bone marrow and peripheral blood neutropenia (110). In addition, CXCL12 also regulates the senescent return of neutrophils to the bone marrow for clearance (94). In this process, neutrophils increase CXCR-4

expression on their surface, becoming susceptible to CXCL12 in the bone marrow, which facilitates their re-entry via phagocytosis by bone marrow macrophages (94).

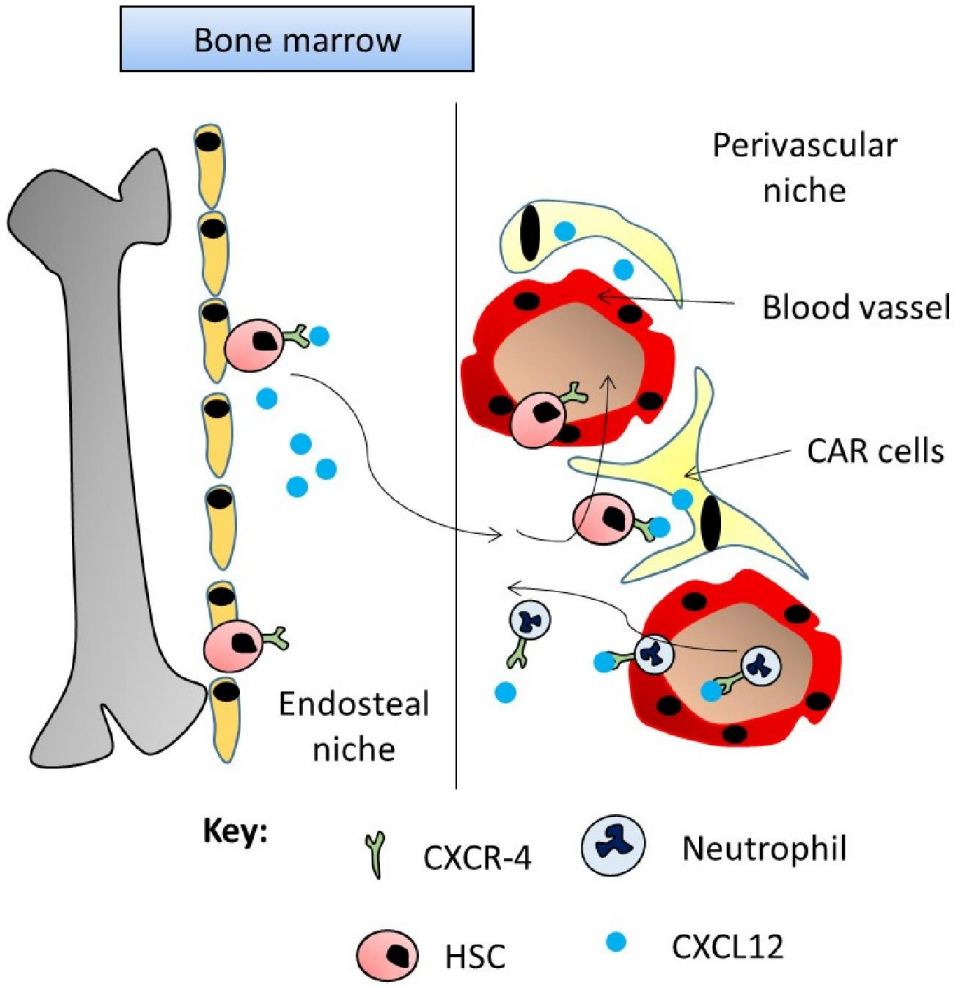

Figure 7. Homeostatic chemokines in hematopoietic stem cell homing or trafficking. Bone marrow. HSCs reside in two different niches within the bone marrow. The hypoxic endosteal niche is generated by bone-lining cells producing CXCL12, which keeps the cells largely in an immobile and quiescent state. The perivascular niche is formed by perivascular CXCL12 abundant reticular (CAR) cells, which support homing within the bone marrow, cell division, and evasion of blood cells into the blood stream. Neutrophils are shown at the bottom of the figure, and immature lymphocytes in the upper part, respectively. Senescent neutrophils also return to the bone marrow for phagocytic clearance upon upregulation of CXCR-4.

Further support comes from CXCL12 or CXCR-4-deficient mice, which show a severe defect of myelopoiesis (111). It is of note that the central role of CXCL12/CXCR-4 in regulating HSC homing has been exploited for clinical purposes: a single injection of a CXCR-4 antagonist is sufficient to mobilize HSCs and other progenitor cells from the bone marrow into the peripheral blood (112); therefore representing a possible therapeutic approach used beyond mobilization of HPSCs (113). Inside the kidney, podocytes produce the vascular endothelial growth factor (VEGF) to maintain normal glomerular capillaries and contribute to endothelial regeneration after glomerular injury (114).

CXCL12 expressed by mature podocytes acts on endothelial cells but also on other glomerular cells, such as RPCs from BC identified as CD24+ and CD133+ cells, that showed increased CXCL12/CXCR-7-mediated survival *in-vitro* after H_2O_2 stimulation (88). The CXCL12 ability to maintain tissue in homeostasis by regulating podocytes, capillary endothelial cells and RPCs, could be crucial to modulate the outcome of kidney disease. Moreover, the consequent aspect necessary to be defined is the pathogenic role of CXCL12 during kidney disease.

1.10. Pathogenic roles of CXCL12 during kidney disease

Glomerulonephritis. In human biopsies of IgA nephropathy and extra-capillary glomerulonephritis, high levels of CXCR-4 expression was revealed in hyperplastic lesions by immune-fluorescent staining, associated with a positivity for $CD24^+$ progenitor cells (115). On the contrary, in patients with membrane nephropathy or diabetes, the positivity of CXCR-4 expression was faint (115). Moreover, in a mouse model of diabetic nephropathy, the podocytes were the major producer of CXCL12 as demonstrated by CXCL12 protein quantification and tissue staining (83). CXCL12 is produced by podocytes in a state of health similar to that during glomerular disease (83, 116). Interestingly, CXCL12 expression can be further increased by podocytes during glomerulonephritis. This deregulation of CXCL12 production seems to be related to the development of nephritis (116). The reversal of nephritis in New Zealand Black/New Zealand White (NZB/W) mice treated with an anti-CXCL12 monoclonal antibody (mAb) had effects on both levels, systemically and locally (116). The CXCL12/CXCR-4 axis is involved in such excessive epithelial hyperplasia, which is presented as crescentic glomerulonephritis (35, 117). Crescentic glomerulonephritis and collapsing glomerulopathy are both characterized by podocyte loss and inappropriate hyperplasia of mal-differentiated epithelial cells (118). It has been demonstrated that in the tip lesion as well as in FSGS, both characterized by some hyperplasia, glomerular RPCs are the main constituents of the proliferative lesion (52). RPCs can also consequently form tip lesion as described during FSGS and diabetic nephropathy (52). In diabetic nephropathy CXCL12 is located within the cytoplasm of the podocytes during the advanced phase of the disease (83). In a study by *Rizzo, et al*. CXCR-4 was found to be expressed by activated PECs and CXCL12 was produced by podocytes in Munich Wistar Frömter (MWF) rats, which develop progressive glomerular injury (115). Using a diabetic C57BLKS db/db mouse model, *Sayyed, et al.* showed that blockade of CXCL12 ameliorates glomerular disease markers and increases the number of podocytes to maintain the peritubular vasculature without affecting glucose levels or glomerular macrophages infiltration (83). Furthermore, *Darisipudi, et al.* revealed that CXCL12 blockade increases the differentiation capacity of RPCs towards podocytes, and reduces the loss of nephron levels in the total kidney of diabetic mice (82). Along the same line,

CXCR-4 re-expression in adult podocytes could drive autocrine actions of nephrosclerosis, a common manifestation of chronic microvascular disease (119). This may also include mobilization and detachment of podocytes from the glomerular basement membrane, a process known to lead to glomerulosclerosis and chronic kidney disease. Together, the data emphasize the fact that blocking CXCL12 and its receptors in a time-dependent way could be an important tool to modulate and ameliorate glomerular pathologies (109).

Tubular injury. Acute kidney injury (AKI) is characterized by a rapid decrease in excretory renal function and sometimes also with a decrease in urinary output within hours to days, either due to a decline in renal blood perfusion, intrarenal injuries such as acute tubular necrosis (ATN) or urinary outflow obstruction (120). During ATN, increased hypoxia level, can induce tubular cells CXCL12 secretion. The distal convolute tubules and collecting ducts also showed high expression levels of CXCL12 in the cytoplasm and CXCR-4 on the plasma membrane (121). Proximal tubules were also positive for CXCL12, whereas the renal interstitium was negative (121). CXCL12 can trigger neutrophil infiltration during an ischemic insult leading the tubular inflammation (121). The renal ischemia-reperfusion (IR) injury is a common cause for AKI, associated with high morbidity and mortality, that can affect native and transplanted kidneys (122). As for the glomerular compartment, the CXCL12 expression is increased during kidney IR. In particular, bilateral IR induces a strong expression of CXCL12 in tubular epithelial cells (TECs) of ischemic kidneys after one day compared to contro-lateral kidneys (123). However, CXCL12 levels return to baseline after 10 days following surgery. *Stokman, et al*. have investigated this increased production of CXCL12 to answer the question whether high levels of CXCL12 are a pre-requisite for starting the regeneration phase of the tubular compartment after IR via bone marrow stem cells (HSCs) mobilization and differentiation towards TECs (123). Surprisingly, blocking CXCL12 with an antisense oligonucleotides (ASON) did not alter the influx of HSCs and had no effect on tubular regeneration compare to treatment with nonsense oligonucleotides (NSON) (123). Instead, ASON-CXCL12 showed that CXCL12 was required to improve TECs survival during IR compared to CXCL12-nonsense oligonucleotides (NSON) blockade (123). Together, CXCL12 displays opposite roles during IR injury: (1) CXCL12 is an important chemoattractant for neutrophils during tubular injury as shown in Figure 8, and (2) it is a crucial factor in avoiding cell death of TECs as well as helping the recovery of TECs after IR. (3) CXCL12 also triggers the infiltration of immune cells towards the injured tubular compartment to promote healing by serving as a survival factor for tubular cells; however this concept remains to be evaluated in more details.

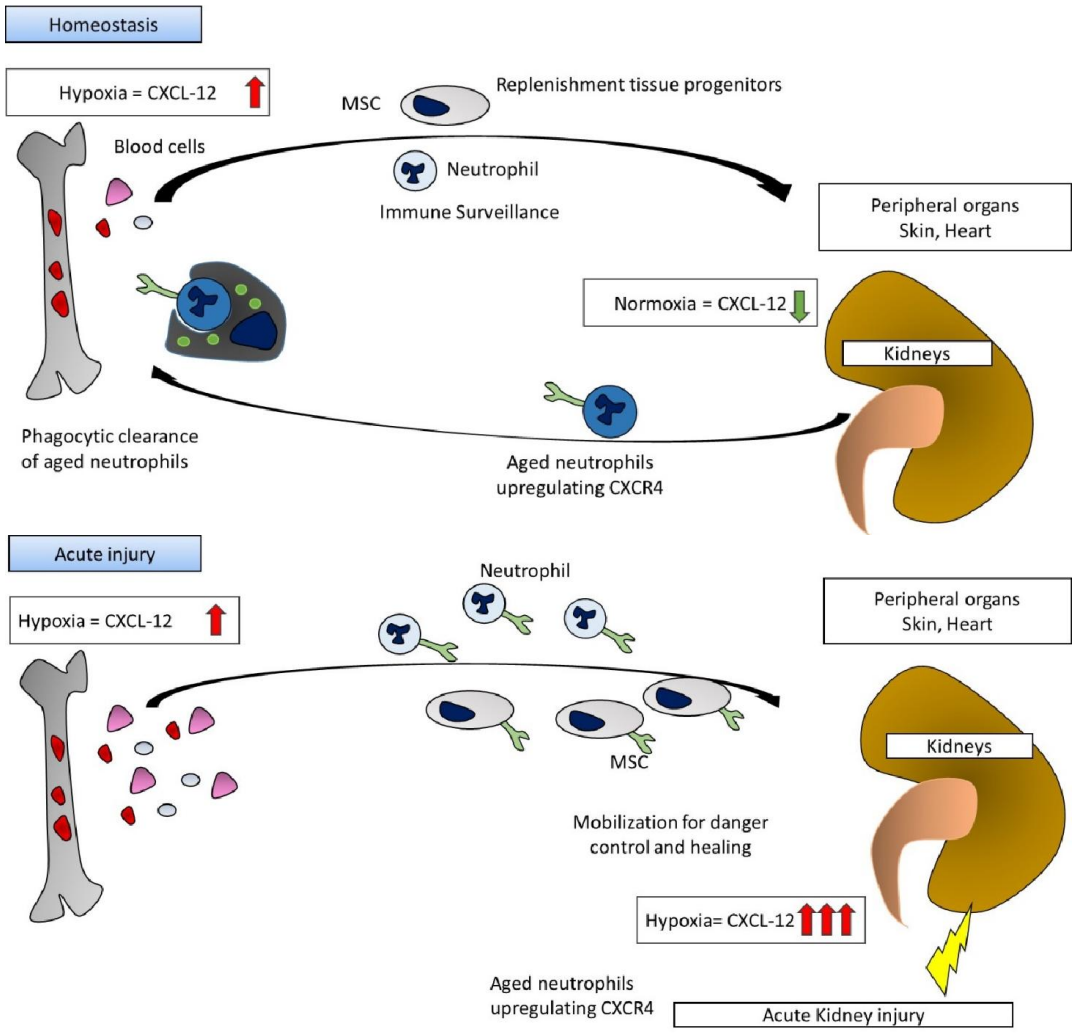

Figure 8. Figure 6. CXCL12 in homeostasis and AKI. In the upper panel, CXCL12 effects on the neutrophils clearance are shown. Also, CXCL12 has a role in many tissue progenitor replenishment. In the bone marrow, as well as in other organs CXCL12 effects are strongly regulated by the hypoxia. In the lower panel is shown how, during acute injury the increased level of hypoxia can lead to several tissues to secrete higher levels of CXCL12 with subsequential inflammatory cell recruitment in the diseased compartment.

1.11. CXCL12 and kidney regeneration

Commonly, in adult tissues, stem cells are the principal players involved in self-renewal, proliferation, and multipotent differentiation capability *in-vivo* (124). The mammalian kidney shares with other organs the ability to partially resolve the damaged structures after injury. Tubular integrity, for instance, can be restored after acute damage, and glomerular disorders can sometimes undergo regression by re-epithelialization (53, 125). Research on the functional role of RPCs has been of great interest in the last years due to a potential importance of RPCs for *de-novo* regeneration of podocyte loss following glomerular injury (28). *Mazzinghi, et al.* identified the mechanisms that are involved in the therapeutic homing of human renal progenitors into the injured kidney (88). Using a radioactive assay, they were able to show the expression of CXCR-4 and CXCR-7 on the surface of human renal progenitors (88). A dual blockade of CXCR-4 and CXCR-7 to assess the regenerative capacity of injected human RPCs during kidney damage was induced by glycerol injection in SCID (88). They further demonstrated that the interaction between CXCL12 and both receptors are important for the homing and regeneration of the kidney. Of note, CXCR-4 is required for RPC chemotaxis and migration, while CXCR-7 is necessary for RPCs transendothelial migration and subsequently the adhesion to the extracellular compartment (88). Another study showed that blocking CXCL12 for 8 weeks in a male diabetic C57BLKS db/db uninephrectomized mouse model resulted in increased numbers of infiltrating cells in each glomerulus that were positive for the podocyte marker Wilms-tumor protein1 (WT-1) compared to control mice (82). Also, total kidney mRNA-RT-PCR evaluation of the podocyte marker nephrin showed an increased expression following blockade of CXCL12 (82). Furthermore, *Darisipudi, et al. (82)* showed that blocking CXCL12 during RPC differentiation toward podocyte lineage under VRAD medium stimulation *in vitro* that the mRNA level of nephrin increased in podocytes (82). CXCL12 is also known to play a key role during EPCs mobilization. To investigate this, *Bo, et al.* designed a tubular ischemia precondition (IPC) before inducing a severe IR damage (126). They were able to raise CXCL12 and VEGF levels in the kidney and the subsequent mobilization of EPCs towards the tubular compartment resulting in a better AKI outcome (126). These data suggest that EPCs and CXCL12 have a renal protective role in the late phase of IR injury by regulating endothelial cell dysfunction (126).

1.12. Spiegelmer, a next generation aptamer

Klussman, et al. (86, 127-129) and *Darisipudi, et al.* (82), showed the CXCL12 was a good target inside and outside the glomerular diseases. Within this thesis, the CXCL12 antagonist from NOXXON Pharma called NOX-A12 was used (113), a chiral molecule specific for CXCL12 that was obtained via SELEX technology (Figure 9). This Spiegelmer (NOX-A12 antagonist) has been identified

to be highly selective, non-immunogenic, save and body well-tolerated and highly stable in plasma. The preparation of the mirror-image target that was required for the screening process is important and sometimes challenging step, particularly when targets are chemically or biologically more complex. Whereas, smaller peptide targets that are more easily accessible for the Spiegelmer discovery and development. Until now, several different studies and clinical trials have been successfully undertaken using the NOX-A12 antagonist animal models e.g.: CXCL12 Inhibition during bone marrow cancer therapy (128-130) as well as preclinical and clinical studies e.g. Spiegelmer NOX-A12, interferes with chronic lymphocytic leukemia cell motility and causes chemosensitization (131). Therefore NOX-A12 was used to inhibit CXCL12 in all experiments within this thesis.

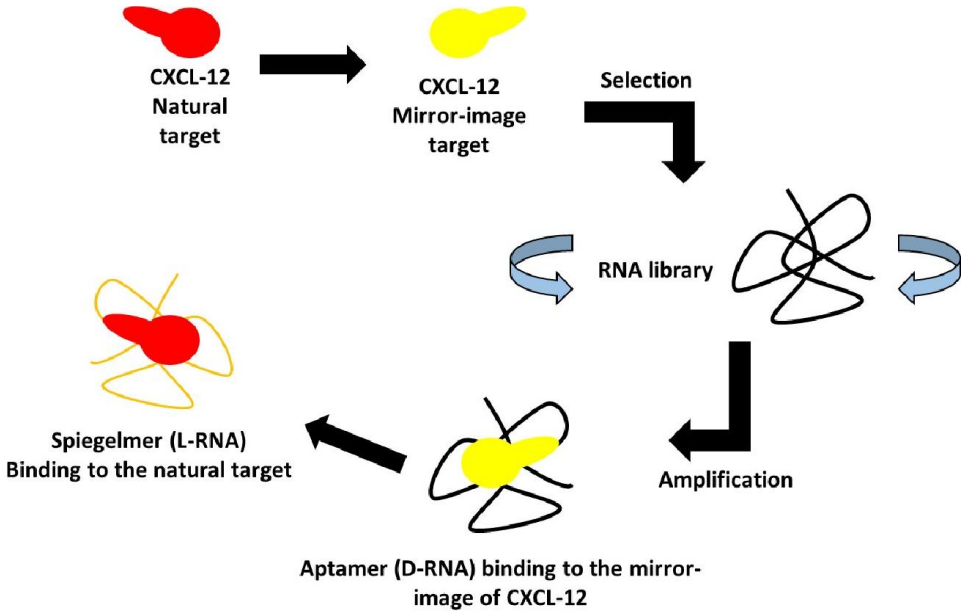

Figure 9. The representative process to obtain an RNA-spiegelmer against the chemokine CXCL12. Mirror image of CXCL12 is synthesized. RNA aptamers binding to the mirror-image are selected by *in-vitro* synthetic ribonucleotide library in the natural D-configuration. The D-configuration is required because stereoselective enzymes are used for amplification, cloning, and sequencing of bound sequences. The finals identified sequences were synthesized using an (L)-ribonucleotides like an NOX-A12 spiegelmer after poly-etilen glycol molecular stabilization.

2. Hypotheses

In search of a potential cure for progressive glomerulosclerosis we previously found that blocking the chemokine CXCL12 protected mice with type 2 diabetes from albuminuria, podocyte loss, progressive glomerulosclerosis and CKD (82, 83). The pathophysiology behind this renoprotective effect is unclear. During glomerular disease, podocytes are the major producer of CXCL12. The role of CXCL12 in the glomerulus was studied intensively by *Romagnani, et al.* (88) in the field of RPC recruitment and survival during glomerular disease, however, the mechanisms are still not fully understood, especially the release of CXCL12 by podocytes under healthy and disease conditions.

Therefore, the following hypotheses were raised:

- CXCL12 produced by podocytes may serve as an autocrine survival factor for podocytes during glomerular injury.
- CXCL12 drives the proliferation and differentiation of RPCs toward the podocytes lineage during glomerular disease by inhibiting Notch

3. Materials and Methods

3.1 Instruments and Chemicals

3.1.1 Chemicals and Reagents

RNeasy Mini Kit	Qiagen GmbH, Hilden, Germany
RT-PCR primers	Metabion, Munich, Germany
Cell culture:	
DMEM-F12 medium	Sigma, Munich, Germany
RPMI-1640 medium	GIBCO/Invitrogen, Paisley, Scotland, UK
FBS	Biochrom KG, Berlin, Germany
FBS Hyclone	ThermoScientific, UT, USA
EBM	Lonza, Cologne, Germany
EGM-MV	Lonza, Cologne, Germany
CXCL12	immunotools
Trypsine/EDTA (1×)	PAA Laboratories GmbH, Cölbe, Germany
Penicillin/Streptomycin (100×)	PAA Laboratories GmbH, Cölbe, Germany
All-trans retinoic acid	Sigma, Munich, Germany
Vitamin 3D	Sigma, Munich, Germany
Antibodies:	
Nephrin	Santa Cruz Biotechnologies, Santa Cruz, CA
WT-1	Santa Cruz Biotechnologies, Santa Cruz, CA
DAPI	Invitrogen, Darmstadt, Germany
Alexa Fluor 488 anti-rat IgG1	Invitrogen, Darmstadt, Germany
Alexa Fluor 546 anti-rabbit IgG1	Invitrogen, Darmstadt, Germany
Alexa flour 488 anti-goat	Invitrogen, Darmstadt, Germany
Alexa Fluor 488 anti-mouse IgG1	Invitrogen, Darmstadt, Germany
Alexa Fluor 546 anti-mouse IgG1	Invitrogen, Darmstadt, Germany

HRP linked Anti-Rabbit secondary	Cell signaling, Danvers, MA
HRP linked Anti-Mouse secondary	Cell signaling, Danvers, MA
HRP linked Anti-Goat secondary	Dianova, Hamburg, Germany
β-Actin	Cell signaling, Danvers, MA
Elisa Kits:	
Mouse Albumin	Bethyl Laboratories, TX, USA
Creatinine FS	DiaSys Diagnostic System, Holzheim, Germany
Urea FS	DiaSys Diagnostic System, Holzheim, Germany
Chemicals:	
Acetone	Merck, Darmstadt, Germany
AEC Substrate Packing	Biogenex, San Ramon, USA
Bovines Serum Albumin	Roche Diagnostics, Mannheim, Germany
Skim milk powder	Merck, Darmstadt, Germany
DEPC	Fluka, Buchs, Switzerland
DMSO	Merck, Darmstadt, Germany
EDTA	Calbiochem, SanDiego, USA
30% Acrylamide	Carl Roth GmbH, Karlsruhe, Germany
TEMED	Santa Cruz Biotechnology, Santa Cruz, CA
Eosin	Sigma, Deisenhofen, Germany
Ethanol	Merck, Darmstadt, Germany
Formalin	Merck, Darmstadt, Germany
Hydroxyethyl cellulose	Sigma-Aldrich, Steinheim, Germany
HCl (5N)	Merck, Darmstadt, Germany
Isopropanol	Merck, Darmstadt, Germany
Calcium chloride	Merck, Darmstadt, Germany
Calcium dihydrogenphosphate	Merck, Darmstadt, Germany

Calcium hydroxide	Merck, Darmstadt, Germany
Beta mercaptoethanol	Roth, Karlsruhe, Germany
Sodium acetate	Merck, Darmstadt, Germany
Sodium chloride	Merck, Darmstadt, Germany
Sodium citrate	Merck, Darmstadt, Germany
Sodium dihydrogenphosphate	Merck, Darmstadt, Germany
Penicillin	Sigma, Deisenhofen, Germany
Roti-Aqua-Phenol	Carl Roth GmbH, Karlsruhe, Germany
Streptomycin	Sigma, Deisenhofen, Germany
Tissue Freezing Medium	Leica, Nussloch, Germany
Trypan Blue	Sigma, Deisenhofen, Germany
Xylol	Merck, Darmstadt, Germany
Miscellaneous:	
LDH	Roche diagnostic, Switzerland
Cell Titer 96 Proliferation Assay	Promega, Mannheim, Germany
Pre-separation Filters	Miltenyl Biotec, Bergish Gladbach, Germany
Super Frost® Plus microscope slides	Menzel-Gläser, Braunschweig, Germany
Needles	BD Drogheda, Ireland
Pipette's tip 1-1000µL	Eppendorf, Hamburg, Germany
Syringes	Becton Dickinson GmbH, Heidelberg, Germany
Plastic histocasettes	NeoLab, Heidelberg, Germany
Tissue culture dishes Ø 100x20mm	TPP, Trasadingen, Switzerland
Tissue culture dishes Ø 150x20mm	TPP, Trasadingen, Switzerland
Tissue culture dishes Ø 35x10mm	Becton Dickinson, Franklin Lakes, NJ, USA
Tissue culture flasks 150 cm2	TPP, Trasadingen, Switzerland
Tubes 15 and 50 mL	TPP, Trasadingen, Switzerland

Tubes 1.5 and 2 mL	TPP, Trasadingen, Switzerland
Balance:	
Analytic Balance, BP 110 S	Sartorius, Göttingen, Germany
Mettler PJ 3000	Mettler-Toledo, Greifensee, Switzerland
Cell Incubators:	
Type B5060 EC-CO2	Heraeus Sepatech, München, Germany
Centrifuges:	
Heraeus, Minifuge T	VWR International, Darmstadt, Germany
Heraeus, Biofuge primo	Kendro Laboratory Products, Hanau, Germany
Heraeus, Sepatech Biofuge A	Heraeus Sepatech, München, Germany
ELISA-Reader:	
Tecan, GENios Plus	Tecan, Crailsheim, Germany
Confocal microscopy	
LSM501 META laser	CarlZeiss, Jena, Germany (Leica)
Leica SP5 AOBS	Leica
Real-Time System:	
Light Cycler 480, Roche	Roche Diagnostics, Mannheim, Germany
Chameleon Ultra-II two-photon	(Coherent)
Other Equipments:	
Nanodrop	PEQLAB Biotechnology, Erlangen, Germany
Cryostat CM 3000	Leica Microsystems, Bensheim, Germany
Homogenizer ULTRA-TURRAX	IKA GmbH, Staufen, Germany
Microtome HM 340E	Microm, Heidelberg, Germany
pH meter WTW	WTW GmbH, Weilheim, Germany
Thermomixer 5436	Eppendorf, Hamburg, Germany
Vortex Genie 2™	Bender & Hobein AG, Zürich, Switzerland

Water bath HI 1210	Leica Microsystems, Bensheim, Germany
qRT-PCR syber green LC-480	Roche, Mannheim, Germany

If not stated otherwise, all other reagents were of analytical grade and are commercially available from Invitrogen and Sigma-Aldrich.

3.2 Experimental procedures

3.2.1 Animal models

The experiments were performed in Germany and Italy according to the Italian and German animal care and were approved by local government authorities. Balb/cAncrl, mice were obtained from Charles-Rriver, Germany. Balb/cAncrl Ancrl mice were purchased from Charles River Laboratories (Sulzfeld, Germany), and NPHS2-rtTA;tetO-Cre;Rosa26-TomatoRedGFP and hNPHS2.rtTA;TetO.Cre;iDTR mice were obtained from Prof.Tobias Hüber (132) (University of Freiburg, Germany) and Prof. Waismann A (133) (University of Mainz), Pax2.rtTA;TetO.Cre;mT/mG mice were developed by crossing the mT/mG reporter strain B6.129(Cg)-Gt(ROSA)26Sor$^{tm4(ACTB-tdTomato,-EGFP)Luo}$/J from Prof. Romagnani P. (University of Florence, Italy) (27). Mice were housed in groups of five mice in standard housing condition with a 12-hour light/dark cycle. Cages, nest lets, food, and water were sterilized by autoclaving before use and mice were allowed to unlimited access to food and water.

3.2.2 Experimental design

In this experimental thesis, several mouse disease models have been used, which are described in more detail within this section:

A) CXCL12 blockade in ADR-induced nephropathy
B) Therapeutic blockade of CXCL12 in an ADR-induced nephropathy mouse model
C) NPHS2.rtTa:TetO.Cre;iDTR;mT/mG-induced nephropathy and CXCL12 blockade
D) ADR-induced nephropathy and CXCL12 blockade in an induced PAX2 lineage-tracing genetic mouse model

A) CXCL12 blockade in Adriamycin-induced nephropathy

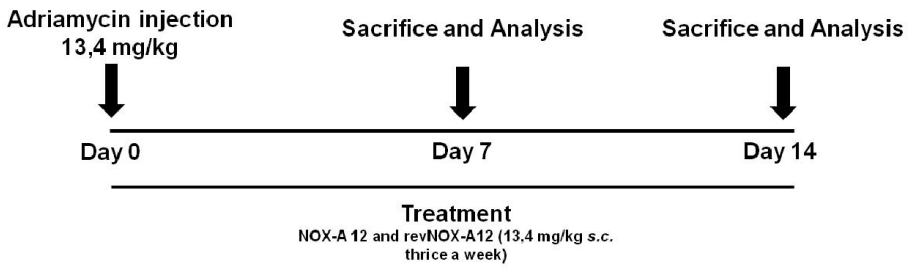

Figure 10. Treatment protocol A

ADR nephropathy was induced in 6-weeks old Balb/cAncrl mice, which received a single tail vein injection of 13.4mg/kg doxorubicin hydrochloride (Pharmacia&Upjohn, Erlangen, Germany) on day 0. Mice received three subcutaneous injections of NOX-A12 (13.4mg/kg) or revNOX-A12 in 5% sucrose (B.Braun, Melsungen, Germany). Group size was n=6-8 mice in each experiment. After 7 days plasma and urine samples were collected before sacrifice by cervical dislocation and kidney tissues harvested. The kidneys were divided into three parts. One part was immediately flash frozen in liquid nitrogen and then further stored at -80^{0}C for protein isolation and cryo sections, the second part was collected in RNA later solution (Ambion, CA, USA) and stored at -20^{0}C for RNA isolation and the third part of the kidney was kept in formalin to fix the tissue before embedding in paraffin for histological analysis.

B) Therapeutic blockade of CXCL12 in an adriamycin -induced nephropathy model

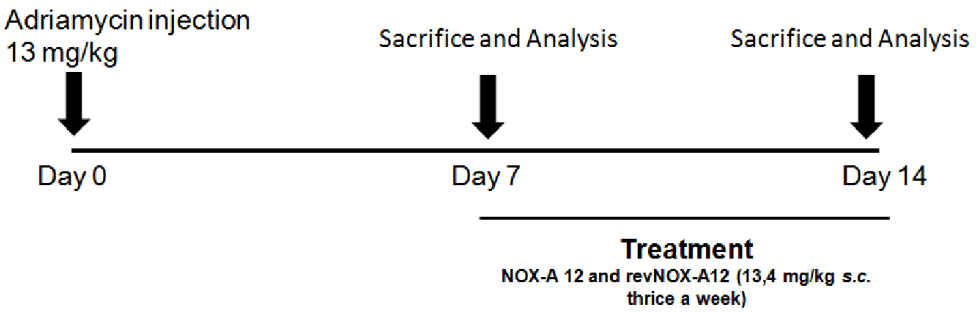

Figure 11. Treatment protocol B

ADR nephropathy was induced in 6-week old Balb/cAncrl mice, which received a single tail vein injection of 13.4mg/kg doxorubicin hydrochloride (Pharmacia&Upjohn, Erlangen, Germany) to induce a nephropathy. Mice received three subcutaneous injections of NOX-A12 (13.4mg/kg) or revNOX-A12 in 5% sucrose (B. Brown) on day 7 until day 14. Group size was n=6-8 mice in each experiment. At the end of the study, plasma and urine samples were collected before sacrifice by

cervical dislocation and kidney tissues harvested. The kidneys were divided into three parts, as described before.

C) ADR-induced nephropathy and CXCL12 blockade in an induced *Pax2.rtTA;TetO.Cre;mT/mG* lineage-tracing genetic mouse model

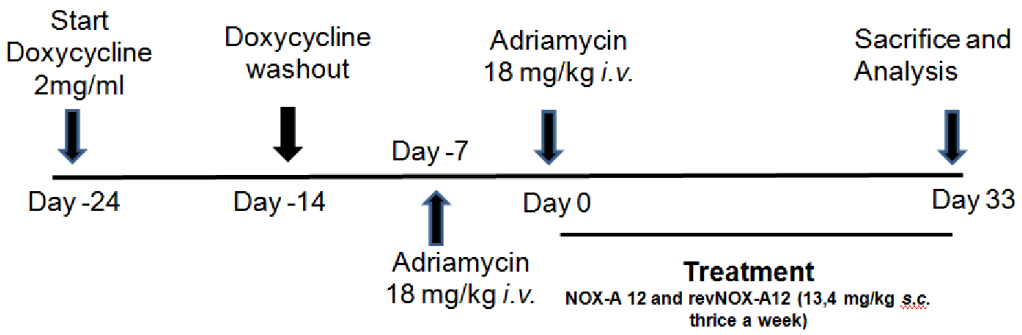

Figure 12. Treatment protocol C

Reporter *Pax2.rtTA;TetO.Cre;mT/mG* transgene recombination was induced at 6 weeks of age by administration of doxycycline hyclate (2 mg/ml, Sigma-Aldrich) in drinking water additioned of 2.5% sucrose (Sigma-Aldrich), for 10 days. *Pax2.rtTA;TetO.Cre;mT/mG* induced at the age of 8-9 week-old male and female old mice received by two successive tail veil injections of 18 mg/kg doxorubicin hydrochloride (Sigma-Aldrich) on the day -7 and day 0. Mice received subcutaneous injections with 13.4mg/kg of the CXCL12 inhibitor NOX-A12 (NOXXON, Berlin, DE) in 5% sucrose (vehicle) or control CXCL12 inhibitor revNOX-A12 (NOXXON, Berlin, DE), thrice a week. Mice were sacrificed at the end of the experimental period of 33 days (n=8), kidneys were collected, incubated in 4% PFA in PBS for 2 hours at 4°C followed by immersion in a 15% sucrose solution in PBS for 2 hours at 4°C and subsequently in a 30% sucrose solution in PBS overnight at 4°C, then frozen kidneys were collected as detailed above and analyzed by confocal microscopy. At least 4 healthy mice were included in each experiment. Urinary albumin and creatinine ratio was evaluated on spot urine using the system described below.

D) *NPHS2;TetO.Cre;iDTR/mT/mG*-induced nephropathy and CXCL12 blockade

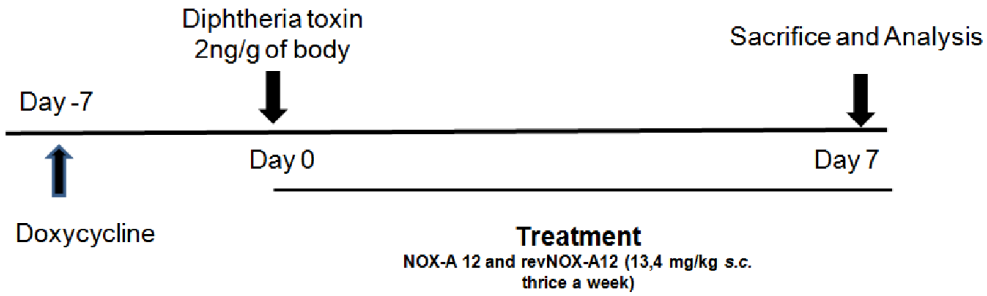

Figure 13. Treatment protocol D

hNPHS2.rtTA;TetO.Cre;iDTR mice (Podocin-iDTR received doxycycline hydrochloride (Sigma-Aldrich) via the drinking water (2mg/ml with 5% sucrose, protected from light) during pregnancy and nursing to induce transgene recombination. To increase induction efficiency, the mice received doxycycline (2mg/ml) orally from P6 to P18 three times per week. Diphtheria toxin (DT) (Sigma-Aldrich) was injected once intraperitoneally, to induce mild podocyte depletion with DT 2ng/g body weight. For blocking CXCL12, mice received 13.4mg/kg of the CXCL12 inhibitor NOX-A12 (NOXXON) in 5% sucrose (vehicle) or control CXCL12 inhibitor revNOX-A12 (NOXXON) subcutaneously thrice a week. On day 7, mice were euthanized by cervical dislocation, and kidneys harvested. Blood and urine were collected before sacrifice to evaluate the functional parameters of the kidney damage. Kidneys were harvested as described above.

3.3 CXCL12 inhibitor

Spiegelmers were modified with 40Kd branched polyethylene glycol (PEG) at 5'-end. The antagonist binds CXCL12 with sub-nanomolar affinities. All spiegelmers were dissolved in isotonic 5% glucose (B. Brown).

Sequences:

- NOX-A12 (CXCL12 antagonist)
  5'GGCGACAUUGGUUGGGCAUGAGGCGAGGCCCUUUGAUGAAUCCGCGGCCA-3'
- revNOX-A12 (control antagonist)
  5'GCAUGGACUGAUCCUAGUCGGUUAUUAGAUCUAGUGUGGUGCG-3'

3.4 Blood and urine sample collection

Urine samples were collected using the approved methods. Collected urine was stored at -20^{0}C until used for further biochemical analysis. At the end of the study blood samples were collected by retro-orbital bleeding technique under isoflurane anesthesia in microcentrifuge tubes containing EDTA (10µl of 0.5M solution per 200µl of blood). Samples were centrifuged at 8000 rpm for 5 minutes and plasma was separated and stored at -20^{0}C until used for analysis. BUN levels were measured by BUN Standard FS (DiaSys Diagnostic Systems).

3.5 Urinary albumin to creatinine ratio

Mouse Albumin ELISA Quantification Set (Bethyl, Montgomery, TX), and Creatinine Assay kit were used as per manufacturer's instructions. Mouse albumin is an indirect competitive ELISA designed to monitor urinary albumin. In the assay procedure, sample and rabbit anti-murine albumin capture antibody are added to albumin-coated wells. The antibody interacts and binds with the albumin immobilized to the stationary phase or with albumin in the fluid phase, hence the notion of competitive binding. Generally, albumin levels in urine samples from FSGS mice were quite high, therefore, urine samples were diluted 1000 times (receipt provided by the kit) before estimation. In short, primary antibody rabbit anti-murine albumin were added into the respective wells of an NUNC 96well maxisorbp (Sigma-Aldrich) plate (pH 9.6 carbonate-bicarbonate buffer 1:100) and incubated overnight at 4°C. The plate was washed 3 times (TRIS-NaCl 1x buffer+ 0.05% Tween 20). The coated plate was incubated for 1 hour at room temperature (RT) with blocking buffer (TRIS-NaCl 1times + BSA 1%) to reduce the aspecific bindings. The plate was washed 3 times. Diluted samples/standards were added and incubated at room temperature (RT) for 60 minutes. After incubation, each well was washed 3 times with wash buffer. Anti-rabbit HRP conjugated detection antibody) was added and the plate was incubated in dark for further 60 minutes. After HRP-conjugate incubation, each well was washed 3 times with wash buffer and incubates for 5-10 minutes in the dark at RT. TMB reagent (freshly prepared by mixing equal volumes of two substrate reagents) was added and incubated in dark until color reaction was completed followed by addition of 50µl stop solution (1N H_2SO_4). The absorbance was read at 450 nm within 10 minutes after adding the stop solution with an ELISA plate reader. The albumin content in each sample was determined using the equation of regression line generated by plotting absorbance of different standards against their known concentrations.

Urinary creatinine and plasma creatinine levels were measured using Jaffe´s enzymatic reaction using a Creatinine FS kit (DiaSys Diagnostic system, GmbH, Holzheim, Germany). Urine samples were diluted 10 times with distilled water. Different dilutions of the standard were

prepared using the stock provided with the kit. Working mono-reagent was prepared by mixing 4 parts of reagent 1 (R1) and 1 part of reagent 2 (R2) provided with the kit. Then, 10µl of each diluted sample and standard was added into a 96 well plate with a flat bottom (Nunc maxisorb plate). The mono-reagent (200µl) was added to each well, and immediately after 1 minute of incubation, the absorbance of the reaction mixture was measured at 492nm using an ELISA plate reader. This was repeated after 1 and 2 minutes of additional incubation. The change in absorbance (Δ A) was calculated as Δ A = [(A-2 – A-1) sample or standard] – [(A2 – A-1) blank]. And creatinine content of samples was calculated as Creatinine (mg/dl) = ΔA sample /ΔA standard * Concentration of standard (mg/dl)Urinary albumin to creatinine ratio was calculated after converting values for albumin and creatinine to similar units (mg/dl). Albumin content for each sample calculated (mg/dl) was divided by creatinine content (mg/dl) for the same sample.

3.6 Immunostaining and confocal imaging

All immunofluorescent studies were performed on five micrometer-thick frozen sections and analyzed with an LSM510 META laser confocal microscope (Carl Zeiss, Jena, Germany). Five µm thick frozen sections were cut and fixed in cold formalin (4% in PBS or Saline) for 20 minutes and washed for 5 minutes in PBS. Specific blocking buffer was prepared in PBS 1x+ 3% BSA+ diluted serum host of the secondary antibody and added. Sections were incubated for 30 minutes at room temperature. Afterwards, sections were incubated with diluted primary antibody for 15 minutes at 37°C followed by 1 hour at 4 °C. After washing for 5 minutes with PBS 1x, 200µl of the specific secondary antibody (diluted 1:1000) was added and the sections incubated for 30 minutes in the dark at room temperature. At the end of the incubation with the secondary antibody, the sections were washed for 5 minutes followed by the second staining performed as previously described. The nuclei staining were performed using DAPI or To-Pro-3 (1:1000 Life Technologies, Darmstadt, Germany). The following primary antibodies were used: pig anti-mouse nephrin (1:100, Acris Antibodies, Herford, Germany), rabbit anti-mouse WT-1 (1:25, Santa Cruz Biotechnology, Santa Cruz, CA), anti-rabbit CXCL12 (1:100; R&D, Minneapolis, MN), NICD-1 C-20 rabbit goat polyclonal IgG (1:10, Santa Cruz, USA), NICD3 rabbit polyclonal (1:10, ABCAM, UK), anti-SYN (mAb, G1D4, Progen, Heidelberg, Germany). H3-Ser10 (Cell Signaling, Danvers, MA), α-tubulin (Sigma-Aldrich). Secondary antibodies were obtained from Molecular Probes (Life Technologies, Monza, Italy) using different fluorochrome of the spectrum, 643, 544, 488nm. Immunofluorescent staining were evaluated using LSM 510 confocal microscope and LSM software (Carl Zeiss, Germany). Confocal microscopy was performed on 10µm sections of renal frozen tissues by using a Leica SP5 AOBS confocal microscope (Leica) equipped with a Chameleon Ultra-II two-photon laser (Coherent). Nuclei were counterstained with To-pro-3 (1:1000 Life Technologies) or DAPI (Life Technologies 1:1000). The degree of

glomerulosclerosis was assessed by observing 50 randomly selected glomeruli from each mouse kidney from PAS-stained kidney sections under a light microscope (Leitz DMR, Leica Microsystems, Bensheim, Germany). These glomeruli were then further classified as having no lesions, segmental lesions (<50 of glomerulus) or global lesions (>50% of glomerulus). Cellular crescents were assessed separately when more than a single layer of PECs was present around the inner circumference of BC.

3.7 Periodic acid-Schiff staining

For immunohistological studies one part of each kidney from each mouse was fixed in formalin (4% in PBS or Saline) overnight and processed using tissue processors (Leica) and paraffin blocks were prepared. 2µm thick paraffin-embedded sections were cut. De-paraffinization was carried out using xylene (3 * 5 minutes) followed by re-hydration by incubating the sections in 100% absolute ethanol (3 * 3 minutes), 95% ethanol (2 * 3 minutes) and 70% ethanol (1 * 3 minutes) followed by washing with distilled water (2 * 5 minutes). Rehydrated sections were incubated with Periodic acid (2% in distilled water) for 5 minutes followed by washing with distilled water for 5 minutes. Then sections were incubated with Schiff solution for 20 minutes at room temperature followed by washing with tap water for 7 minutes and counter staining with Hematoxylin solution (1* 2 minutes). This was followed by washing with tap water (1* 5 minutes) and finally sections were dipped in alcohol 90% and dried and closed with cover slips. For routine histology and morphometric analysis, 4µm sections were stained with the periodic acid-Schiff (PAS) reagent. For immunohistochemistry, sections were deparaffinized, rehydrated, transferred into citrate buffer, and either autoclaved or microwave-treated for antigen retrieval and processed as described (134). The frozen tissues were fixed in paraformaldehyde 4% for 2 hours, then 2 hours in 15% Sucrose/PBS1x solution and overnight in 30% Sucrose/PBS 1x solution at 4°C.

Table 2. Representative images of glomerular lesions

Score	Lesion in Glomeruli
No lesion (0)	None
Segmental Lesion (1)	≤ 50 %
Global Lesion (2)	≥ 50 %

All sections in each group were quantified as a percentage of glomeruli with each score (mean ± SEM).

3.8 Podocyte loss quantification

Podocyte quantification in *Pax2.rtTA;TetO.Cre;mT/mG* mice we quantified: 1) the percentage of podocyte loss (P) = 100 – mean of n° of total podocyte loss (green/blue + red/blue cells) at day 33 in proteinuric mice/mean of n° of total podocytes in healthy mice x 100; 2) the percentage of newly generated podocytes (P) = mean of n° of regenerated podocytes (red/blue new cells)/mean of n° of total podocytes at day 33 in proteinuric mice x 100 – mean of n° of regenerated podocytes (red/blue cells)/mean of n° of total podocytes in healthy x 100; 3) total percentage of lost podocytes (ablated podocytes, P) = P + Podocyte ablated and loss new. The percentage of regenerated podocytes over lost podocytes was thus = P /P x 100. Similar formulas were used in *Pax2.rtTA;TetO.Cre;mT/mG* mice, where podocytes were quantified as the number of SYN+ or WT-1+ cells per glomerular section in 15 glomeruli of at least four sections for each mouse counted by two independent observers.

3.9 Cell culture studies

Isolation and culture of human renal progenitors CD24+CD133+

RPCs were characterized and isolated from human renal biopsies as described (28, 45, 88, 135). In brief, kidney biopsies were processed and sieved for isolating glomeruli (60, 80, and 150 mesh). During this process, the glomeruli were separated from the tubules through graded mesh screening. To enrich the number of capsulated glomeruli, non-enzymatic digestion was performed. The glomerular suspension was collected and plated on fibronectin-coated dishes (10µg/ml; Sigma-Aldrich). After 4 to 5 days in culture, isolated glomeruli adhered to the plate resulting in cellular outgrowth. Glomeruli were detached, and the cellular outgrowth was cultured as a bulk. The cells were cultured with Endothelial Cell Growth Medium (EGM-MV) 20% FBS (Hyclone, Logan, UT) media and they were checked for simultaneous expression of the surface marker CD133 and CD24 by flow cytometer analysis. Generation of clones from CD24+CD133+ PECs was performed by limiting the dilution in fibronectin-coated 96-well plates in EGM-MV 20% FBS. $CD24^+CD133^+$ PECs were also maintained in culture as a bulk, and routine cell passaging was performed. All experiments were performed using cells at least at passage 3. Cells were grown at 37^0C supplied with 5% CO_2. Trypsin and EDTA (1:1 vol/vol) was used for splitting the cells. Cells were counted using a Neubauer chamber and the desired numbers of cells were used for experiments.

RPCs for RNA extraction were seeded at a density of $10x10^5$ cells/well in six-well plates in

Endothelial Cell Basal Medium (EBM) medium (LONZA, Basel, Switzerland) and grown overnight to the confluence. The cells were then incubated with 100nM human CXCL12 (Immunotools, Friesoythe, Germany), 1mg/ml NOX-A12 or revNOX-A12 and incubated at 37°C, 5% CO_2 for 24 hours. For the proliferation/ viability assays, the human RPCs were seeded in 96-well plates (8000 cells/well) and incubate at 37°C in EBM medium (LONZA). The RPCs were then incubated with 100nM CXCL12, NOX-A12 1mg/ml or revNOX-A12m (NOXXON), 10µM of the γ-secretase inhibitor IX DAPT (N-[N-(3,5-Difluorophenacetyl)-L-alanyl]-S-phenylglycine t-butyl ester) that was obtained from Merck, KGaA, Darmstadt, Germany or their combination for 24 hours and CellTiter 96 Non-Radioactive Cell Proliferation Assay (MTT assay) was performed (Promega, Madison, WI) according to the manufacturer's instructions. Experiments were performed in quintuplicate.

Differentiation of RPCs into podocytes

Human RPC differentiation toward podocytes were obtained as follow: RPCs were incubated in the podocyte differentiation medium VRAD (Dulbecco Eagle Modified Medium Ham f-12 (DMEM-F12)(LONZA) enriched with: 10% FBS (Hyclone), All-trans-retinoic acid (ATRA) 100µM (Sigma-Aldrich) and 100nM Vitamin D-3 (Sigma-Aldrich) incubation for 48 hours with 37°C and 5% CO_2 (27, 28, 135). During the differentiation, podocytes were incubated with: control EBM medium (LONZA), 10% Fetal Bovine serum (FBS) (Hyclone), VRAD medium with DMEM-F12 (Sigma-Aldrich) plus (All-trans retinoic acid, ATRA 100uM, Sigma-Aldrich) and 10µM Vitamin D3 (Sigma-Aldrich), 100nM CXCL12 (r-human, Immunotools, Friesoythe, Germany), NOX-A12 1mg/ml or revNOX-A12 or a combination of both. Total mRNA was isolated from the podocytes and analyzed for podocyte expression levels of the principal podocyte markers: nephrin, CD2AP and podocalyxin for the podocyte cytotoxicity assay, podocytes were obtained as described before, and incubated for 24 hours with: doxorubicin 10µM, CXCL12 100nM (Immunotools), NOXA-12 1mg/ml, revNOX-A12 1mg/ml and DAPT 10µM (Merck) or a combination of both. LDH assay was performed (Roche, Switzerland) according to the manufacturer's instructions. Experiments were performed in quintuplicate.

Preparation of necrotic supernatants from podocytes

For the podocyte necrotic supernatant (NS) proliferation assay, 2500cells/ml podocytes were obtained as described before and 3 cycles of heating from -80°C to 60°C in DMEM F-12 medium (Sigma-Aldrich) were performed to get NS. Human RPCs were incubated for 24 hours with: 30µL/mL NS plus 1mg/ml NOX-A12, revNOXA-12 or CXCL12 100nM and DAPT 10µM (Merck). MTT assay was performed (Promega) according to the manufacturer's instructions. Experiments were

performed in quintuplicate. For the podocyte cytotoxicity assay, podocytes were obtained as described before and incubated for 24 hours with: doxorubicin 10µM, CXCL12 100nM (Immunotools), NOXA-12 1mg/ml, revNOX-A12 1mg/ml and DAPT 10µM (Merck) or a combination of both. LDH assay was performed (Roche, Switzerland) according to the manufacturer's instructions. MTT assay was performed (Promega, Madison, WI) according to the manufacturer's instructions. Experiments were performed in quintuplicate.

Cell freezing and thawing

At earlier passages large amounts of cells were grown under standard culture conditions and were frozen for future use. Cells to be frozen were detached from the culture plates and counted using the Neubauer's chamber. One million (10^6) cells were centrifuged under sterile conditions for 5 minutes at 1000 rpm. The cell pellet was maintained on ice and carefully re-suspended in cold freezing medium (90% respective culture medium and 10% DMSO) by pipetting the suspension repeatedly up and down. One ml aliquots were quickly dispensed into freezing vials. The cells were located in the freezing chamber at -80^0C overnight. The next day, all aliquots were transferred to liquid nitrogen. In order to thaw cells, a frozen vial was removed from liquid nitrogen and put into a water bath at 37^0C for 5 minutes. The cells were then resuspended in 10ml of warm complete growth medium and transferred into new culture plates. After 12 hours, cells were observed under the microscope and the medium was changed once more

3.10 Protein isolation and western blotting

Protein from kidney tissues as well as cells were extracted using lysis buffer (Tris-HCl 50mM, NaCl 150mM, sodium orthovanadate 100µM, sodium deoxycholate 0.5%, NP40 4%, Triton X-100 2%, EDTA 5mM, sucrose 300mM, and Roche protease inhibitors). Total cellular extracts were prepared in protein lysis buffer (Tris 10mM, NaCl 10mM, ethylenediaminetetraacetic acid 10mM, HEPES 1mol/l, glycerol 20%, MgCl2 1 mol/l, dithiothreitol 1mol/l, Triton, 10% sodium fluoride 1mol/l, and Roche protease inhibitors). After determination of protein concentrations, 50µg of the kidney protein or 10µg of protein extracted from cells was mixed with 5 × sodium dodecyl sulfate loading buffer (100mmol/l Tris-HCl, 4% sodium dodecyl sulfate, 20% glycerol, and 0.2% bromophenol blue) for western blot analysis. Samples were heated at 95°C for 5 minutes. Proteins were separated by sodium dodecyl sulfate-polyacrylamide gel electrophoresis and then transferred to a polyvinylidene difluoride membrane. Nonspecific binding to the membrane was blocked for 1 hour at room temperature with 5% bovine serum albumin in tris-buffered saline buffer (20mmol/l Tris-HCl, 150mmol/l NaCl, and 0.1% Tween 20). The membranes were incubated overnight at 4°C with primary antibodies, goat antibody against mouse NICD1, NICD2 and, NICD3 (ABCAM, UK) and rabbit

antibody against ß actin (Cell signaling). Secondary antibodies were a peroxidase-conjugated donkey anti-goat IgG (Dianova, Hamburg, Germany) and an anti-rabbit IgG (Cell signaling, and β-actin (Cell signaling), followed by incubation with the secondary antibody anti-biotin or anti-rabbit IgG labeled with HRP. Immunostained bands were detected.

3.11 RNA isolation from cells and tissue

At the end of the experiment, cells were harvested under sterile conditions for RNA isolation. Immediately after kidney isolation, a small piece of a kidney from each mouse was preserved in RNA-later (Ambion, CA, USA) and stored at -20^{0}C until processed for RNA isolation. RNA isolation was performed using RNA isolation kit from Ambion according to the protocol provided. The harvested cells were washed two times with sterile PBS and centrifuged. The supernatant was discarded and the pellet was resuspended in 350µl lysis buffer containing 10µg/ml beta-mercaptoethanol and frozen at –80 °C until RNA isolation. Tissues (30mg) preserved in RNA-later were homogenized using a blade homogenizer for 30 seconds at 4°C in lysis buffer (600µl) containing β-mercaptoethanol (10µl/ml). During RNA isolation, the samples were thawed and 350µl of 70% ethanol diluted in 1% diethyl pyrocarbonate-treated water (DEPC water) was added to the samples and mixed well. This mixture was then loaded onto RNeasy mini columns held in 2ml collection tubes and centrifuged at 12000 g for 15 seconds. The flow-through was discarded and the columns were loaded with 700µl of Wash buffer I and centrifuged at 12000 g for 15 seconds. The collection tubes were discarded together with the flow-through and the columns were transferred to fresh 2ml collection tubes. 500µl of Wash Buffer II was pipetted onto the column and centrifuged at 12000 xg for 15 seconds, and the flow-through was discarded. This step was repeated and the column was rendered dry by centrifugation and placed into a 1.5ml fresh collection tube. Then, 40µl of RNase-free water was pipetted directly on the silica-gel membrane and was centrifuged to collect the RNA solution. Isolated RNA was measured, checked for purity and stored at -80^{0}C.

RNA quantification and purity check

The isolated RNA samples were quantified using a Nanodrop (PEQLAB Biotechnology GMBH, Erlangen, Germany). The ratio of optical densities at 260 nm and 280 nm is an indicator for RNA purity (indicative of protein contamination in the RNA samples). Only samples with a ratio of 1.8 or more were considered to be of acceptable quality.

3.12 cDNA synthesis and real-time PCR

The RNA samples, isolated according to procedures described above, were processed for cDNA conversion using reverse transcriptase II (Invitrogen, Karlsruhe, Germany). RNA samples were diluted in DEPC water to a concentration of 2µg / 30µl. A master mix was prepared with the following reagents: 9µl of 5 x buffer (Invitrogen, Karlsruhe, Germany), 1µl of 25mM dNTP mixture (Amersham Pharmacia Biotech, Freiburg, Germany), 2µl of 0.1M DTT (Invitrogen, Karlsruhe, Germany), 1µl of 40U/µl RNasin (Promega, Mannheim, Germany), 0.5µl of 15µg/ml linear acrylamide (Ambion Ltd, 36 Cambridgeshire, UK), 0.5 µl of Hexanucleotide (Roche, Mannheim, Germany), 1µl of Superscript (Invitrogen, Karlsruhe, Germany) or ddH2O as a control. The master mix was made to a volume of 13.2µl and added to 1µg / 20µl RNA samples were taken in separate DEPC treated microcentrifuge tubes, which were mixed and placed at 42°C on a thermal shaker incubator for 1 hour. After 1 hour, the cDNA samples were collected and placed at -20°C until use for RT-PCR analysis. The cDNA samples prepared as described above were diluted 1:10 for real-time polymerase-chain-reaction (RT-PCR). Two µl of diluted cDNA samples was mixed with SYBR green master mix (10µl), forward primer (0.6µl) and, reverse primer (0.6µl), both specific for the gene of interest, Taq polymerase (0.16µl) and distilled water (6.64µl). The RT-PCR was performed using Light Cycler480. Pre-incubation was carried out for 5 minutes at 95^0C to activate the polymerase and complete denaturation of cDNA samples. cDNA was amplified for 45 cycles, each comprising of 15 seconds incubation at 95^0C and 45 seconds incubation at 60^0C. The melting curve was set for initial 95^0C for 5 seconds followed by 65^0C for 1 minute with continuous heating. The RT-PCR of the reference gene (18S rRNA) was carried out under similar conditions. The CT values were calculated using the Light Cycler480 and the results were normalized with respect to the reference gene expression. In all cases controls consisting of ddH2O were negative for target or reference genes. All designed SYBR green primers for all genes evaluated were obtained from Metabion (Metabion, Martinsried, Germany).

3.13 Statistical analysis

Data are presented as mean ± SEM. A comparison of groups was performed using paired Mann-Withney U to compare two groups or one-way ANOVA with posthoc Bonferroni`s correction was used for multiple comparisons. A value of $p < 0.05$ was considered to indicate statistical significance.

Table 3. Human Primers for RT

Target	Primer sequence	
Notch-1	Forward Primer 5'-3'	**GTGAACTGCTCTGAGGAGATC**
	Reverse Primer 5'-3'	**GGATTGCAGTCGTCCACGTTGA**
Notch-2	Forward Primer 5'-3'	**GTGCCTATGTCCATCTGGATGG**
	Reverse Primer 5'-3'	**AGACACCTGAGTGCTGGCACAA**
Notch-3	Forward Primer 5'-3'	**TACTGGTAGCCACTGTGAGCAG**
	Reverse Primer 5'-3'	**CAGTTATCACCATTGTAGCCAGG**
Dll-1	Forward Primer 5'-3'	**TGCCTGGATGTGATGAGCAGCA**
	Reverse Primer 5'-3'	**ACAGCCTGGATAGCGGATACAC**
Jag-1	Forward Primer 5'-3'	**TGCTACAACCGTGCCAGTGACT**
	Reverse Primer 5'-3'	**TCAGGTGTGTCGTTGGAAGCCA**
Jag-2	Forward Primer 5'-3'	**GCTGCTACGACCTGGTCAATGA**
	Reverse Primer 5'-3'	**AGGTGTAGGCATCGCACTGGAA**
Hey-1	Forward Primer 5'-3'	**TGTCTGAGCTGAGAAGGCTGGT**
	Reverse Primer 5'-3'	**TTCAGGTGATCCACGGTCATCTG**
Hes-1	Forward Primer 5'-3'	**GGAAATGACAGTGAAGCACCTCC**
	Reverse Primer 5'-3'	**GAAGCGGGTCACCTCGTTCATG**
Nephrin	Forward Primer 5'-3'	**GTCTGCACTGTCGATGCCAATC**
	Reverse Primer 5'-3'	**CCAGTTTGGCATGGTGAATCCG**
Podocin	Forward Primer 5'-3'	**CTGTGAGTGGCTTCTTGTCCTC**
	Reverse Primer 5'-3'	**CCTTTGGCTCTTCCAGGAAGCA**
Podocalyxin	Forward Primer 5'-3'	**CCTGAACCTCACAGGAAACACC**
	Reverse Primer 5'-3'	**TGGAACAGATGCCAGCCGTATG**
CD2AP	Forward Primer 5'-3'	**CCAAAGCCTGAACTGATAGCTGC**
	Reverse Primer 5'-3'	**GGACTTGTGGAGCTGCTGGTTT**
18s	Forward Primer 5'-3'	**GCAATTATTCCCCATGAACG**
	Reverse Primer 5'-3'	**AGGGCCTCACTAAACCATCC**

List of abbreviations sees Abbreviations section 9

Table 4. Murine Primers for RT

Target	Primer sequence	
Notch-1	Forward Primer 5'-3'	**GCTGCCTCTTTGATGGCTTCGA**
	Reverse Primer 5'-3'	**CACATTCGGCACTGTTACAGCC**
Notch-2	Forward Primer 5'-3'	**CCACCTGCAATGACTTCATCGG**
	Reverse Primer 5'-3'	**TCGATGCAGGTGCCTCCATTCT**
Notch-3	Forward Primer 5'-3'	**GGTAGTCACTGTGAACACGAGG**
	Reverse Primer 5'-3'	**CAACTGTCACCAGCATAGCCAG**
Dll-1	Forward Primer 5'-3'	**GCTGGAAGTAGATGAGTGTGCTC**
	Reverse Primer 5'-3'	**CACAGACCTTGCCATAGAAGCC**
Jag-1	Forward Primer 5'-3'	**TGCGTGGTCAATGGAGACTCCT**
	Reverse Primer 5'-3'	**TCGCACCGATACCAGTTGTCTC**
Jag-2	Forward Primer 5'-3'	**CGCTGCTATGACCTGGTCAATG**
	Reverse Primer 5'-3'	**TGTAGGCGTCACACTGGAACTC**
Hey-1	Forward Primer 5'-3'	**CCAACGACATCGTCCCAGGTTT**
	Reverse Primer 5'-3'	**CTGCTTCTCAAAGGCACTGGGT**
Hes-1	Forward Primer 5'-3'	**GGAAATGACTGTGAAGCACCTCC**
	Reverse Primer 5'-3'	**GAAGCGGGTCACCTCGTTCATG**
Nephrin	Forward Primer 5'-3'	**CAGCGAAGGTCATAAGGGTC**
	Reverse Primer 5'-3'	**CACCTGTATGACGAGGTGGA**
Podocin	Forward Primer 5'-3'	**CAGGAAGCAGATGTCCCAGT**
	Reverse Primer 5'-3'	**TGACGTTCCCTTTTTCCATC**
CD2AP	Forward Primer 5'-3'	**CATCCCTCGTCTCCCATTTA**
	Reverse Primer 5'-3'	**TATCCGAGTTGGGGAAATCA**
Synaptopodin	Forward Primer 5'-3'	**GCCAGGGACCAGCCAGATA**
	Reverse Primer 5'-3'	**AGGAGCCCAGGCCTTCTCT**
WT-1	Forward Primer 5'-3'	**GGTTTTCTCGCTCAGACCAGCT**
	Reverse Primer 5'-3'	**ATGAGTCCTGGTGTGGGTCTTC**
18s	Forward Primer 5'-3'	**GCAATTATTCCCCATGAACG**
	Reverse Primer 5'-3'	**AGGGCCTCACTAAACCATCC**

List of abbreviations sees Abbreviations section 9 (Notch primers Niranjan T et al 2010)

4. Results

4.1.Effects of podocyte-derived CXCL12 in a mouse model of specific podocyte depletion

4.1.1. CXCL12 is a podocyte survival factor during a specific podocyte depletion model

To answer the specific question about CXCL12 and podocyte survival we used specific podocyte depletion system *NPHS2/rtTa-tetO-CMV/iCre/iDTR/TomatoRed* (*Podocin*-iDTR/mT/mG) mice were obtained from our collaborator in Freiburg (132) that have a fluorescent reporter system endogenous green florescent protein(green)/endogenous red florescent protein(red) meaning that all podocytes express the human diphtheria toxin receptor (DTR) on their cell membrane after pre-stimulation with the antibiotic doxycycline (methods section 2.2). Figure 15A illustrates a representative confocal microscopy image of a healthy doxycycline-induced *Podocin*-iDTR/mT/mG mouse to test the model efficiency (genome cartoon). After doxycycline-induced expression of the DTR, mice received a single injection of the human diphtheria toxin (DT) to induce podocyte depletion by DT toxicity followed by Diphtheria toxin nephropathy. Immediately after the induction of the disease, *Podocin*-iDTR/mT/mG mice were treated with the CXCL12 inhibitor NOX-A12 or the control compound revNOX-A12. (see methods part 2.2). The urinary albumin /creatinine ratio (UACR) showed a significant progression of the disease in mice that were treated with the CXCL12 inhibitor compared to the inhibitor control (Figure 15B). Following blockade of CXCL12, blood urea nitrogen and creatinine levels were also significantly increased in *Podocin*-iDTR/mT/mG mice (Figure 15C) indicating that CXCL12 acts as a survival factor for podocytes during Diphtheria toxin nephropathy.

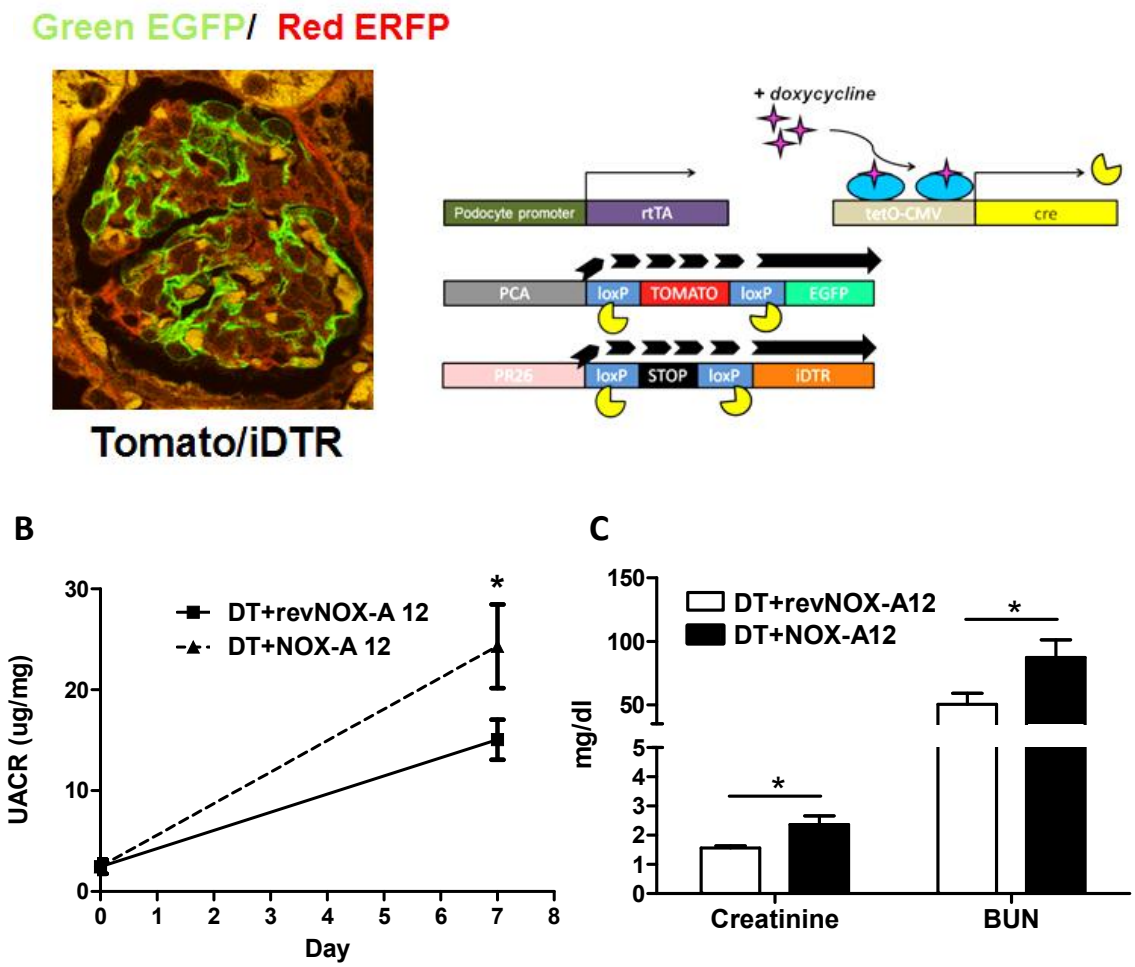

Figure 15. CXCL12 is blocked aggravates Diphtheria toxin nephropathy. *NHP2rtTA/Tet-ON-iCRE/ iDTR/mG/mG* mice were induced to Diphtheria toxin nephropathy as described in methods section 2.2). Two groups of mice CXCL12 inhibitor NOX-A12) or control revNOX-A12 from day 0 until day 7. (**A**) Schematic of the genetic model of *Podocin*-iDTR/mT/mG mouse model of diphtheria toxin nephropathy and a representative IF of an induced mouse to check the efficiency of the system. (**B, C)** CXCL12 blockade increased UACR **(B)**, BUN and creatinine **(C)** in the Diphtheria toxin nephropathy compared to the control group. The data are means ± SEM from 6-7 animals per NOX-A12 group. *p<0.05 versus revNOX-A12 group.

4.1.2. CXCL12 blockade aggravates diphtheria toxin-induced nephropathy renal pathology

Next, we performed PAS staining on kidney sections to displayed the histopathology score. As illustrated in Figure 16A, NOX-A12 treatment increased the glomerular sclerosis score was aggravated compared to the control group after 7 days. In particular, the percentage of global glomerular lesions increased when CXCL12 was inhibited, whereas the quantity of normal glomeruli and glomeruli with segmental lesions was reduced (Figure 16B).

A

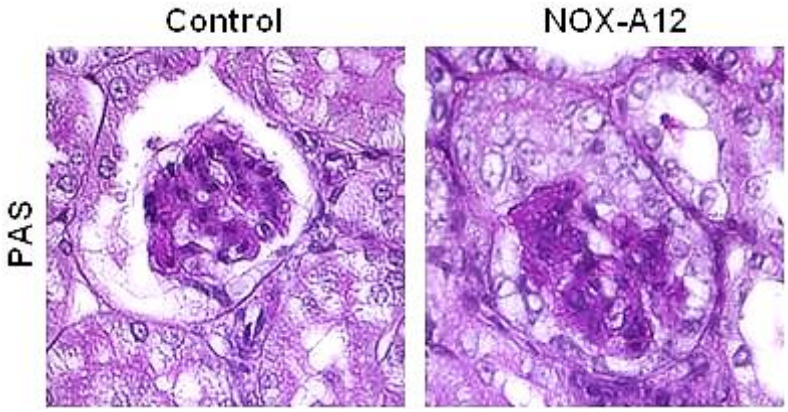

B

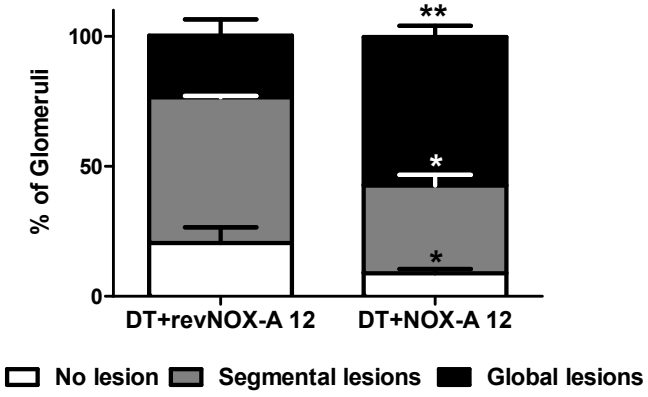

Figure 16: CXCL12 blockade increases the severity of Diphtheria toxin nephropathy. (**A**) Representative pictures of PAS- stained kidney sections in the DTN mouse model after CXCL12 blockade**.** (**B**) The glomerular injury score showed worsening of glomerular injury when CXCL12 was blocked compared to control. CXCL12 blockade significantly increased the number of global glomerular lesions on day 7 during Diphtheria toxin nephropathy compared to the control group. The data are means ± SEM from 6-7 animals in each NOX-A12 group, *p<0.05, **p<0.01 versus revNOX-A12group at day 7. Original magnification 400x.

4.1.3. Podocyte numbers decreased after CXCL12 blockade in Diphtheria toxin nephropathy

To determine the podocyte score I performed at the end of the study, IF staining for Nephrin/WT-1. The results showed that during Diphteria toxin nephropathy, inhibition of CXCL12 reduced the number of podocytes compared to control (Figure 17B). The decreased number of podocytes was associated with decreased levels of total kidney mRNA for the podocyte-specific markers *Nephrin, Podocin, Synaptopodin* and *CD2AP* after NOX-A12 treatment during DTN (Figure 17B).

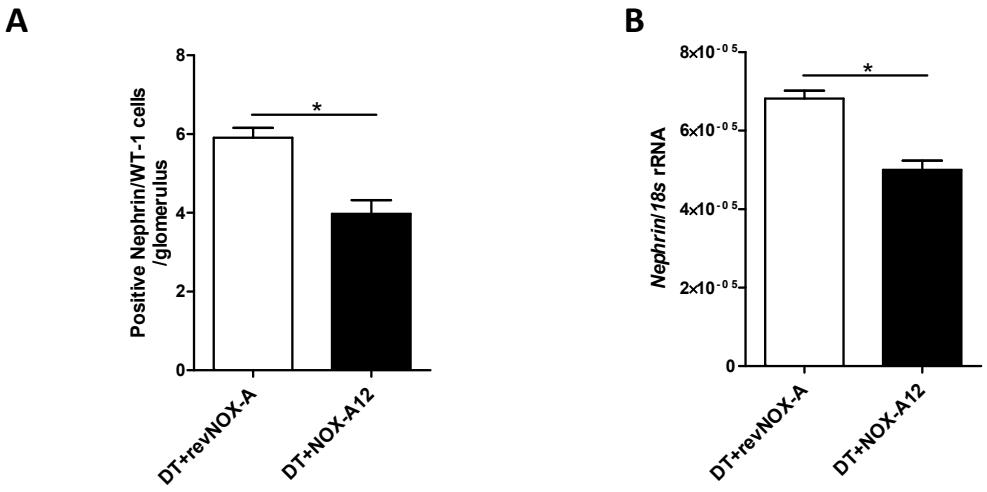

Figure 17. Podocyte evaluation of Diphtheria toxin nephropathy. (**A**) CXCL12 blockade decreased the total number of Nephrin/WT-1 double positive cells per glomerulus on day 7 during Diphtheria toxin nephropathy compared to control revNOX-A12. (**B**) Blockade of CXCL12 in diphtheria toxin nephropathy reduced nephrin renal mRNA levels in the kidney. The data are means ± SEM from 6-7 animals in each NOX-12 treated group, *p<0.05 versus revNOX-A12 group at day 7.

Finally, I determined the impact of the CXCL12 blockade on the survival of *Podocin*-iDTR/iDTR mice, which were in homozygosis for the iDTR during Diphtheria toxin nephropathy. As shown in Figure 18, we observed a significant difference in the survival Kaplan-Maier analysis (Figure 18A) on day 2 after Diphtheria toxin nephropathy onset was observed. During the first 2 days, more than 60% of the NOX-A12-treated *Podocin*-iDTR/iDTR mice died, whereas 40% of the remaining mice survived until sacrifice on day 7. These data indicate that *Podocin*-iDTR/iDTR mice in homozygosis loss more podocytes (more than 50%) after a single diphtheria injection compared to *Podocin*-iDTR/mT/mG mice and that these mice were much more susceptible to Diphtheria toxin nephropathy in combination with the CXCL12 blockade. Together, the data suggests that CXCL12 produced by podocytes acts as an autocrine survival factor during glomerular injury.

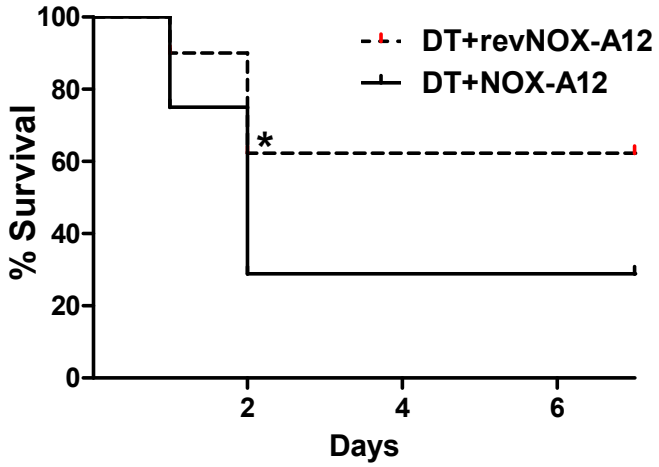

Figure 18: Kaplan-Meier in *Podocin*-iDTR/iDTR mouse model of Diphtheria toxin nephropathy. In a homozygote *Podocin*-iDTR/iDTR mouse, I induced with diphtheria toxin injection a Diphtheria toxin nephropathy-DTN, CXCL12 blockade decreased the survival ratio more the 60% in the NOX-A12 group at day 2 during Diphtheria toxin nephropathy compare to the control revNOX-A12. The data are means ± SEM from 10-13 animals in each NOX-A12 group, *p<0.05 versus revNOX-A12 at day 2.

4.2.CXCL12 is a podocyte survival factor by reduces mitotic catastrophe

To further investigate the role of CXCL12 as podocyte survival factor, firstly human RPC-derived podocytes were challenged *in-vitro* with the well-known death stimulus ADR in the presence of NOX-A12 or revNOX-A12. Secondly, to mimic the *in-vitro* system, we used a mouse model *of* ADR podocyte depletion.

CXCL12 acts as a podocyte survival factor during adriamycin-induced cell death

RPCs were differentiated into podocytes using VRAD medium for 48 hours as described in the methods. Following differentiation, RPCs were stimulated with ADR, a well-known podocyte cytotoxic drug, for 24 hours and measured the cytotoxic effect of ADR on podocytes using a photometric lactate dehydrogenase (LDH) assay. After establishing the optimal concentration of ADR for the LDH assay *in-vitro*, the CXCL12 podocytes pro-survival effect was investigated. Human RPCs were differentiated into podocytes in the presence of VRAD medium prior to the treatment with 10µM ADR. As demonstrated in Figure 19B, ADR induced cell death in podocytes; however, this cytotoxic effect was significantly decreased following stimulation with CXCL12. Upon blockade of CXCL12 using the NOX-A12 spiegelmer, the cytotoxic effect of ADR on podocytes was reversed compared to control revNOX-A12. Taken together, CXCL12 was identified as an autocrine survival factor for podocytes.

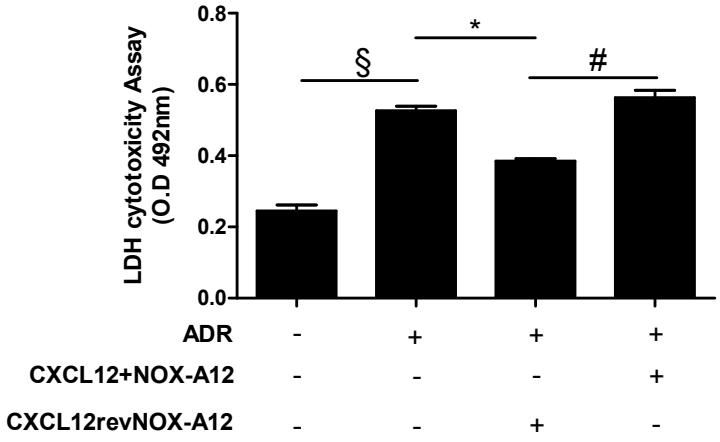

Figure 19: Adriamycin induced podocyte death can be reduced by CXCL12 treatment *in-vitro*. Treatment with CXCL12 significantly reduced ADR cytotoxicity; CXCL12 blockade by NOX-A12 restored this cytotoxic effect of ADR on podocytes. This data suggested that CXCL12 was a survival factor for podocytes. Data are means ± SEM 2-3 experiments, (§ $p<0.01$ normal podocyte versus ADR treatment), (* $p<0.05$ ADR treated podocyte versus ADR+CXCL12),(# $p<0.05$ ADR+CXCL12+NOX-A12 versus revNOX-A12 treated group) after 24h.

4.2.1. CXCL12 acts as a podocyte survival factor during adriamycin-induced catastrophic mitotic cell death

The functional significance of the constitutive release of CXCL12 by podocytes is still not fully clear. This raises the question of how CXCL12 acts as a survival factor for podocytes. Reports by *Lasagni et al.* and *Mulay et al,* (42, 64, 136) have shown that after an ADR-induced podocyte injury, podocytes detach or die via catastrophic mitosis (CM). Further work has reported an involvement of the Notch signaling pathway in CM activation(64). However, the role of CXCL12 during podocyte CM has not been investigated before; therefore, human podocytes were exposed to ADR with or without CXCL12 in the presence of either the active or inactive CXCL12 inhibitor. Moreover, the Notch inhibitor DAPT was used as a control. IF staining was performed to study the catastrophe mitosis (CM). CM was assessed by a double IF of histone H3 Serine 10 phosphorylated (H3-Ser10) a maker of CM activation (green), α-tubulin as a cytoskeleton integrity marker (red) and the chromatin-nuclear staining To-pro-3 (blue) (Figure 20). As illustrated in Figure 20-panel 1, human RPC showed a normal mitotic spindle and well-divided chromosomes. Mature podocytes, on the other hand, did not proliferate (Figure 20-panel 2), only when ADR was added into the medium and aberrant chromosomal division occurred (Figure 20-panel 3). Interestingly, following the addition of CXCL12 into the medium prevented such aberrant nuclear divisions(Figure 20-panel 4). Upon CXCL12 blockade using NOX-A12, CM started again in comparison to the control inhibitor (Figure 20-panel 5-

6). As expected, inhibition of Notch signaling with DAPT restored the normal podocyte structure (Figure 20-panel 7). However, combined treatment of DAPT and CXCL12 had no additive effect on CM (Figure 20-panel 8) as well as adding the CXCL12 inhibitor and control revNOX-A12 alone had no effect on preventing cathastrophic mitosis (Figure 20-panel 9-10). This data indicated that CXCL12 inhibition accelerated the podocytes loss via catastophic mitosis. Thus, intrinsic CXCL12 is a podocyte survival factor during toxic injury-induced CM of podocytes.

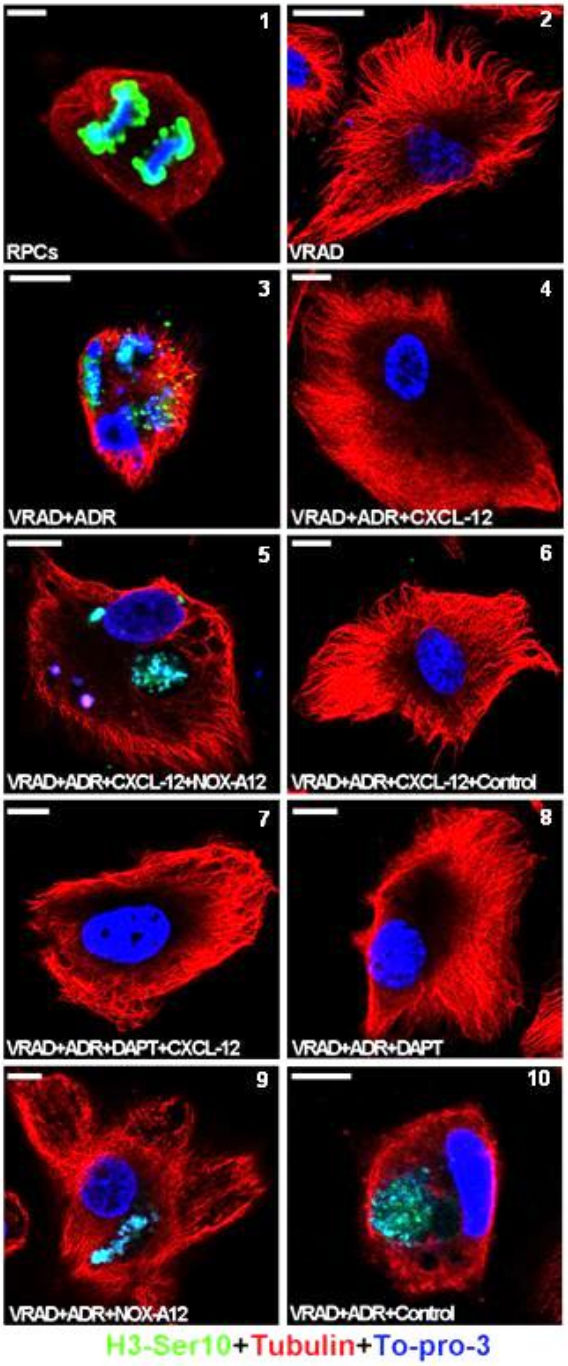

Figure 20. CXCL12 reduces catastrophic mitosis *in-vitro*. Immunostaining of podocytes for H3-Ser10 in green. Tubulin staining marks the mitotic spindle in red. To-pro-3 marks the chromatin in blue. Note that RPCs proliferate by forming normal mitotic spindles and appropriate chromosomal alignment in the anaphase plate in between the spindles (control) (**1**). Mature podocytes (**2**) do not proliferate in culture but ADR induced aberrant chromosomal division and mitotic catastrophe leading to cell death (**3**). This process is inhibited by CXCL12 (**4**). CXCL12 blockade induced CM (**5**) compared with the control inhibitor treatment (**6**). Podocytes were protected from CM in the presence of the Notch pathway inhibitor DAPT (**8**). The combination of CXCL12 and DAPT had no additive effects on CM (**8**). Treatment of NOX-A12 and revNOX-A12 had no protective effects on CM (**9-10**). Representative images, original magnification 1000x (scale bar 10µm).

4.3. The effect of CXCL12 during a murine model of Adriamycin-induced nephropathy

In this section, I used a Balb/c mouse model of FSGS to investigate the effect of podocyte's derived CXCL12. FSGS can be pharmacologically induced via ADR tail vein injection (see methods 2.2). The disease developed within a few days after the induction of AN. This model was reliable, fast and the injury could be modulated in a dose-dependent manner.

4.3.1. Podocytes are the major source of CXCL12 during focal segmental glomerular sclerosis

In the past *Darisipudi et al.* (82) showed that during diabetic nephropathy, podocytes were the main source of CXCL12. Human podocytes were obtained from RPCs and IF staining was performed for the podocyte marker WT-1 (red), CXCL12 (green), and the blue nuclear marker DAPI (Figure 21A). The staining clearly showed that CXCL12 was produced from the podocytes (WT-1 and DAPI co-stained, which appears as violet). To further identify the source of CXCL12 during AN, we performed an immune-staining for CXCL12 from kidneys of ADR-treated and non-treated (healthy) mice. Podocytes were positive for CXCL12 in the glomerulus even under healthy conditions (Figure 21A). During AN, podocytes expressed CXCL12 after 7 and 14 days, as shown in Figure 21B. IF co-staining showed that CXCL12 was mainly expressed in the cytosol of podocytes, whereas podocytes stained positively stained for WT-1 in the nucleus (Figure 21C).

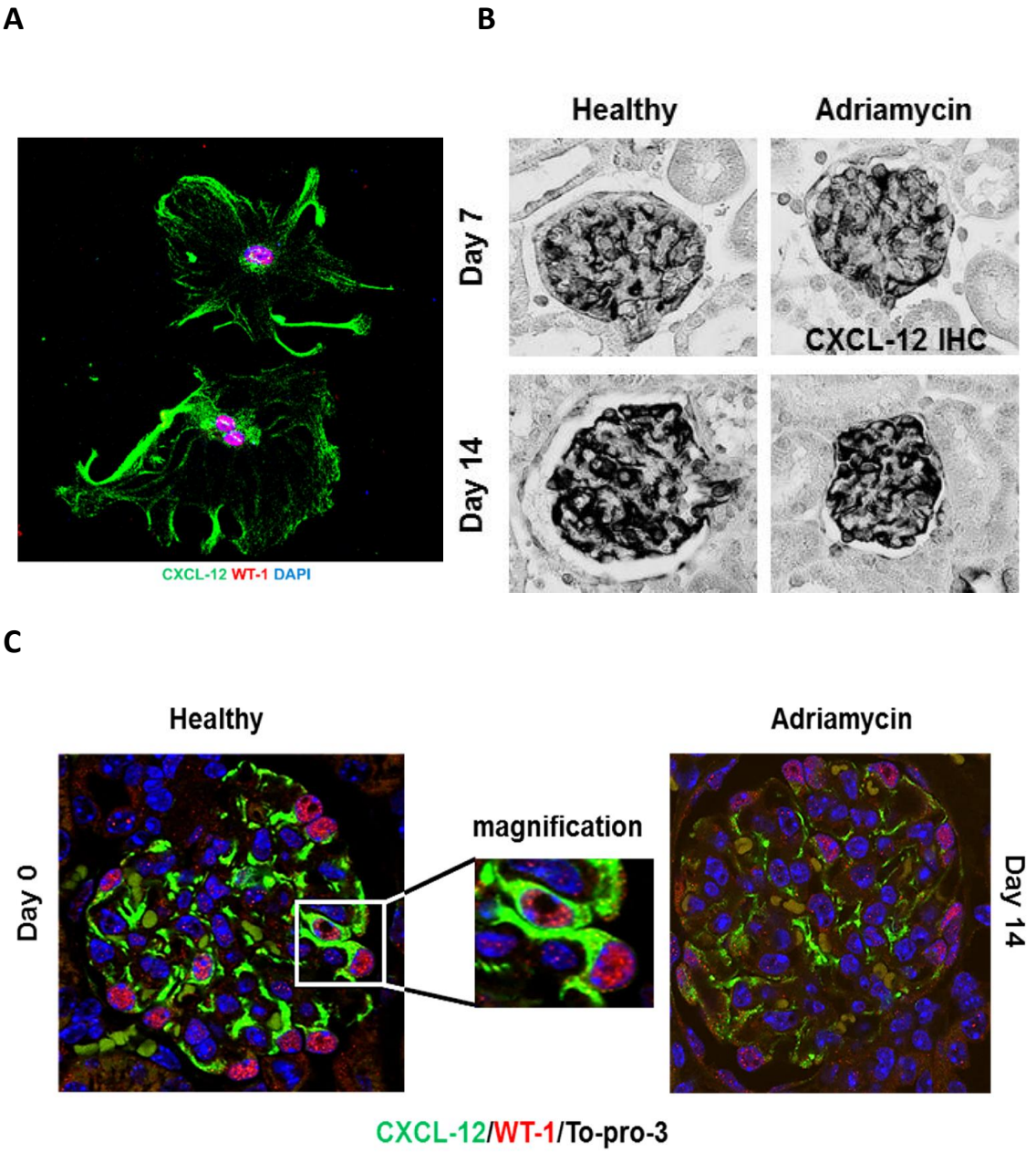

Figure 21. CXCL12 is produced by podocytes. (**A**) RPCs derived podocyte IF staining: (red) WT-1, (Blue) DAPI, (green) CXCL12 IF (**B**) Using IHC staining for CXCL12 we showed CXCL12 production by podocytes in healthy and AN kidneys after 7 and 14 days. (**C**) Glomerular immune-fluorescent (IF) co-staining for CXCL12 (green) and WT-1 (red) and blue nuclei (To-pro-3) showed that CXCL12 was expressed in the cytosol of podocytes in healthy and ADR-injured mice. Representative images, the original magnification of **A** is 600x, **B** is 400x and **C** high magnification 600x.

4.3.2. Urine Albumin/Creatinine ratio and blood urea level in Adriamycin nephropathy

During AN, the loss of podocytes was associated with UACR. After injecting mice with ADR, the UACR significantly increased on day 7 and 14 compared to control -treated healthy mice (Figure 22A). As a consequence of AN, also, the BUN significantly increased on day 14 compared to control mice indicating a compromised excretory function of the kidney (Figure 22B).

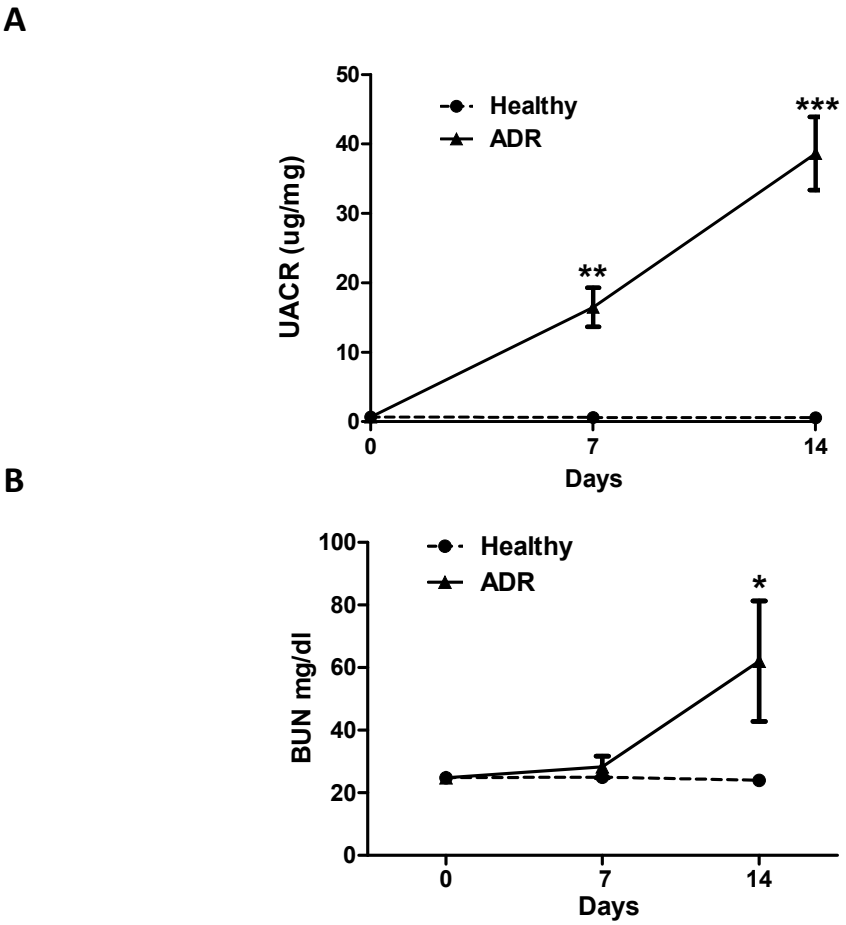

Figure 22. Characterization Adriamycin nephropathy mouse model. Wild-type Balb/c mice received an intravenous injection of ADR (13.4mg/kg) to induce AN or PBS only as control and urine was collected on day 7 and 14. (**A**) ADR induced an aggravation of kidney injury as demonstrated by increased urine albumin/creatinine ratio on day 7 and 14 during AN compared to healthy control group. (**B**) Plasma levels of urea (BUN) showed an evident increment at day 14 in the ADR group compared to PBS control. The data are means ± SEM from 6-7 animals per healthy group*p<0.05, **p<0.01, *** p<0.001 versus ADR group at day 7 and 14.

To further confirm the UACR data, I determined renal histomorphology after AN on day 7 and 14. ADR injection induced a strong glomerulosclerosis in the kidney as demonstrated by PAS staining, in Figure 23A, and more segmental and global lesions were found in the ADR-treated mice compared to the healthy controls (Figure 23B). Thus, glomerular lesion score correlates with the loss

of podocytes following ADR treatment and the lesions are the major cause of the functional loss of the kidney.

A

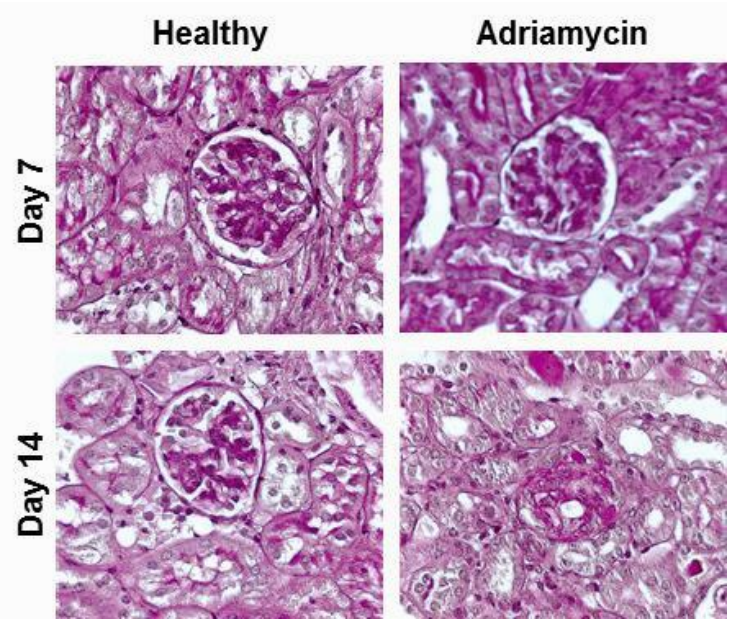

B

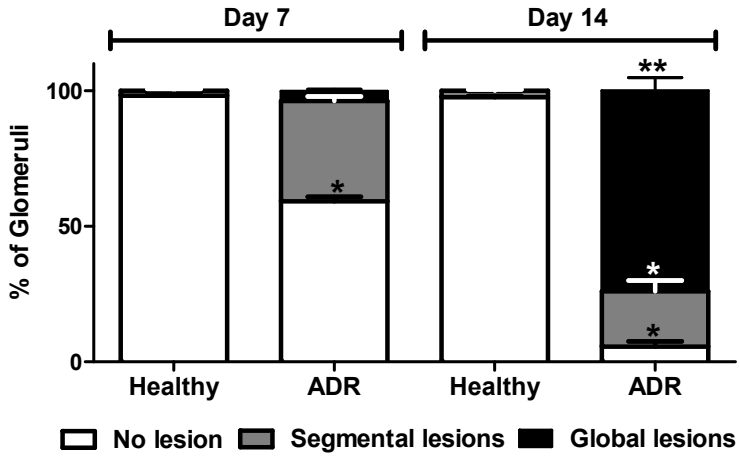

Figure 23. Renal histopathology of Balb/cAncrl mice with Adriamycin nephropathy. Mice were injected with ADR for 7 and 14 days and (**A**) PAS staining of the kidney sections carried out. (**B**) Segmental and global glomerular lesions were determined on day 14 during AN compared to control. The data are means ± SEM from 6-7 animals per healthy group. *p<0.05, **p<0.01, versus ADR group at day 7 and 14. Original magnification 400x.

4.3.3. Podocyte loss in adriamycin-induced focal segmental glomerular sclerosis

ADR induced a reduction in the number of podocytes in the glomerulus. We performed an IF staining for the podocyte markers nephrin and WT-1. Also, I evaluated the staining with a semi-quantitative analysis. The number of double positive cells (nephrin/WT-1) was significantly reduced after ADR injection compared to the control (Figure 24A). The loss of podocytes was a major feature during AN resulting in the severe loss of kidney functions.

A

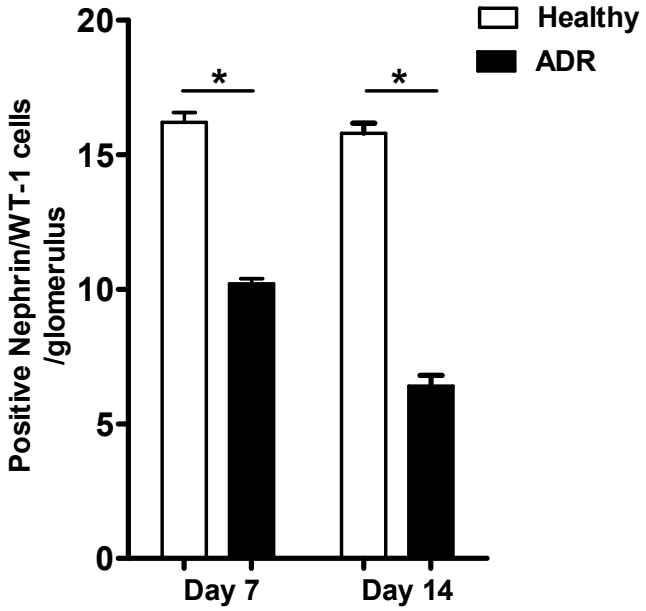

Figure 24. Quantification of podocytes in Balb/cAncrl mice during Adriamycin nephropathy. ADR treatment caused a reduction in the number of podocytes in the glomeruli on day 7 and 14 compared to the healthy group. The data are means ± SEM from 6-7 animals per healthy group. (*p<0.05, **p<0.01, healthy mice group versus ADR group) at day 7 and 14.

Renal mRNA expression levels of podocyte markers in total kidney during Adriamycin nephropathy

To confirm the loss of podocytes during AN, mRNA expression levels of the classical podocyte markers in the kidneys were determined. In the ADR-treated group, a significant reduction in the mRNA expression levels of the podocyte markers was found, e.g.: *Nephrin, Podocin, Synaptopodin* and *CD2AP* on day 7 and 14 compared to the healthy controls (Figure 25).

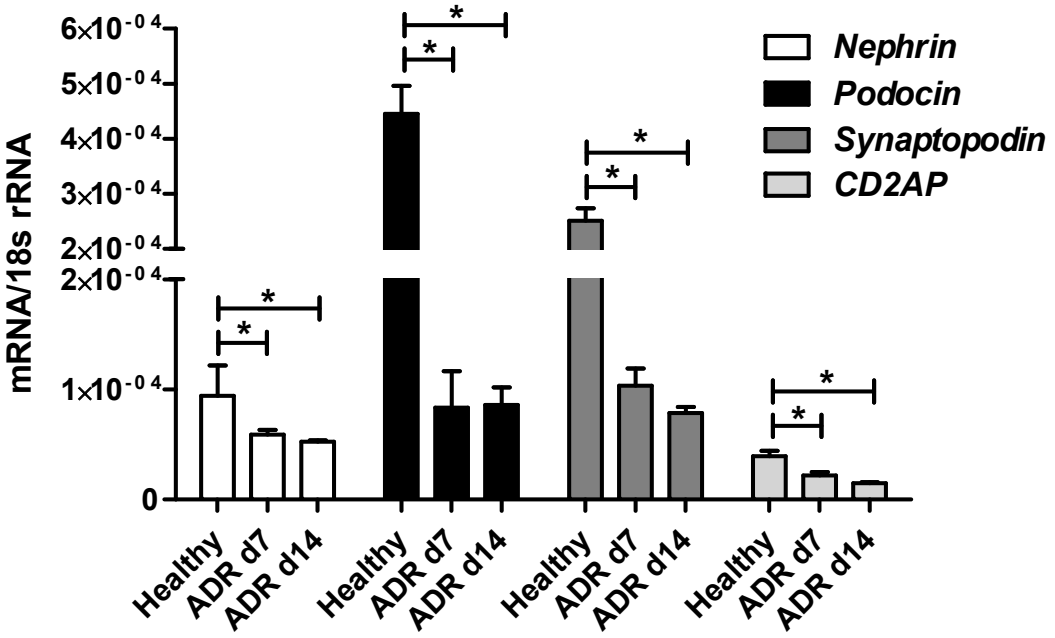

Figure 25. Total kidney mRNA expressions in Adriamycin nephropathy. Wild-type Balb/c mice with AN. Total kidney mRNA from AN mice were analyzed for quantitative real-time PCR for a number of genes including *Nephrin, Podocin, Synaptopodin*, and *CD2AP*. The data are ± SEM from 6-7 animals in each group. (*p<0.05, ADR day 7 and 14 versus healthy group) at day 7 and 14.

4.3.4. The CXCL12 blockade has a dual role on the outcome of Adriamycin nephropathy

To investigate the role of CXCL12 during AN, Balb/c mice were treated with the CXCL12 inhibitor NOX-A12 or control revNOX-A12 for up to 14 days. As demonstrated in Figure 25A, the blockade of CXCL12 had a differential effect on the UACR during AN on day 7 compared to day 14. While the UACR was significantly increased following NOX-A12 treatment on day 7, it decreased after 14 days in comparison to the control revNOX-A12 group (Figure 26A). Furthermore, the BUN levels (Figure 26B), as well as the blood creatinine (Figure 26C), decreased upon treatment with NOX-A12 compared to control revNOX-A12 only on day 14. The data suggests that CXCL12 blockade had only a protective effect during the late phase of AN but not during the early phase.

A

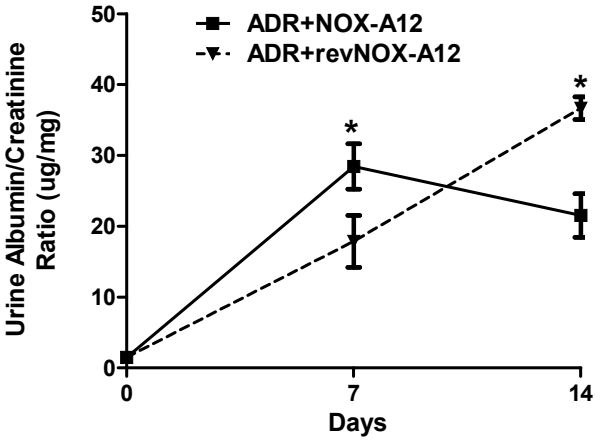

B

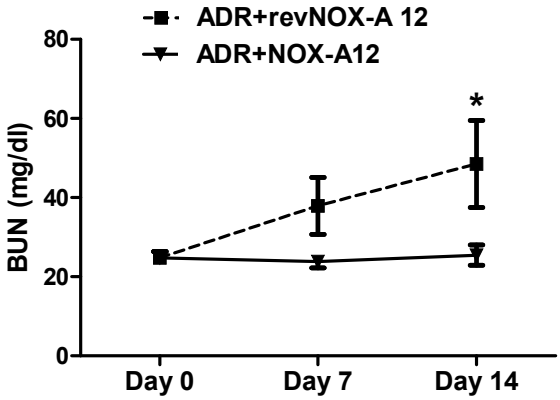

C

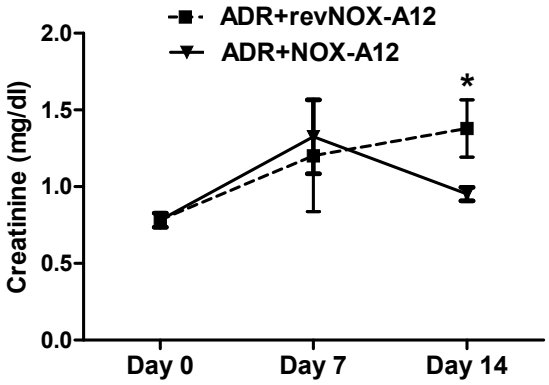

Figure 26. CXCL12 blockade has a dual effect during Adriamycin nephropathy. Balb/c mice received an intravenous injection of ADR to induces AN (see methods 2.2). Two groups of mice received subcutaneous injections of either the CXCL12 inhibitor NOX-A12 or control revNOX-A12 thrice a week. Urine was collected on day 0, 7 and 14 and the disease markes : UACR (**A**), BUN (**B**) blood creatinine (**C**) were measured. Data are mean ± SEM from 6-7 animals per group, *p<0.05 revNOX-A12 versus NOX-A12 at day 7 and 14.

4.3.5. CXCL12 blockade and renal morphology on Adriamycin Nephropathy

To assess morphological changes in the kidney after CXCL12 blockade during AN, whiten the group, we stained the kidney sections for PAS and the level of lesions in the NOX-A12 group vs. the revNOX-A12 group was evaluated. Quantification of glomerular lesions in the NOX-A12-treated AN mice after 7 days showed no difference in the percentage of normal glomeruli (50%), segmental lesions (40%) and global lesions (10%) compared to the control revNOX-A12 group (Figure 27A and B). Although the function of the kidney decreased following CXCL12 blockade after 7 days (Figure 27A), there was no worsening in regards of histological changes between the NOX-A12 and revNOX-A12 group. However, 14 days after AN, the percentage of global lesions increased dramatically (75%), whereas the percentage of normal and segmental glomeruli decreased compared to the early time point. Interestingly, the blockade of CXCL12 with NOX-A12 resulted in a significant decrease in the percentage of global lesions (40%) but in an increase in the percentage of global and normal glomeruli compared to revNOX-A12-treated mice (Figure 27B) indicating that CXCL12 blockade improved the kidney function during AN. Next, I counted the percentage of crescent formations in the glomeruli during AN. As shown in Figure 27C, the percentage of crescents increased during AN injected with revNOX-A12 over time (black bars). As expected, the amount of crescent formation significantly decreased when CXCL12 was blocked during AN (gray bars). The data demonstrated a pathological improvement associated with reduced crescent formation of the kidney following NOX-A12 treatment during AN.

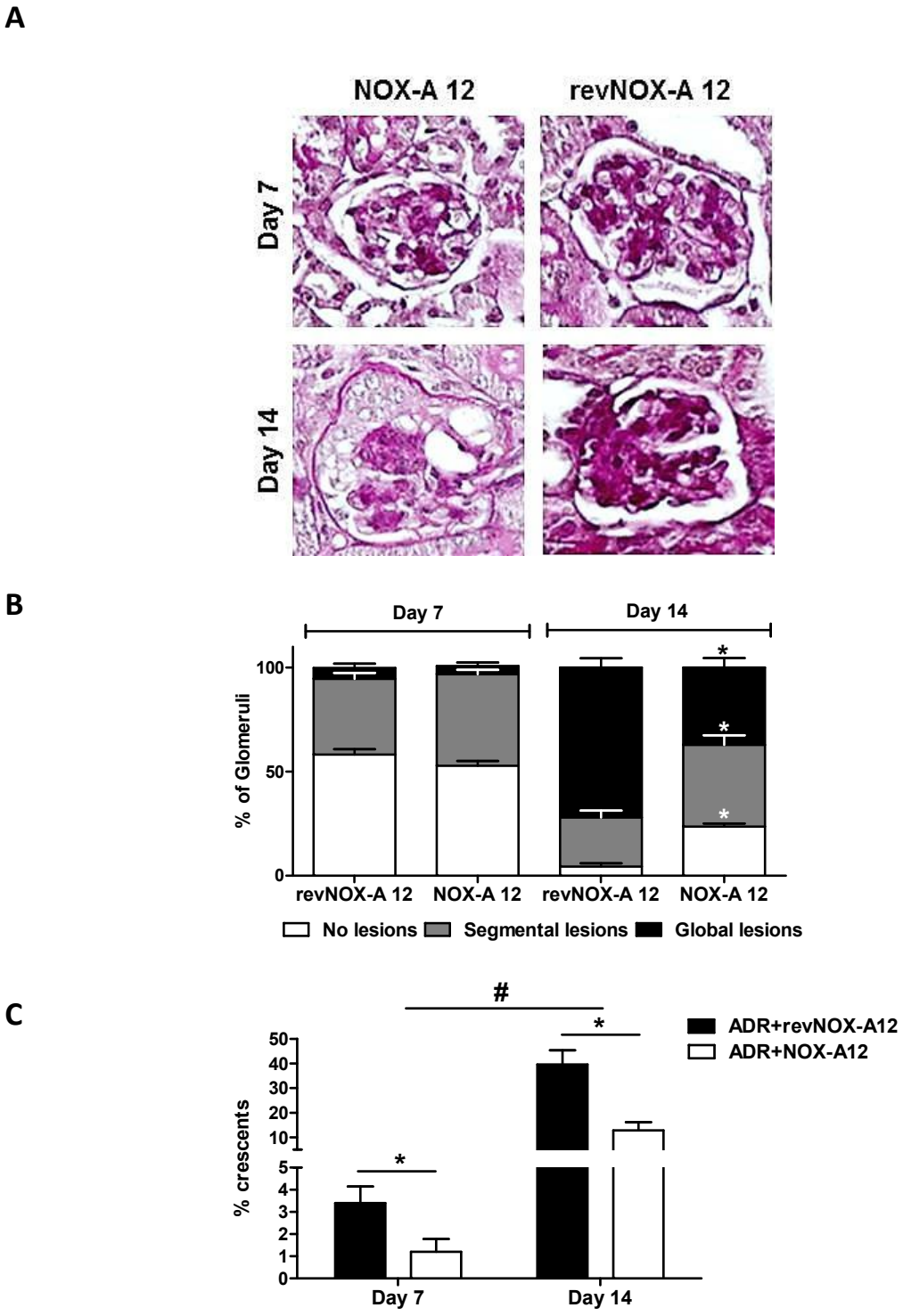

Figure 27: Renal pathology evaluation in Balb/cmice with Adriamycin nephropathy after CXCL12 blockade. (**A**) PAS staining of kidney sections of AN mice in the presence of NOX-A12 or control revNOX-A12 on day 7 and 14. (**B, C**) Quantification of glomerular injury score showed that CXCL12 blockade significantly reduced segmental and global glomerular lesions (**B**) as well as glomerular crescents (**C**) at day 14 during AN. The data are means ± SEM from 6-7 animals per group. (*p<0.05 revNOX-A12 group versus NOX-A12 at day 7 and 14), (#p<0.05 treated mice at day 7 versus day 14). Original magnification 400x.

4.3.6. Podocyte counts after CXCL12 blockade during Adriamycin nephropathy

Previous *in-vitro* experiments have shown that CXCL12 can act as a survival factor for podocytes. During the characterization of AN mouse model, we showed that the number of podocytes in the glomerulus was reduced after ADR treatment. We further evaluated the number of podocytes after CXCL12 blockade during AN. CXCL12 inhibitor had a differential effect on the function of the kidney on day 7 compared to day 14 (Figure 28A). We stained kidney sections with an IF for nephrin (green) and WT-1 (red), the staining showed differents in the podocyte counts when the mice were treated with NOX-A12 or revNOX-A12 during AN (Figure 28A). Interestingly, following CXCL12 blockade, the number of podocytes significantly decreased on day 7compared with the control whereas increased after 14 days of AN (Figure 28B). This data is in line with the differential effect of CXCL12 on the kidney function: UACR, BUN, and creatinine during AN.

A

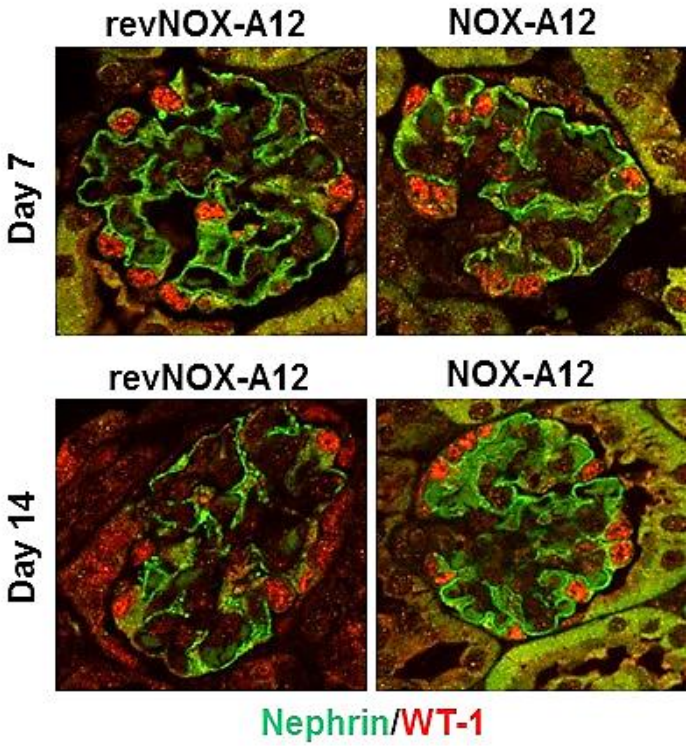

B

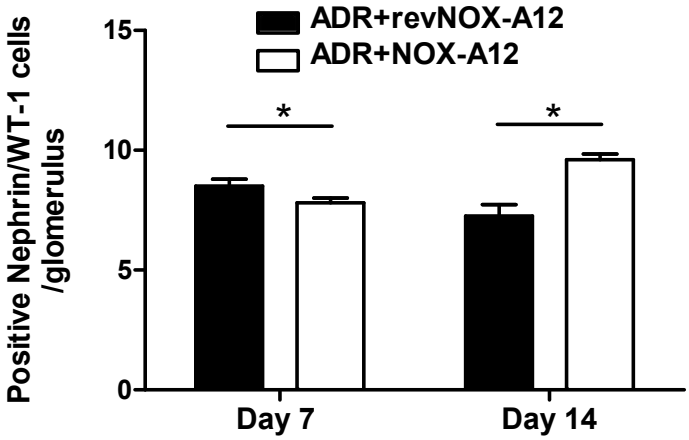

Figure 28. CXC-12 blockade reduces podocyte number in the early phase but increased them in the late. Podocytes quantification in wt Balb/cAncrl mice with AN after CXCL12 blockade. While using semi-quantitative IF staining for podocytes positive for nephrin (green) and WT-1 (red) (**A**), we were able to show that CXCL12 blockade significantly reduced the number of podocytes at day 7 but increased them at day 14 during AN (**B**). The data are means ± SEM from 6-7 animals in each group. (*p<0.05, **p<0.01 NOX-A12 treatment versus revNOX-A12 at day 7 and 14 after AN), (original magnification 400x).

4.3.7. Renal mRNA expression levels of podocyte markers in total kidney of Adriamycin nephropathy with CXCL12 blockade

To confirm the increased number of podocytes during AN treatment with NOX-A12 and revNOX-A12 after 14 days, I evaluated the mRNA expression levels for the classical podocyte markers. RT-PCR analysis showed no difference in the mRNA expression levels of the podocyte marker nephrin and WT-1 in the NOX-A12 as well as revNOX-A12 treated mice on day 7 (data not shown). In contrast, the mRNA levels of *Nephrin* and *WT-1* following NOX-A12 treatment were increased in comparison to the control group on day 14 (Figure 29). These data indicating that CXCL12 blockade has a general benefit for podocytes on AN day 14.

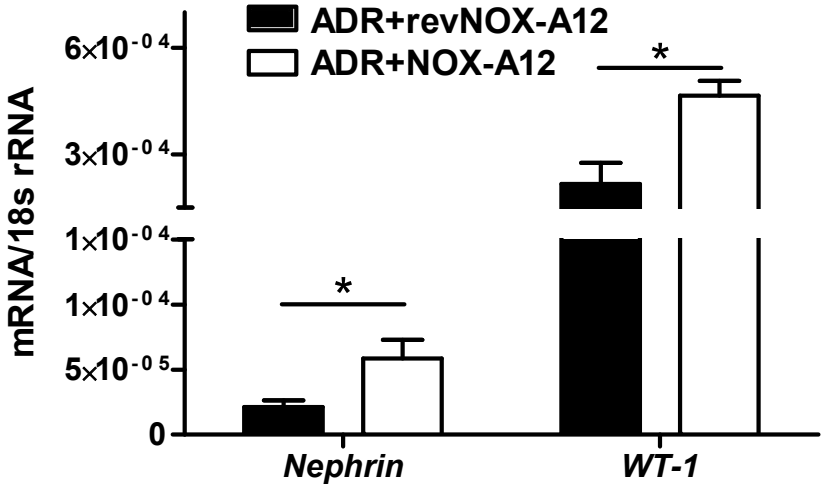

Figure 29: mRNA expression levels from the kidney Balb/c mice following CXCL12 blockade during Adriamycin nephropaty. mRNA was isolated from kidneys of AN mice on day 14 and quantitative real-time PCR for the podocyte markers: *Nephrin* and *WT-1* was carried out. The mRNA expression levels were significantly increased after CXCL12 blockade compares with control revNOX-A12 during AN. The data are means ± SEM from 6-7 animals in each group.(*p<0.05 NOX-A12 treated group versus revNOX-A12 group) at day 14.

4.4.The role of CXCL12 in human renal progenitor cells and human podocytes in-vitro

Previously, *Darisipudi et al.* showed that the blockade of CXCL12 in diabetic glomerulosclerosis ameliorates diabetic outcomes including slowing down the onset of proteinuria and increasing the number of podocytes. Furthermore, *Sargrinati et al. and Ronconi et al*. (28, 44) identified a specific stem cell population within the human glomerular urinary pole that is positive for both stem cell markers CD133 and CD24. Following glomerular damage, this stem cell population can become activated and migrate to the glomerular vascular pole into the Bowman´s capsule, and differentiate into *de-novo* podocytes. This raised the question of whether the increased number of podocytes was a direct consequence of RPCs regeneration due to the blockade of CXCL12 as demonstrated in the study by *Darisipudi et al*.? In the following section, several experiments were performed to study the effect of CXCL12 on RPCs, in particular on their proliferation and differentiation capacity toward podocytes *in-vitro*.

4.4.1. CXCL12 reduces human renal progenitor cell proliferation capability in-vitro

Recently, *Mazzinghi et al.* (88) showed that RPCs express the chemokine receptors for CXCL12 better known as CXCR-4 and CXCR-7. In this study, the authors demonstrated that CXCL12 is necessary for maintaining RPCs quiescence under homeostatic condition. CXCL12 is mainly produced by podocytes during homeostasis as well as during inflammatory conditions. Podocytes, as well as the RPCs, express the CXCL12 receptors CXCR-4 and CXCR-7 (Table 1). To investigate the effect of CXCL12 on RPCs, RPCs were stimulated with culture medium containing 20% FBS in the presence of NOX-A12 or control revNOX-A12. FBS was used as a strong pro-proliferation stimulus for RPCs. I determined the proliferative capacity and cell viability of RPCs using the colorimetric MTT assay. As shown in Figure 30A, stimulation with 20% FBS-induced proliferation of RPCs indicated by a significant increase in the optical density (O.D.) value (very light gray bar) that was reduced when RPCs were co-incubated with CXCL12 (blue bar). This suppressive effect of CXCL12 on the proliferation of RPCs was restored following pre-incubation with the NOX-A12 inhibitor (green bar). revNOX-A12 served as a control showing the specificity of NOX-A12 (yellow bar). To mimic the physiological condition in the human glomerulus, I differentiated RPCs into podocytes and after 24 hours the supernatants containing podocyte-derived CXCL12 (PDCXCL12) were collected (Figure 30B). I cultured then, RPCs in the absence or presence of podocyte-derived CXCL-12. The data in Figure 32C showed that 20% FBS-induced the proliferation of RPCs that was significantly reduced when podocyte-derived was present in the culture (blue bar) indicating that podocytes are major

source of CXCL12 in the glomerulus and that secreted CXCL12 reduced the capability of RPCs to proliferate (Figure 30C).

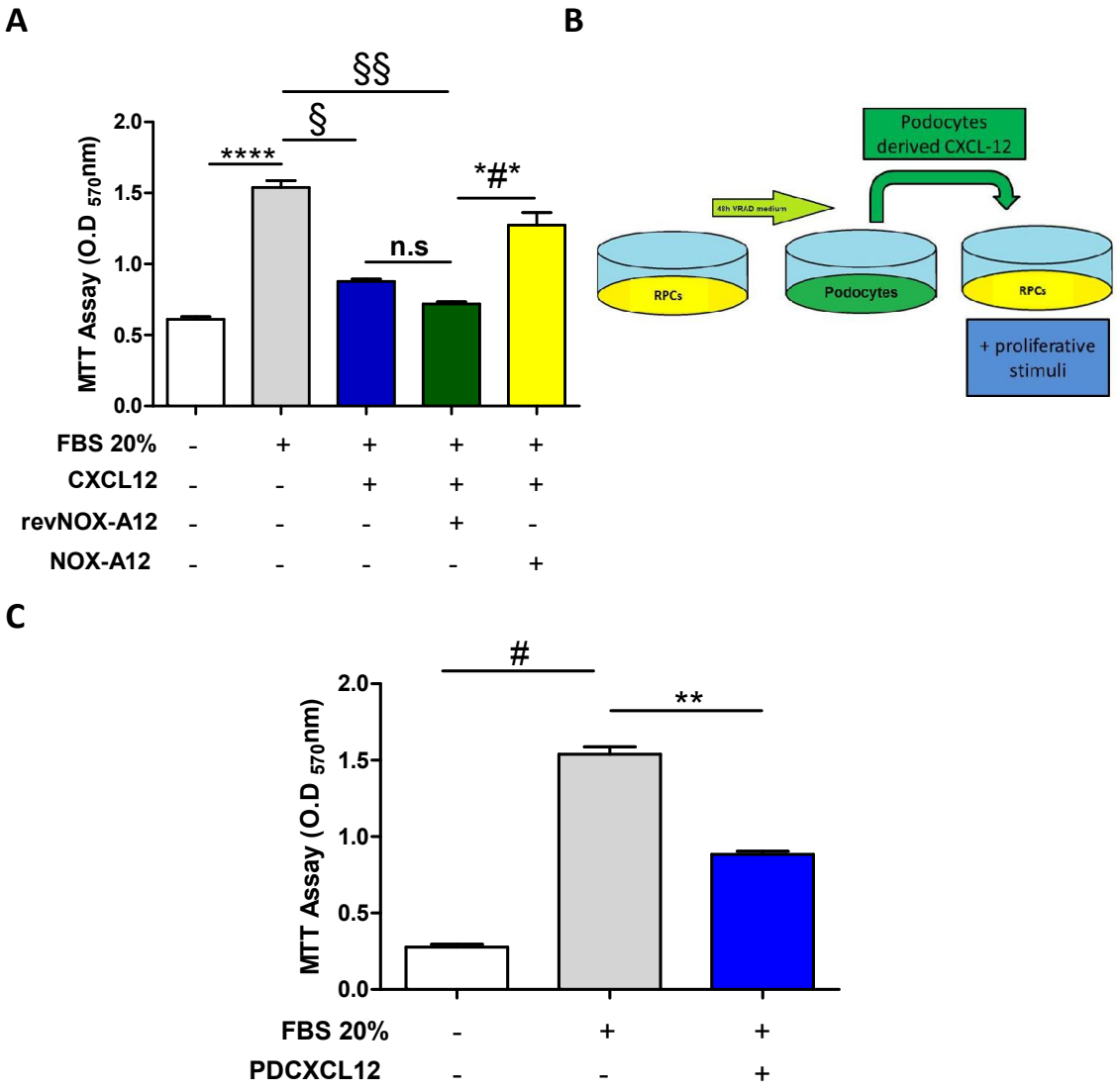

Figure 30: Podocyte-derived CXCL12 reduces human renal progenitor cell proliferation capability. (**A**) I used MTT assay to measure the capacity of human RPCs to proliferate in the presence of the stimulus FBS (20%) or in combination with CXCL12. Human RPCs were also co-incubated with the NOX-A12 inhibitor or revNOX-A12 for 24 hours. The stimulated human RPCs proliferated less when CXCL12 (blue bar) was added. NOX-A12 (yellow bar) inhibitor partially restored the proliferation capability compared to the control (green bar). (**B**) The experimental layout of the *in-vitro* experiment. (**C**) RPCs were cultured with 20% FBS in the absence or presence of podocyte-derived CXCL12 for 24 hours. Podocyte-derived CXCL12PODOCYTE DERIVED CXCL12 significantly reduced the proliferation capability of RPCs. (****p<0.0001 human RPCs treated with control medium versus 20% FBS medium), (§p<0.0001 RPCs treated with 20% FBS versus 20% FBS medium plus CXCL12) (§§p<0.001 RPCs treated with 20% medium versus 20% medium plus CXCL12 and revNOX-A12),(*#*p<0.01 RPCs treated with 20% FBS plus CXCL12 and revNOX-A12 versus 20% FBS plus CXCL12 and NOX-A12), (#p<0.0001 control medium versus 20% FBS medium), (**p<0.01 enriched 20% medium versus enriched medium plus podocyte-derived CXCL12), (n.s not significant) after 24h.

4.4.2. Necrotic supernatants from lysed podocytes imply human renal progenitors cell proliferation via Notch signaling in-vitro

During glomerular disease, loss of podocytes is one of the most important features responsible for the progression of the injury process. Previously, podocyte derived CXCL12 has caused the reduction of RPCs activity. To investigate whether soluble factors from dying podocytes can affect RPCs proliferation, I designed an *in-vitro* experiment, where RPCs were first differentiated into podocytes. After obtaining a sufficient number of podocytes, necrotic supernatants were prepared as described in section 2.11 and illustrated in Figure 31A. Podocyte-derived necrotic supernatants (NS) were added in three different concentrations (1, 10 and 100µl/ml) to RPCs and I determined the proliferative capacity by MTT assay after 24 hours. As demonstrated in Figure 31B, RPCs proliferate best when 10µl/ml NS is added to the culture. For all further experiments., I used 10µl/ml of NS for all the

A

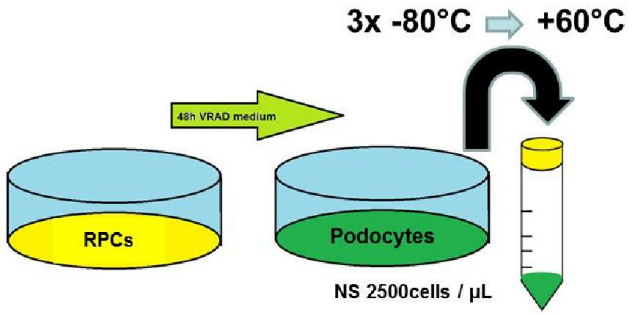

B

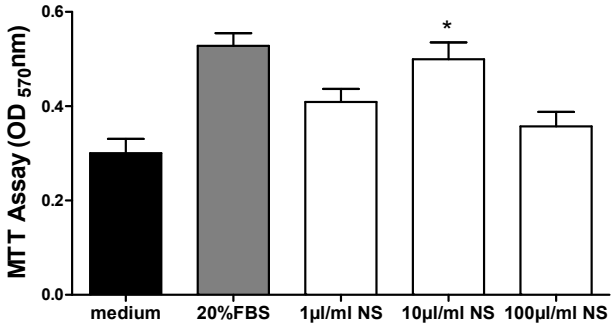

Figure 31. Proliferative capacity of renal progenitor cells in the presence of necrotic supernatants obtained from podocytes. (**A**) Podocyte NS was obtained like shown in the cartoon. (**B**) RPCs were stimulated with varying concentrations of NS (1, 10 and 100µl/ml) and 20% FBS (control medium) and cell proliferation was quantified using MTT assay after 24 hours. Data are means ± SEM of 2-3 experiments (* $p<0.05$ human RPCs treated with control medium versus RPCs treated with NS after 24h)

Next, fresh RPCs were cultured with 10µl NS in the presence of the CXCL12 inhibitor NOX-A12 and control revNOX-A12 for 24 hours. The MTT assay results showed that blocking CXCL12 in the NS increased significantly the capability of RPCs to proliferate (yellow bar) compared to the controls NS (red bar) or NS+revNOX-A12 (blue bar) (Figure 32). These results indicated that CXCL12 was present in the NS and that CXCL12 inhibition increased the NS-induced proliferation of RPCs. It is currently unknown how exactly CXCL12 in the NS suppresses RPCs proliferation. To investigate this, I co-incubated RPCs with NS in the absence or presence of the Notch pathway inhibitor DAPT and/or NOX-A12.

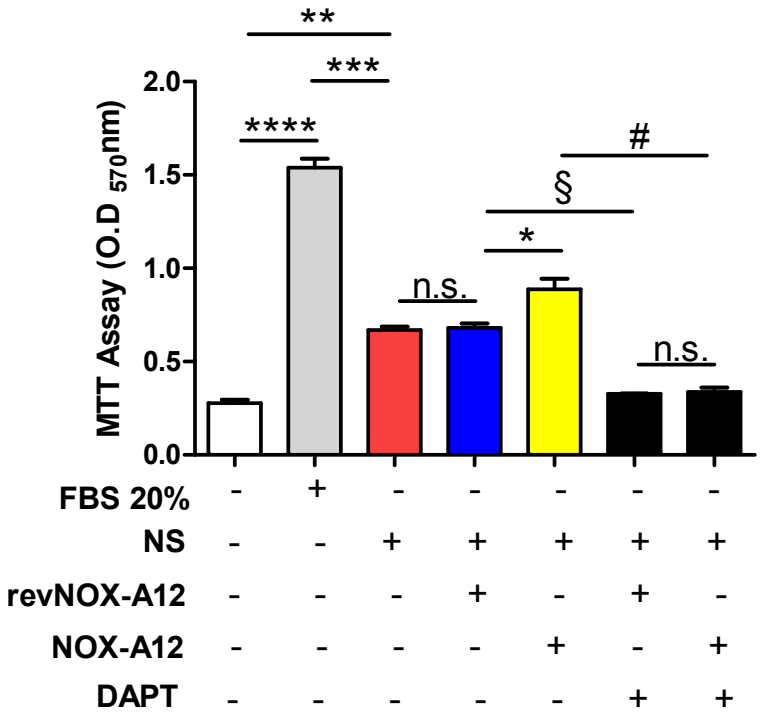

Figure 32. Necrotic supernatant induces renal progenitor cell proliferation via Notch pathway. MTT assay was carried out and O.D. measured at 570 nm. NS-induced RPCs proliferation (red bar), the inhibition of NS-CXCL12 with NOX-A12 (yellow bar) increased much more the RPCs proliferation compare with the NS (red bar) and NS+revNOX-A12 (blue bar). Further, Incubation with DAPT the inhibitor of the Notch signaling pathway drastically reduced the RPCs proliferation capability (black bar). Inhibition of CXCL12 with NOXA-12 or revNOX-A12 had no effect in the presence of DAPT had no supplementary effects. Data are means ± SEM of 2-3 experiments. (****p<0.0001 RPCs treated with control medium versus RPCs treated with 20% FBS), (**p<0.01 treated RPCs with control medium versus NS treated RPCs), (***p<0.001 treated RPCs with 20% FBS versus NS treated RPCs), (n.s. not significant), (*p<0.05 treated RPCs with NS plus revNOX-A12 versus RPCs treated with NS+NOX-A12), (§p<0.01 treated RPCs with NS plus revNOX-A12 versus RPCs treated NS plus NS plus revNOX-A12 and DAPT), (#(**p<0.01 treated RPCs with NS plus NOX-A12 versus RPCs treated with NS and NOX-A12 plus DAPT) at 24h.

Upon blockade of the Notch pro-proliferative pathway using DAPT the capacity of RPCs to proliferative was reduced, whereas stimulation with DAPT in combination with NOX-A12 had no further effect on RPCs proliferation (black bars).

4.4.3. The role of necrotic supernatant-podocyte-derived CXCL12 and the Notch pathway on renal progenitor cells

The RPCs increased proliferation upon blockade of CXCL12 could be reversed leading to increased activity of the Notch signaling pathway during AN. *Lasagni et al,* (64) have previously shown that the activation of the Notch signaling pathway in podocytes can act as a trigger for cell death as well as for prolonged Notch pathway activation during AN, increased RPC proliferation and differentiation toward podocyte lineage. In the next paragraphs, we investigated the impact of CXCL12 on RPCs and the cross-regulation between Notch pathway and CXCL12. To test this connection, I stimulated RPCs with 10µl/ml NS and I evaluated the mRNA expression levels of the receptors *Notch-1, Notch-2* and *Notch-3*, the ligands and the downstream genes *Hey-1* and *Hes-1* of the Notch pathway. Real-time qPCR showed that the mRNA levels of all tested genes were significantly increased significantly increased following NOX-A12 treatment compared to revNOX-A12 indicating that NS-derived CXCL12 inhibited Notch signaling activity and, therefore, proliferation of RPCs (Figure 33).

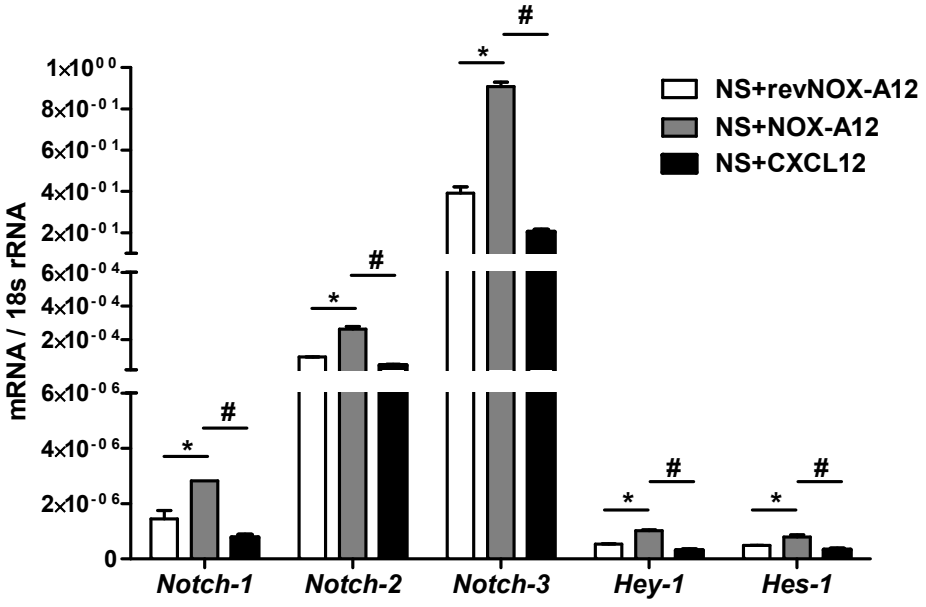

Figure 33: Notch pathway is overactivated when CXCL12 is removed from the prodocyte-derived necrotic supernatant. mRNA was isolated from RPCs after NS treatment. The graph showed an increased expression of the receptors *Notch-1, Notch-2* and *Notch-3*, the ligands and downstream effector genes *Hey-1* and *Hes-1* of Notch pathway mRNA in RPCs stimulated with NS when CXCL12 was blocked. Data are means ± SEM of 2-3 experiments, * $p<0.05$ RPCs treated with NS plus reNOX-A12 versus RPCs treated with NS plus NOX-A12), (# $p<0.01$ RPCs treated with NS plus NOX-A12 versus RPCs treated with NS plus an extrinsic surplus of CXCL12) at 24h.

To confirm the mRNA expression levels, I performed a western blot analysis to evaluate the expression of the most activated nuclear domain of the Notch receptor 3(NICD-3). The data shows an increase in the protein levels of NICD-3 in NS-stimulated human RPCs when CXCL12 was blocked compared to the controls (Figure 34).

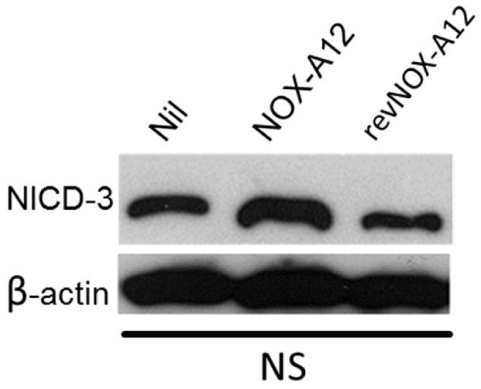

Figure 34. CXCL12 blockade increases the level of activated the Notch intracellular domain-3. Western Blot of RPCs stimulated with NS showed Notch NICD-3 activation after CXCL12 blockade. Data are representative 2-3 experiments. Protein loading was corrected for sample protein concentrations and Beta-actin was used as a control.

In conclusion, within this section I show that: 1) CXCL12 is present in podocyte necrotic supernatants; that 2) Notch signaling is important for RPC proliferation and that 3) CXCL12 can act as a direct regulator of the Notch signaling pathway.

Previously, I showed that CXCL12 released from dying podocytes reduced the activity of RPCs via inhibiting the Notch signaling pathway. Next, to confirm the role of CXCL12, I cultured RPCs without NS but in the presence of the Notch inhibitor DAPT, CXCL12 as well as the proliferative stimulus FBS. The MTT assay performed revealed that 20% FBS-induced the proliferation of RPCs (Figure 35, light gray bar) and that upon addition of DAPT (black bar) or CXCL12 (dark gray bar) the proliferative capacity of RPCs was significantly reduced compared to FBS alone. However, inhibiting proliferation of RPCs with CXCL12 was less effective as DAPT treatment alone and the combination treatment of DAPT and CXCL12 had no further effect on RPCs proliferation (squared bar).

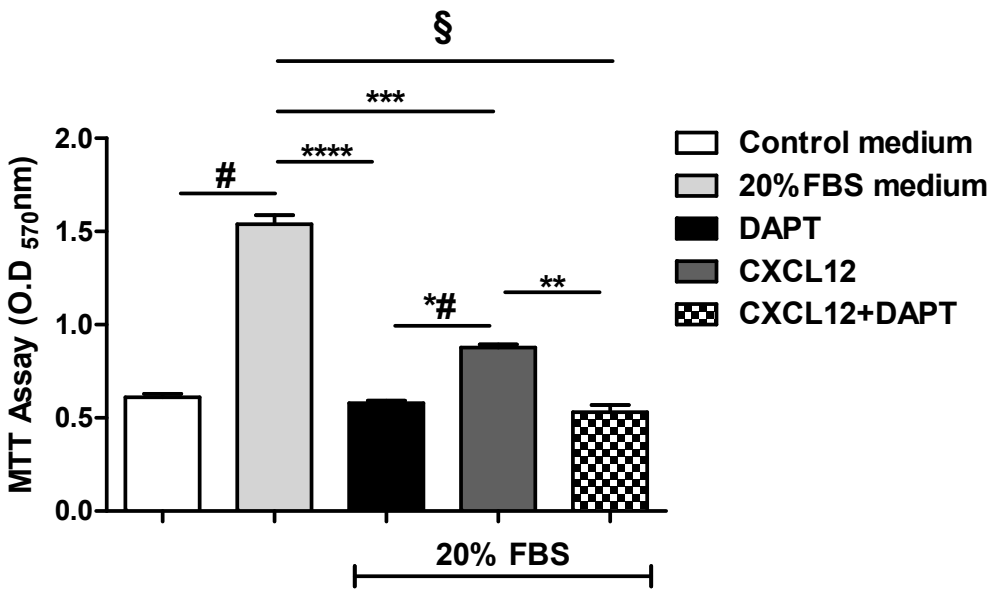

Figure 35: CXCL12 decreases progenitor cells activation by blocking Notch pathway. RPCs stimulated with 20% FBS increased their proliferation capability (light gray). The proliferation was significantly reduced in the presence of Notch inhibitor DAPT in the medium. Also, the stimulation of the RPCs with CXCL12 reduced again the proliferation (gray bar). The combined stimulation with DAPT and CXCL12 no further decreased the RPCs proliferation as DAPT performed alone (square bar). Data are means ± SEM of 2-3 experiments (# $p<0.0001$ RPCs treated with control medium versus 20% FBS treated RPCs), (****$p<0.0001$ RPCs treated with 20% FBS versus RPCs treated with 20% plus DAPT), (***$p<0.001$ RPCs treated with 20% FBS versus RPCs treated 20% FBS plus CXCL12) (§$p<0.0001$ RPCs treated with 20% FBS versus RPCs treated with 20% FBS plus combination of DAPT and CXCL-12), (*# $p<0.01$ RPC treated with 20% FBS plus DAPT versus RPCs treated with 20% FBS plus CXCL-12), (**$p<0.01$ RPCs treated with 20% FBS plus CXCL-12 versus RPCs treated with 20% FBS plus combination of CXCL-12+DAPT) after 24h.

Together, the *in-vitro* data within this section suggest that podocytes are the main source of CXCL12 and that podocyte-derived CXCL12has a suppressive effect on RPCs proliferation. Also, CXCL12 shows cross-linked effects with the Notch pathway.

4.4.4. Effects of CXCL12 on human renal progenitor cells differentiation towards podocyte lineage

Previously*, Darisipudi, et al.* (82) showed that in a mouse model of diabetic nephropathy, CXCL12 blockade resulted in an increase in the number of Nephrin/WT-1 double positive cells (82). Previously, I showed that podocyte-derived CXCL12 had the ability to act as a homeostatic chemokine by reducing the proliferative capacity of RPCs. Less RPCs proliferation can result in less *de-novo* podocyte production. To investigate the direct CXCL12 impact on the podocyte differentiation process, I cultured RPCs into podocytes in the presence of VRAD medium for 48 hours (28). After stimulation, I determined the expression of different podocyte markers using real-time PCR. As shown in Figure 36, the mRNA expression levels of the typical podocyte markers including

Nephrin, Podocalyxin, and *CD2AP* significantly increased after stimulation with VRAD medium compared to control medium (green bar). However, when human RPCs were stimulated with CXCL12 during the differentiation process, the mRNA levels of all three tested podocyte markers decreased. This suppressive effect of CXCL12 on *Nephrin, Podocalyxin* and *CD2AP* mRNA expression was partially rescued by blocking CXCL12 with the NOX-A12 antibody in comparison to the control revNOX-A12 antibody. This results show that CXCL12 reduce the capability of RPCs to differentiate into podocyte.

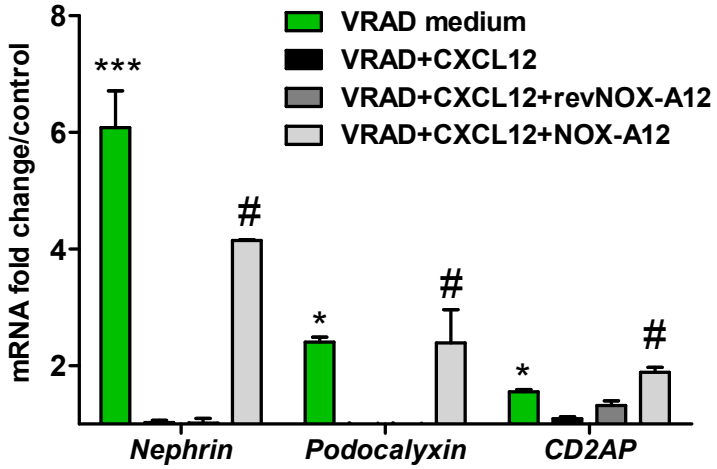

Figure 36. CXCL12 reduces renal progenitor cell differentiation towards podocyte lineage. (**A**) RPCs were differentiated without (EBM control media) or with VRAD medium (see methods 2.11) into podocytes and then treated with CXCL12 alone or in combination with NOX-A12 or revNOX-A12 for 48 hours. qPCR analysis was performed on human RPCs looking at the mRNA expression levels of *Nephrin, Podocalyxin,* and *CD2AP*. Data are means ± SEM of the 2-3 experiment. (* $p<0.05$, *** $p<0.001$ RPCs stimulated with control medium versus RPCs stimulated with VRAD medium), (#$p<0.05$ RPCs stimulated with VRAD plus CXCL12 and NOX-A12 versus RPCs treated with VRAD medium plus CXCL12 and revNOX-A-12.

4.4.5. Blocking CXCL12 increases renal mRNA expression levels of Notch pathway genes during Adriamycin nephropathy

Previous *in-vitro* studies showed that stimulation with NS was able to reduce the proliferative capability of RPCs, associated with a negative regulation of the Notch signaling pathway by CXCL12. To investigate if CXCL12 can also trigger a reduction of Notch expression levels *in-vivo*, I performed a qPCR expression analysis on total kidney mRNA from mice following AN, treated with /without CXCL12 inhibitor. As shown in Figure 37, the mRNA expression levels of the Notch receptors *Notch-1, Notch-2 and Notch-3* increased during AN, day 7 and 14, when CXCL12 was blocked using the NOX-A12 inhibitor compared with the control. (Figure 37A, black bars). Similar to the Notch receptor mRNA profile, the mRNA expression levels of the Notch ligands *Jag-1, Jag-2* and *Dll-1* (Figure 37B) as well as the downstream effectors genes *Hes-1* and *Hey-1* (Figure 37C) were significantly up-regulated following treatment with NOX-A12 compared to control revNOX-A12 on day 7 and 14.

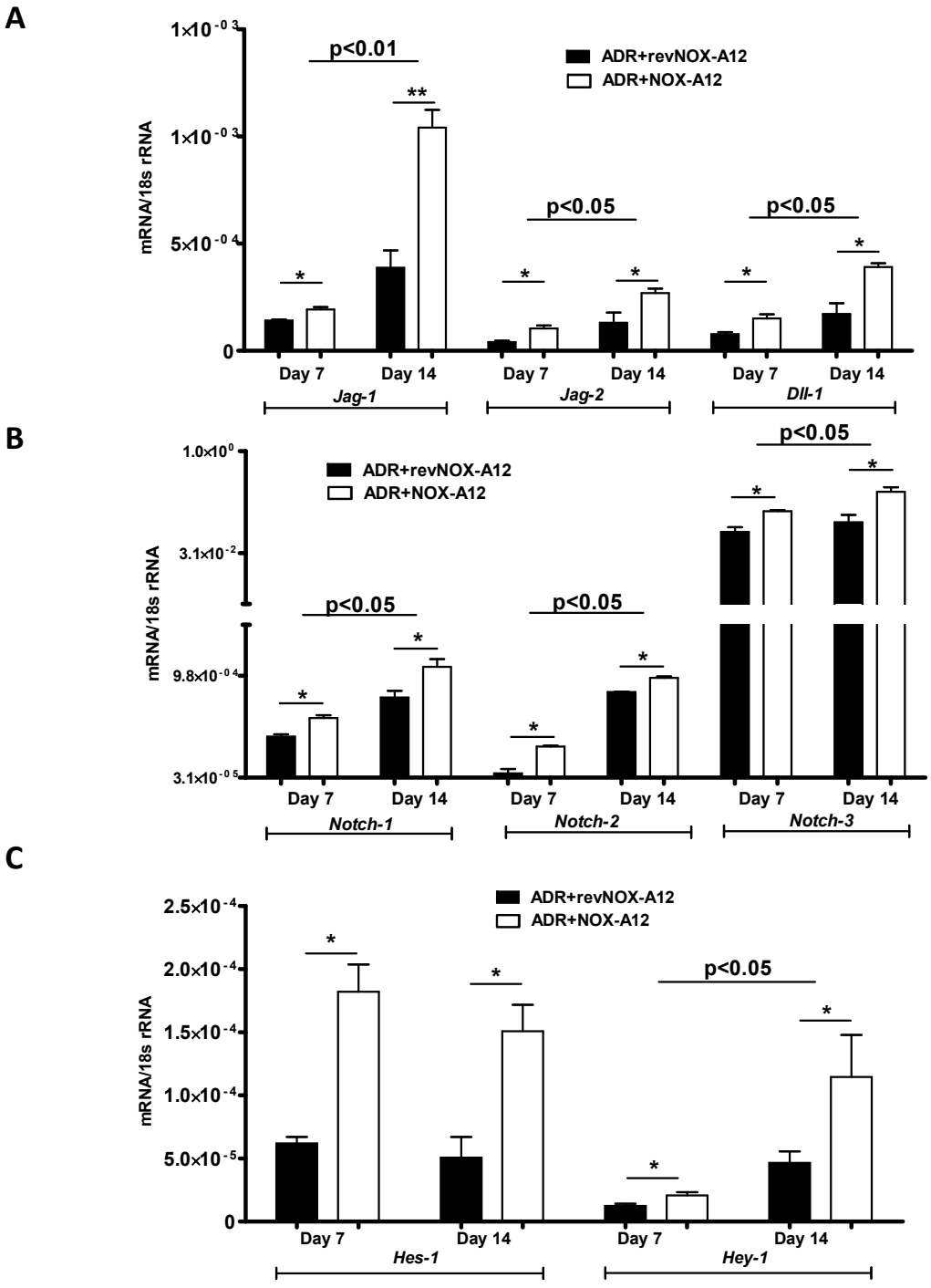

Figure 37. Upregulation of Notch-related genes following CXCL12 blockade during Adriamycin nephropathy. mRNA was isolated from kidneys of AN mice following CXCL12 blockade and showed an increased expression of the receptors *Notch-1, Notch-2* and *Notch-3* (**A**), the ligands *Jag-1, Jag-2* and *Dll-1* (**B**) and the downstream effectors genes *Hes-1* and *Hey-1* (**C**) of the Notch pathway in kidneys on day 7 and 14. Data are ± SEM from 6-7 animals in each group. (*p<0.05, **p<0.01 ADR treated mice with NOX-A12 versus mice treated with ADR and revNOX-A12) at day 7 and 14.

4.4.6. The Notch pathway intracellular domains are highly expressed in the injured glomerulus following CXCL12 blockade Adriamycin nephropathy

To confirm that CXCL12 was responsible for the inhibition of Notch signaling activity during AN, We stained kidney sections from mice treated with NOX-A12 or revNOX-A12 during AN on day 7 and 14 for the Notch intracellular domain 1 (NICD-1) and NICD-3. As showed in Figure 38A, the expression of NICD-3 (green) in the kidneys of AN was increased compared to healthy mice on day 7 (Figure 38A upper panel), in contrast, the expression of NICD-3 decreased on day 14. The fluorescent intensity of NICD-3 was stronger in kidney sections of mice treated with NOX-A12 compared to control revNOX-A12 during AN on day 7 and 14 (Figure 38A, lower panel). Especially on day 7, NICD-3 was highly expressed inside the podocyte cytosol and in the parietal epithelial cells, compared to the revNOX-A12 (Figure 38A lower panel). *Lasagni, et al.* (64) showed that NICD-3 activation in podocyte was a triggering signal to go under proliferation program. This program occurs due to the podocyte structural characteristics cannot be done. When the cell cycle of podocytes is abolished, they died via CM. (Here, in this thesis were presented only *in-vitro* direct experiment about ADR-induced CM and its regulation. At the moment the direct prove of this mechanism Notch pathway-CM and CXCL12 *in-vivo* are under evaluation with animal experiments (64). Together with the previous mRNA data and these IF sections, I confirmed that podocyte's derived CXCL12 had a homeostatic-down regulation of Notch role, on the RPCs but also on the podocytes. Continuing on the work of *Lasagni, et al.* (64), we also checked the NICD-3 signal at the day 14 during the regeneration phase of AN. NICD-3 was much stronger inside the PECs (activated RPCs) during the regeneration phase of the model (Figure 38A low pictures). Indeed, on day 14 mice treated with NOX-A12 represent a stronger NICD-3 signal in PECs compared to revNOX-A12 indicating that the proliferation of PECs via Notch pathway was a consequence of more *de-novo* podocyte regeneration. In addition, this staining showed that CXCL12 had a suppressive effect on the activity of NICD-3 during AN. This was also the case for NICD-1 on day 14 (Figure 38B).

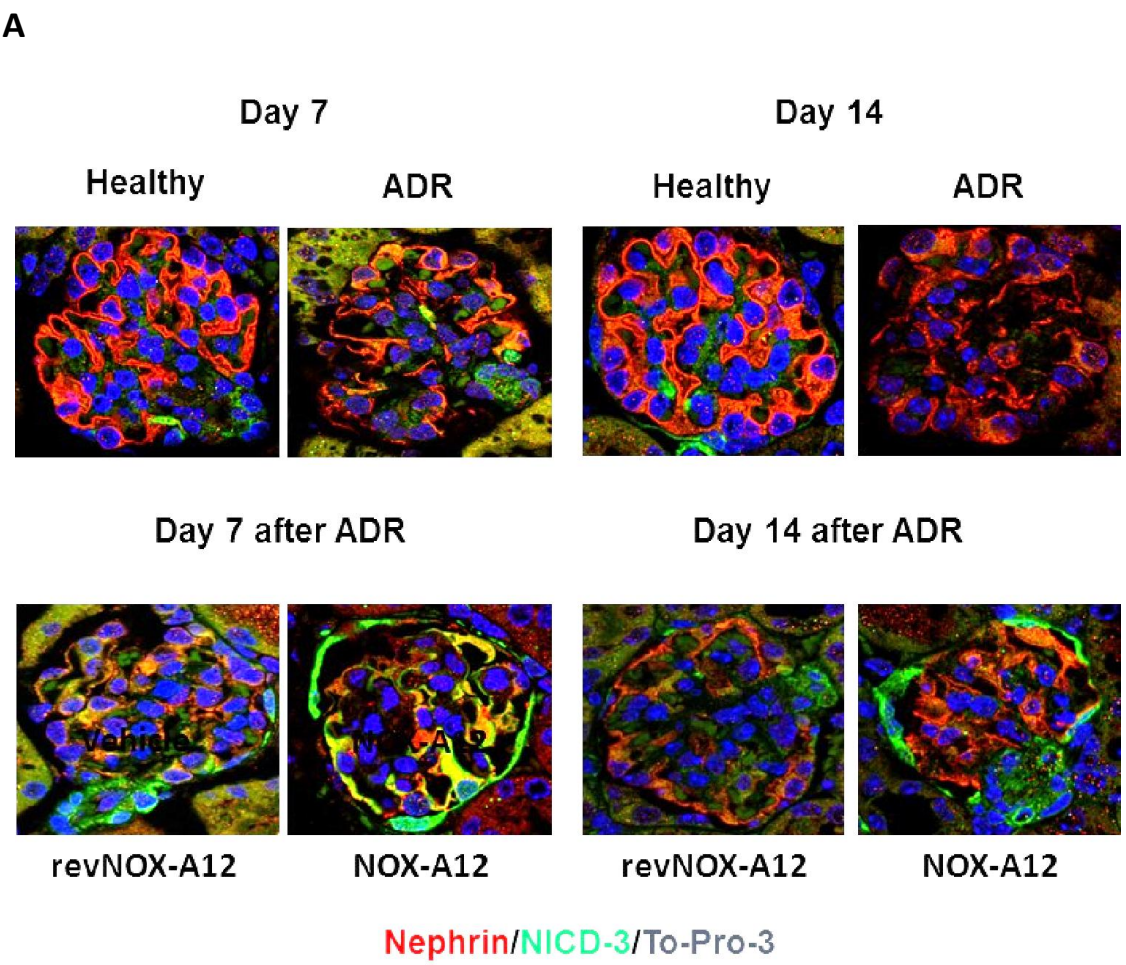

Figure 38. CXCL12 down-regulates Notch 1-3 signaling activity in Adriamycin nephropathy. (**A**) Representative images of kidney sections stained for the activated Notch-domain NICD-3 demonstrated that CXCL12 blockade increased the positivity for NICD-3 on day 7 and 14 compared with the control or healthy status. (**B**) Representative images of kidney sections stained for activated Notch-domain NICD-1 on day 14; here the PECs were positive when treated with NOX-A12 compare to revNOX-A12. Original magnification is 200x.

Together, the *in-vitro* and *in-vivo* findings indicate that CXCL12 could act as a survival factor for podocytes in an autocrine manner. In particular, CXCL12 released from dying podocytes is able to down-regulate the expression of Notch signaling in podocytes. CXCL12 is also necessary during the early phase of AN to keep the podocytes alive and to block Notch pathway activation and preventing other podocytes to die via CM. In contrast, during the late phase (day 14) of AN, blocking CXCL12 is beneficial for the activation and further differentiation of RPCs to *de-novo* podocytes resulting in the amelioration of the disease.

4.5.Blockade of CXCL12 during Adriamycin nephropathy using a mouse renal progenitor cell-lineage tracing-system

Are *de-novo* podocytes derived from RPCs within the glomerular stem cell niche or from other stem cell sources? Does glomerular regeneration via RPCs *de-novo* podocyte formation occur during AN *in-vivo*? To further confirm our findings in the AN model, I used a novel technic based on the lineage-tracing-system. Therefore, we obtained a specific mouse strain, tagged with the tracing endogenous red florescent protein /endogenous green florescent protein (ERFG/EGFP) system for the *Pax2* promoter (*Pax2* mT/mG) from our collaborators in Florence. *Pax2* is a critical regulator of the embryonic progenitor population during kidney development in vertebrates (137). Pax2 is co-expressed with CD133 in the adult RPCs, and it was an ideal combination for RPCs lineage tracing along the Bowman´s capsule of the mouse (138). I induced FSGS after activation of the mT/mG tracing system like described in section 2.2. Consequently, I started CXCL12 blockade treatment from time point day 0 until the end of the experiment on day 33. After that, we used a confocal IF to visualize the endogenous mouse *Pax2* reporter and specific podocyte markers to evaluated the impact of mouse RPCs on the podocyte regeneration after AN.

4.5.1. The effect of blocking CXCL12 during Adriamycin nephropathy

I determined the UACR in the *Pax2.rtTA; TetO.Cre; mT/mG* mice during the treatment with the active or inactive CXCL12. CXCL12 inhibition significantly reduced UACR (Figure 39A). Also, the BUN levels were decreased although not significantly upon treatment with NOX-A12 compared to control revNOX-A12 (Figure 39B). The data suggested that CXCL12 blockade had also a protective effect during the regeneration phase of AN in *Pax2* mice.

A

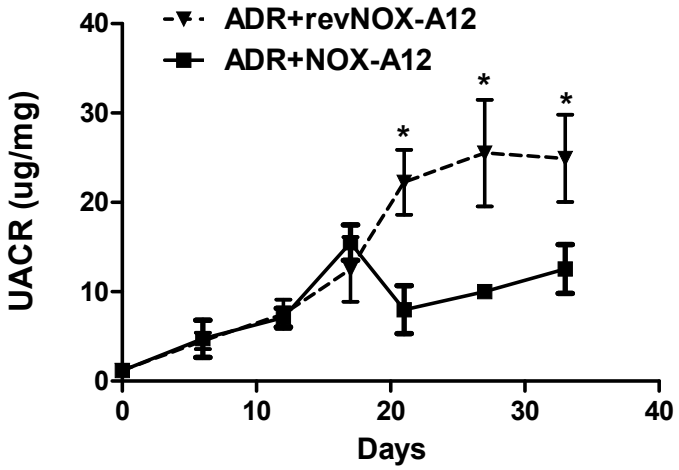

B

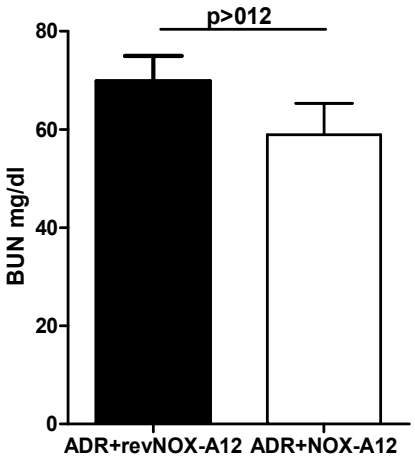

Figure 39: CXCL12 blockade reduces Adriamycin nephropathy disease marker in *Pax2* mice. Adriamycin nephropathy was established as described in methods section 2.2 in *Pax2* mice. Two groups of mice received NOX-A12 and revNOX-A12 as described in methods section 2.2 Urine was collected and the UACR was evaluated along all the treatment period(**A**) and BUN (**B**) measured at the end of the study. Data are means ± SEM from 5 animals group. (*p<0.05 NOX-A12 treated AN mice versus revNOX-A12 group) at day 33.

4.5.2. *Pax2-tagged mouse renal progenitor cells regenerate lost podocytes during Adriamycin nephropathy*

Blocking CXCL12 reduced proteinuria in *Pax2* mice with AN. To determine the expression of Pax2 in the kidneys, I performed IF with the endogenous green and red fluorescent proteins system to identify the *de-novo* mouse podocytes derived from mouse RPCs (Figure 40A). The endogenous red fluorescent protein was used to define the old embryonic Pax2-derived podocytes before the activation of mt/mG system in the glomeruli. The green stained for the de-novo podocyte-derived from the *Pax2* mouse RPCs. Also, we stained with blue color the podocyte marker synaptopodin (Syn) and the nuclei with the marker DAPI (white color). As illustrated in Figure 40B (top panel), the glomerular sections showed a mix of purple cells representing pre-induced podocytes (red color plus Syn in blue and green cells with a blue background as *de-novo* treatment-induced podocytes. The IF staining demonstrated that treatment with the CXCL12 inhibitor NOX-A12 results in more newly derived *de-novo* RPCs (green color) compared to the revNOX-A12 group. Without staining for Syn (blue color), the glomerular sections showed that the NOX-A12 group had more Pax2 activated PECs (green color) in the capsule compared to the control (Figure 40B, lower panel) at day 33.

A

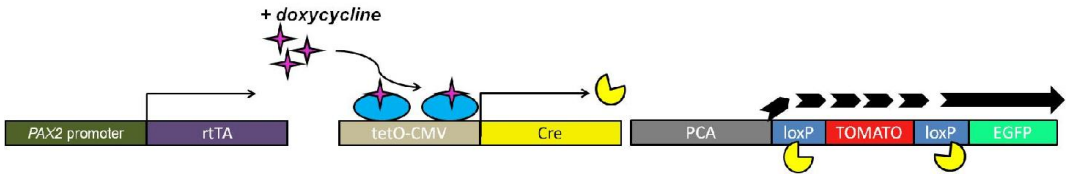

B

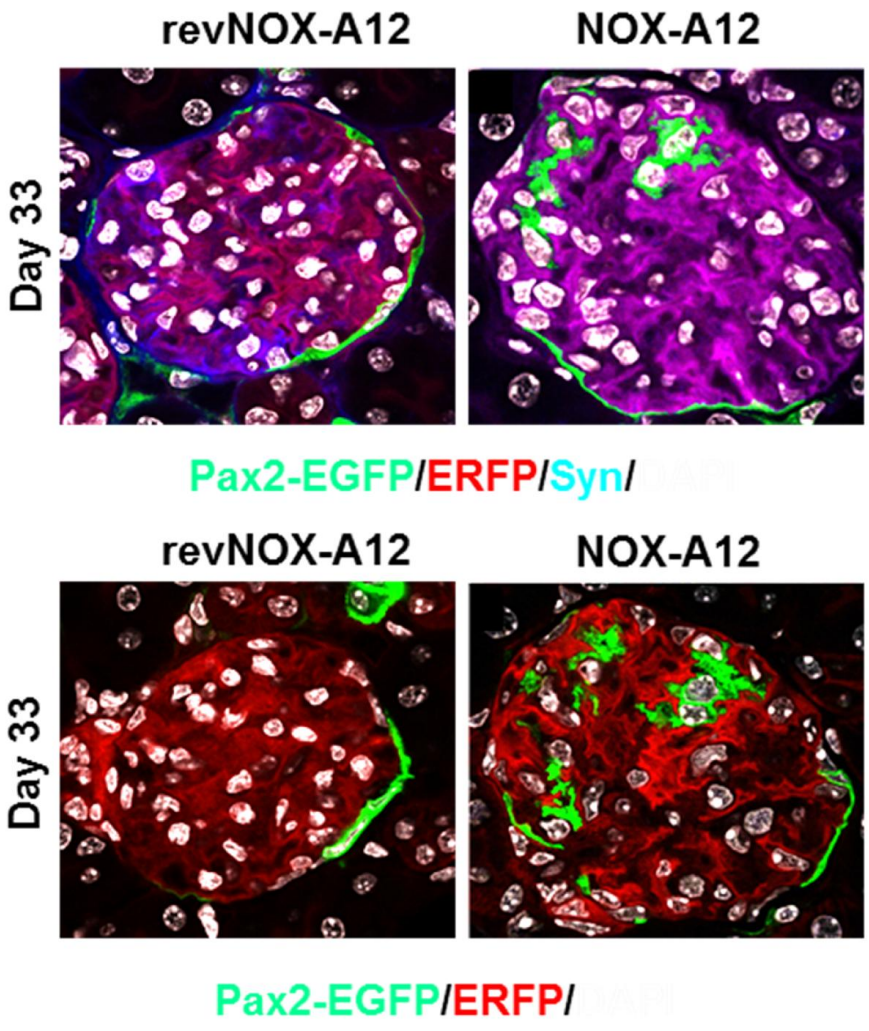

Figure 40. CXCL12 blockade induces activation of renal progenitor cells Pax2 cells toward *de-novo* podocytes in Adriamycin nephropathy. *Pax2* AN was induced as described in methods 2.2. (**A**) *Pax2* mT/mG bgenetic schematic model. (**B**) (upper panel) IF of *Pax2* mouse with red/blue staining of pre-induced podocytes, green stained cells are in the center of the glomerulus that are *de-novo* podocytes derived from the Pax2 mouse renal progenitor. Green cells around the capsule are activated transitional PECs/ podocytes. (**B**) (lower panel) IF of *Pax2* mice without blue Syn staining to better evaluate the foot process of the *de-novo* podocytes (green cells). Representative pictures, original magnification 400x.

To further estimate the impact of mouse RPCs in podocytes regeneration, I determined the total amount of positive Pax2 cell glomeruli inside one entire kidney longitudinal section under the microscope. The resulted data showed a higher Pax2 positivity in the NOX-A12 group, 15% of the total glomeruli were positive, compared with the control treatment were 4.5% of the glomeruli were Pax2 positive (Figure 41A left up graph). Since glomerular damage is focal and segmental in this model, it was possible to assume that not all glomeruli containing Pax2+cell-derived podocytes within the tuft and that not all Pax2+ cells were present within these glomeruli. To further evaluate the activated mouse RPCs, I further counted the total number of absolute n° of Pax2-derived podocyte per glomeruli per all the glomeruli of the longitudinal section. Again the results were significant as NOX-A12-treated mice showed 3 times more Pax2-derived podocytes in absolute counts compared to revNOX-A12 (Figure 41A right up graph). Finally, I estimated the regenerative impact of Pax2 cells during AN while using the *Podo loss* formula of *Lasagni et al,* (27) (see methods 2.10). The percentage of Pax2--derived podocytes-Syn+ over lost podocytes was three times higher in the NOX-A12 treated group (13%) compared to the revNOX-A12 (2.7%) (Figure 41A low graph). Using a high magnification, it was possible to visualize the complex structure of podocytes (green color), the podocyte foot process and the integrated new green podocyte inside the glomerular contest (cells with red color) (Figure 41B).

A

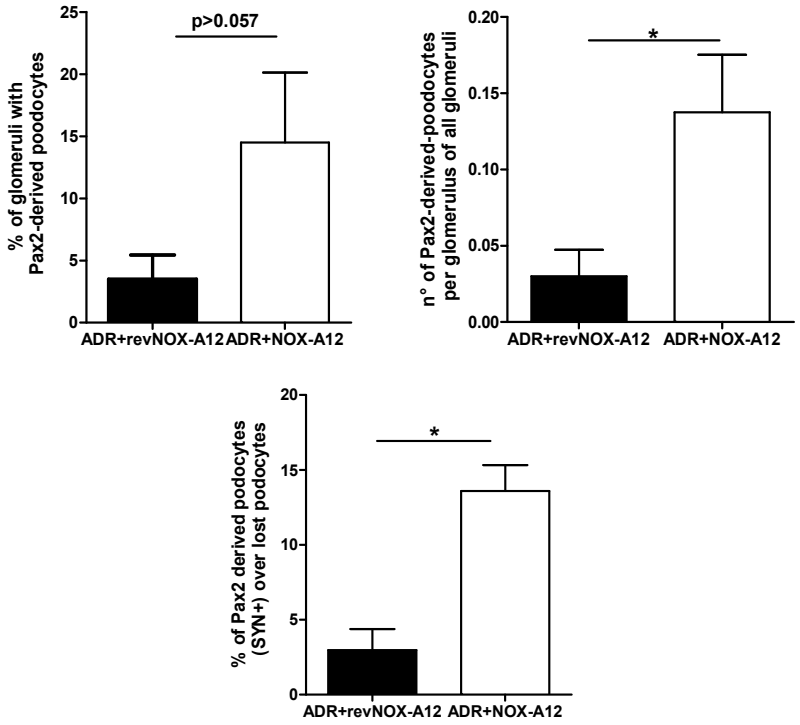

B

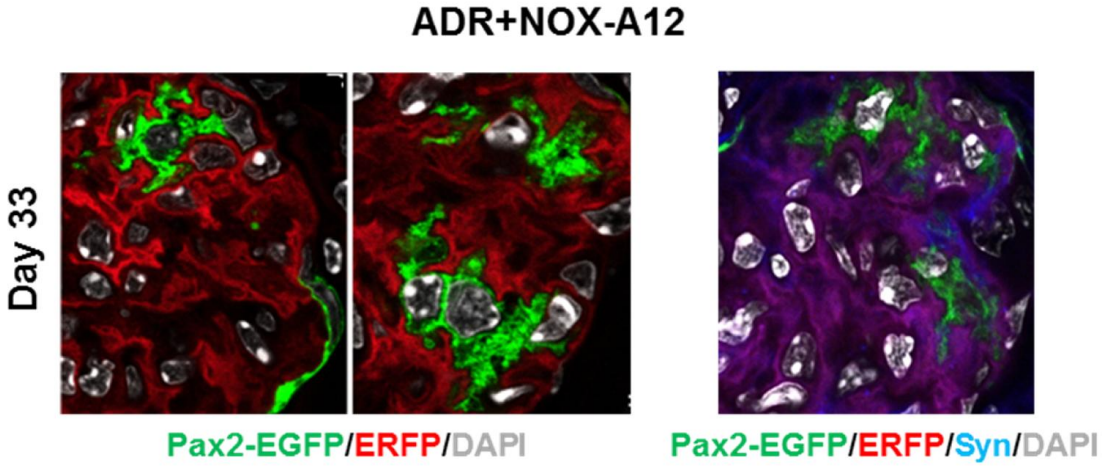

Figure 41. CXCL12 blockade induces activation of the renal prognitor cell-Pax2 cell toward *de-novo* podocytes in a Adriamycin nephropathy. AN was induced as described in methods 2.2. (**A**) Evaluation of the percentage of glomeruli with Pax2 derived podocytes upon treatment with NOX-A12 or revNOX-A12 (left graph), the number of Pax2-derived podocytes per glomerulus of all glomeruli (middle graph), the percentage of Pax2-derived podocytes positive for Syn over lost podocytes (right graph). (**B**) Representatives pictures with high magnification of Pax2-derived podocyte following NOX-A12 treatment on day 33. In panel B-left podocyte with Syn-co-staining, B-right panel, only endogenous IF colors. Data are means of ± SEM from 5 animals per group (*p<0.05 NOX-A12 treated AN mice versus revNOX-A12) group at day 33. Representative pictures, original magnification 600x.

Together, We show that blocking CXCL12 during AN can unblock the mouse RPCs from the CXCL12-induced quiescence, boosting the podocyte regeneration and ameliorates ANdisease markers and glomerular injury.

4.6.Therapeutic blockade of CXCL12 during Adriamycin nephropathy

This conclusive section investigated the possible use of CXCL12 blockade in the established disease contest. Here, I induced AN (see section methods 2.2) where the anti-CXCL12 treatment started one week after the disease induction. To investigate whether blocking CXCL12 therapeutically would be beneficial for the regeneration of RPCs during AN, mice were treated with NOX-A12 one week after the induction of AN till the end of the study. As shown in Figure 42A, the UACR ratio was significantly reduced upon NOX-A12 treatment compared with control revNOX-A12. Besides the UACR, the BUN level also has a decreased trend following NOX-A12 treatment (Figure 42B).

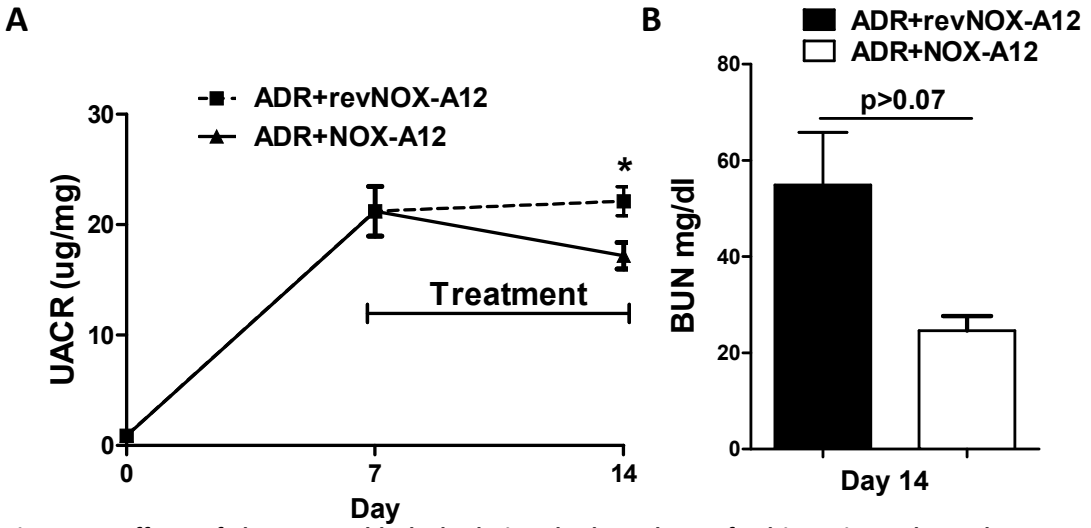

Figure 42. **Effects of the CXCL12 blockade during the late phase of Adriamycin nephropathy**. Mice were treated as described in methods section 2.2 to induce AN. Therapeutic CXCL12 blockade from day 7 protected the kidney during AN compared to the control group as shown by UACR (**A**). BUN also showed a positive trend when CXCL12 was blocked (**B**). The data are means ± SEM from 6-7 animals in each group. (*p<0.05 NOX-A12 treated AN mice versus revNOX-A12) at day 14.

Next, I evaluated the glomerular injury from kidney sections of NOX-A12 treated mice (Figure 43A). The data demonstrated that blocking CXCL12 with the NOX-A12 resulted in a significant increase in the number of normal and segmental lesions per glomeruli, whereas the number of global glomerular lesions decreased compared to the control revNOX-A12 group (Figure 43B). Furthermore, I assessed the percentage of crescent formations during AN, I found that inhibiting CXCL12 decreased the number of crescents in the kidney on day 14 (Figure 43C).

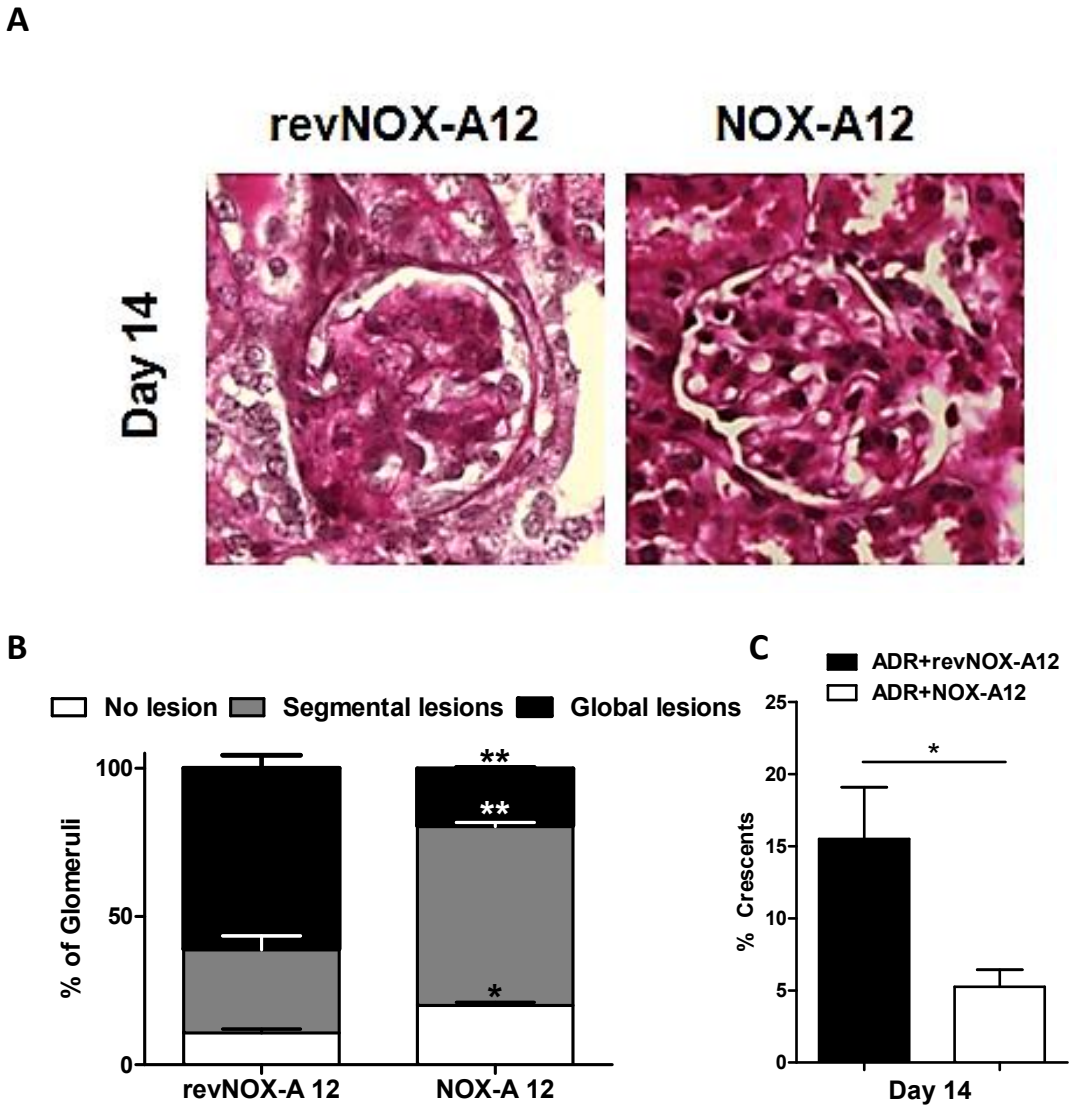

Figure 43. Therapeutic inhibition of CXCL12 decreased global lesions and crescents during Adriamycin nephropathy. Two Balb/c mouse groups of mice received subcutaneous injections of the CXCL12 inhibitor NOX-A12 or control revNOX-A12 from day 7 until day 14 after induction of AN (see,ethods section 2.2). (**A**) PAS staining showed that therapeutic CXCL12 blockade significantly reduced global glomerular lesions (**B**) as well as glomerular crescents on day 14 during AN (**C**). The data are means ± SEM from 6-7 animals per group. (*p<0.05, **p<0.01 NOX-A12 treated AN mice versus revNOX-A12) at day 14. Representative pictures, original magnification 400x.

4.6.1. Therapeutic blockade of CXCL12 in Adriamycin nephropathy increases podocyte numbers at the end of the treatment

After assessing the typical disease markers and morphological changes of the kidney, I evaluated the effect on podocytes using IF for nephrin and WT-1. As shown in Figure 44A, the number of double positive cells (Nephrin/WT-1) increased in the NOX-A12-treated mice compared to the control group, which was quantitatively confirmed by counting the number of podocytes per glomeruli (Figure 44B).

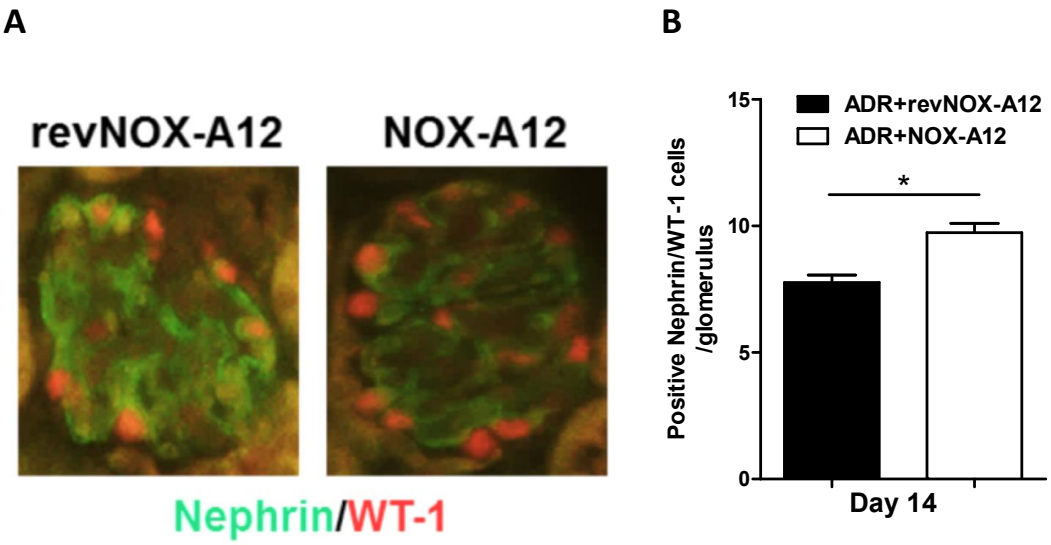

Figure 44. Podocyte counts increased in the kidney of therapeutic CXCL12 blockade Adriamycin nephropathy. Two Balb/c groups of mice received subcutaneous injections of the CXCL12 inhibitor NOX-A12 or revNOX-A12 from day 7 until day 14 after one week of established AN (see methods section 2.2). (**A**) Representative images of kidney glomerulus stained for the podocyte markers nephrin (green) and WT-1 (red). (**B**) Therapeutic CXCL12 blockade significantly increased the number of podocytes on day 14 after one week of treatment. The data are means of ± SEM from 6-7 animals per group. (*p<0.05 NOX-A12 treated AN mice versus revNOX-A12 mice). Original magnification 400x.

4.6.2. Notch pathway is activated in therapeutic blockade of CXCL12

Next, we stained kidney sections from mice treated with or without the CXCL12 inhibitor on day 14 for the activated domain NICD-3 (Figure 45). The fluorescence intensity of the NICD-3-activated domain was up-regulated inside the PECs when CXCL12 was blocked at day 14 compared to revNOX-A12. This indicates that CXCL12 was down-regulating the Notch signalling activity during established AN.

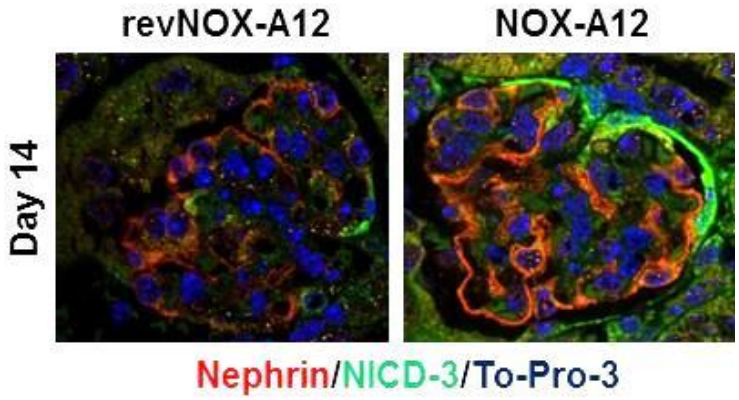

Figure 45. CXCL12 down-regulates Notch signaling activity in established Adriamycin nephropathy. Representative images of kidney sections stained for activated Notch-domain NICD-3 demonstrated that CXCL12 blockade increased the expression of Notch-3 in established AN compared to the control group. Original magnification is 400x.

In conclusion, the data demonstrate that therapeutic CXCL12 blockade was beneficial for a better outcome of established AN, in particular due to the glomerular induced Notch-RPCs-podocyte regeneration. This highlights the therapeutic potential of blocking CXCL12 during an establish FSGS.

5. Discussion

Glomerulonephritis represents an important kidney disease entity, however, little is known about the biological effects of the chemokine CXCL12 in glomerular homeostasis and disease, e.g. in AN. Studies have been performed to explore the role of CXCL12 in diabetic nephropathy (82, 83), however never in AN. This thesis provides further insights into the pathomechanisms involved in the progression during AN, and glomerular regeneration, in particular, the specific effects of CXCL12.

CXCL12 in the glomerulus is produced by podocytes in healthy and sick status. *Darisipudi, et al.* (82, 83) demonstrated that CXCL12 blockade is beneficial during diabetic nephropathy. However, the results of these studies left open questions about the molecular mechanisms of CXCL12. First, why do podocytes produce CXCL12 during glomerular homeostasis and injury? Second, how do the amelioration effects of CXCL12 blockade happen if the immune compartment is not involved? And third, how does CXCL12 blockade increase podocyte counts?

This thesis addressed the role of CXCL12 using several different research approaches:

1) Using mouse disease models based on podocyte-depletion and CXCL12 blockade.

2) Using mouse model based on specific podocyte progenitor lineage tracing.

3) Using RPCs to study the *de-novo* origin of podocytes and a possible link between CXCL12, podocytes and RPCs.

Our data now document a dual homeostatic effect on the terminally differentiated podocytes as well as on their local podocyte progenitor cells during homeostasis, injury, and repair. First, the constitutive expression of CXCL12 has an autocrine survival effect on podocytes, which helps them to withstand stress or injury. Second, CXCL12 expression promotes the quiescence of local podocyte progenitors, a mechanism that may support homeostasis but that also limits their regenerative capacity upon podocyte loss. Thus, while CXCL12 blockade can promote podocyte loss during the injury phase, it may enforce podocyte regeneration and improve long-term outcomes when administered in the regeneration phase of the glomerular disease. Until now, the functional significance of CXCL12 being constitutively released from podocytes is unknown. To test whether podocyte-derived CXCL12 can function in an autocrine manner during podocyte injury, human podocytes were exposed to ADR in the presence of either the active or inactive CXCL12 inhibitor. ADR significantly increased the podocyte cell death ratio. This stimulation was attenuated by extrinsic CXCL12 indicating a pro-survival effect of CXCL12 on human podocytes. CXCL12 inhibitor abrogated this protective effect of CXCL12. Further, we demonstrated in a specific mouse podocyte

depletion system that the blockade of intrinsic CXCL12 significantly aggravated UACR, which was associated with a lower number of podocytes. In another AN model, CXCL12 inhibition aggravated proteinuria in association with more glomerular injury and lower numbers of podocytes at the early time point. The analysis confirmed that CXCL12 inhibition accelerated the loss of preexisting podocytes. Thus, intrinsic CXCL12 was a podocyte survival factor and also reduced the ADR-induced CM by Notch pathway blockade. We further confirmed that CXCL12 was a homeostatic chemokine for mouse and human renal progenitor cells. *In-vitro* experiments demonstrated that extrinsic CXCL12 as well as podocyte-derived CXCL12 blockade increased the capability for the proliferation of renal progenitor cells and for their differentiation toward podocyte lineage. Also, we were able to show that RPCs proliferation was associated with the upregulation of the Notch pathway and that CXCL12 regulated this equilibrium. During a model of AN, CXCL12 blockade regulated the activation and proliferation of RPCs along the BC promoting the *de-novo* differentiation and replacement of lost podocytes during regeneration. This regeneration phenomenon was assessed using a lineage mouse model that showed *de-novo* PAX2-derived podocytes over the AN loss of podocytes. Finally, we determined using a therapeutic interventional mouse model that the late blockade of CXCL12 in established AN was able to promote podocyte regeneration resulting in positive outcomes regarding AN disease markers as well as UACR, BUN, and glomerular injury score. We conclude that CXCL12 inhibition could be a novel therapeutic strategy to promote podocyte regeneration upon injury and to prevent progressive glomerulosclerosis, one of the most common causes for end-stage renal disease.

CXCL12 is constitutively expressed by podocytes

CXCL12 was first described as a growth factor expressed in numerous hematopoietic and non-hematopoietic tissues e.g. bone marrow and lungs (72, 139). CXCL12 is known to be an essential regulator of progenitor cell homing and recruitment (73, 74), which includes bone marrow progenitors of the hematopoietic system as well as committed progenitors in peripheral tissues (75, 76). However, CXCL12 is also known as a "homeostatic" chemokine and it belongs to a category of chemokines that act independently of inflammation (140). In recent years, many studies demonstrated that CXCL12 is produced and secreted from podocytes during primitive glomeruli development and in healthy mature glomeruli, as shown by *Takabatake, at al.* when using a genetic mT/mG lineage-tracing mouse system (106). *Haege, et al*. showed with an elegant dual *in-situ* hybridization of ^{35}S labeled probes for CXCL12 and a DIG-labeled probe for the podocyte marker WT-1, that during capillary tuft development CXCL12/CXCR-4 signaling is necessary between podocytes and glomerular capillaries but also its activity in mature podocytes (103). For example *Balabian, et*

al. showed by IF that CXCL12 was produced by podocytes in the glomeruli of NZB/W mice with lupus nephritis (116). Further, CXCL12 blockade was performed during a mouse model of type 2 diabetic nephropathy, where *Sayyed, et al.* showed using immunofluorescent staining that CXCL12 was produced by podocytes in healthy, early and advanced diabetic nephropathy (83). They further demonstrated that CXCL12 blockade reduced glomerulosclerosis, UACR and increased podocyte counts (83). In this contest, my work confirmed these previous findings (Figure 46). Using immunofluorescent staining for Nephrin and CXCL12 on human-derived podocytes *in-vitro,* we showed that podocytes constitutively express CXCL12. Furthermore, I used immune and immunofluorescent staining on mouse kidney section showing that in healthy and glomerular disease conditions, podocytes are the major glomerular source of CXCL12 and that in normal mature glomeruli, podocytes constitutively express CXCL12 and this continues during AN.

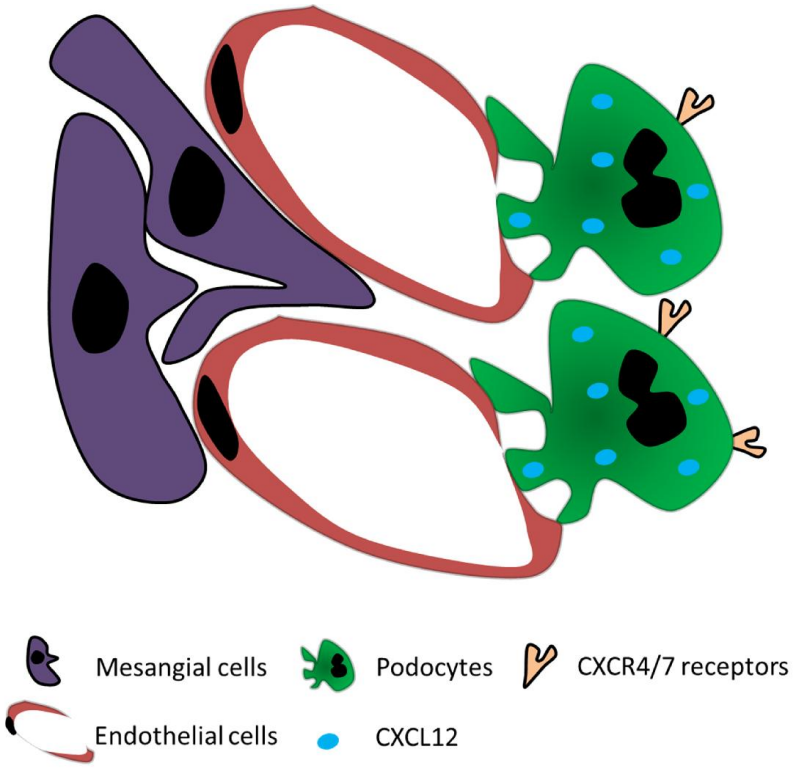

Figure 46. Diagram representing CXCL12 produces by podocytes in the glomerular environment. The podocytes are the glomerulus major source of CXCL12. We showed that during health and injury the CXCL12 Iis secrete the podocyte is to the glomerular environment.

CXCL12 is an autocrine survival factor by preventing Notch-mediated catastrophic mitosis

Podocytes are terminally differentiated cells that constitute their functional contribution to the glomerular filtration barrier via their complex structural interdigitations involving their actin cytoskeleton (3). Upon glomerular injury podocytes frequently enter the cell cycle to undergo hypertrophy but cell cycle arrest is needed to avoid accidental mitosis as mitosis requires the actin cytoskeleton to form the mitotic spindle, a process that is hardly compatible with maintaining the foot processes referred to as "mitotic catastrophe" (70). *Lasagni, et al*. showed with an elegant study, that podocytes catastrophic mitosis molecular mechanisms are connected with the Notch pathway (64). In particularly, they showed with an NICD-infected podocytes, that a persistent Notch pathway activation in podocytes induces the podocytes to cross over the G2/M checkpoint phase of the mitosis (64). Furthermore, podocytes undergoing forced nuclear division are unable to execute cytokinesis for the downregulation of Aurora kinase B, $p21^{Cip1/WAF-1}$ and $p27^{Kip1}$ (64) up which results in polyploid podocytes with a cytoskeleton disruptions, podocyte depletion and cell death via catastrophic mitosis (Figure 47). Moreover, *Lasagni, et al.* showed in human biopsies of FSGS and lupus nephritis by IF that Notch NICD domain1-2-3 as well as the downstream genes *Hey-1* and *Hes-1* were highly expressed in podocytes and RPCs (64). They also demonstrated in SCID mouse model of AN, without the interference of T lymphocytes, that 7 days after AN induction UACR increased in correlation with an over-expression of NICD-1-3 in podocytes co-stained for WT-1 and that this increased expression of NICD-3 correlated with an increased IF staining levels for active H3-Ser10, a marker for catastrophic mitosis. Also, electron microscopy at the late time point after 21 days showed catastrophic mitosis in podocytes (64). The loss of podocytes was reversible, as well as the increased UACR, if the induced AN mice were treated with the Notch pathway inhibitor DAPT. Treatment with DAPT until day 7 resulted in reduced IF positivity for H3-Ser10/Nephrin in podocytes and decreased levels of NICD-1-3 (64). Recently, *Mulay et al.* showed in an *in-vitro* experiment that human RPC-derived podocytes are going under catastrophic mitosis when stimulated with ADR. However, they reduced the impact of the ADR-induced catastrophic mitosis by blocking the cell cycle (136) and showed via IF that podocytes expressed high levels of murine double minute (MDM)-2. While using the MDM2 inhibitor nutlin-3a they were able to arrest the ADR-forced podocyte cell cycle in the G2/M checkpoint (136). Consequently, the arrest of the cell cycle reduced the podocytes in catastrophic mitosis *in-vitro* visible with negative IF staining for H3-Ser10 and normal alpha tubulin staining. *Mulay et al.* furthermore confirmed the effects on podocytes *in-vivo.* Treatment of AN with nutlin-3a ameliorated UACR, BUN, glomerular score compared to the control, and the podocyte count was higher when cell cycle was arrested (136). One further prove was that podocytes crossing the M phase of the cell cycle is required for podocytes to undergo catastrophic mitosis. *Migliorini, et*

al. demonstrated in a SCID AN mouse model treated with interferon-β that podocytes were more positive for H3-Ser10 compared to the control (141). In this context of induced podocyte catastrophic mitosis, my work introduced the concept that CXCL12 reduces catastrophic mitosis. My data provide evidence that podocyte-derived CXCL12 acts in an autocrine survival manner on podocytes by reducing Notch pathway activation and inhibiting aberrant podocyte mitosis leading to podocyte loss, i.e. mitotic catastrophe. Furthermore, using a Diphtheria toxin nephropathy, *in-vivo* model, CXCL12 blockade reduced podocyte counts and increased mortality of Diphtheria toxic treated mice. This was also the case when CXCL12 was blocked during the early time point of AN. Thus, CXCL12 is an intrinsic antagonist of Notch signaling and therefore, supports podocyte quiescence and homeostasis. In turn, Notch signaling is a known inducer of CXCL12 and CXCR-4 implying a balance based on a negative feedback loop between signals (142, 143) As a consequence, CXCL12 inhibition uncouples Notch signaling and subsequently promotes podocyte loss via mitotic catastrophe during acute glomerular injury. Together, we first showed that CXCL12 is an autocrine podocyte survival factor via inhibiting Notch-induced catastrophic mitosis.

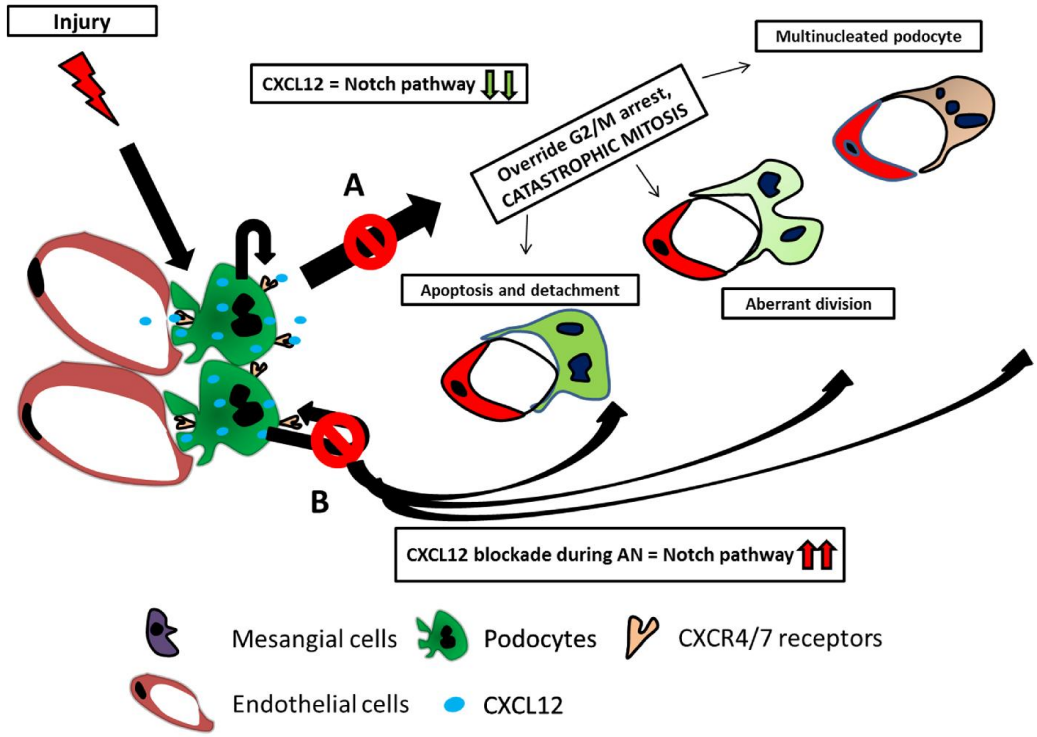

Figure 47. Diagram representing podocytes-derived CXCL12 during Adriamycin nephropathy and Notch-induced catastrophic mitosis. (**A**) During glomerular injury, podocytes produce CXCL12. CXCL12 acts in an autocrine manner in podocytes and can block the Notch pathway. Reducing the activation of the Notch pathway, podocyte cannot override the G2/M phase and undergo catastrophic mitosis. (**B**) CXCL12 blockade induces the activation of the Notch pathway in podocytes and drives them to catastrophic mitosis, apoptosis, and GBM detachment.

Podocyte-derived CXCL12 controls local renal progenitor cell quiescence

In previous studies, CXCL12 has been implicated not only in stem cell adhesion but also in the induction of stem cell proliferation/survival (144-146). In addition, CXCL12 was found to be critical for the development of several organs suggesting that this chemokine may play a role in the migration, adhesion, proliferation and survival of most adult progenitor cells (145). Some groups addressed the origin of such novel podocytes and consistently found intrarenal progenitor cells that permanently reside within the PECs layer along the Bowman´s capsule, called RPCs (27, 135). *Sagrinati, et al.* isolated a CD24+ CD133+ double positive cell population and characterized this population for staminal properties including self-renewal and clonogenic potential. The double positive CD24+ CD133+ PECs in comparison with the double negative control CD24- CD133- cells were able to proliferate for a long time in culture after isolation from the donor. Like the human embryonic kidney cell line (HEK), RPCs overexpressed the transcription factor Oct-4 and Bml-1 compared to the mature double negative cells (135). Furthermore, they enriched the RPCs population and found that RPCs have the capacity to differentiate under appropriate culture condition to multi-lineage cell types, e.g. podocytes and tubular cells within the glomerulus or into osteogenic and adipocyte extraglomerular cell lineage (46, 135). Within the same group, *Mazzinghi, et al*. did an extensive study looking at the role of CXCL12 on RPCs. They found by IF that adult stem cells expressed high levels of the CXCL12 receptors CXCR-4 and 7 using RT-PCR analysis and a ^{125}I-CXCL12 binding assay (88). As mentioned before, CXCL12 is required for the survival and anti-apoptotic effect of bone-marrow stem cells and adult stem cells. *Mazzinghi, et al*. confirmed that CXCL12 mediates the survival of RPCs, when CXCL12 is in close interaction with the receptor CXCR-7. In our study, we showed that podocytes are the major source of CXCL12 in homeostasis and injury, and that CXCL12 is a homeostatic RPC chemokine by reducing the capability of RPCs to proliferate. We also indirectly demonstrated using NS and directly using podocyte-derived CXCL12 that during the intensive loss of podocytes, there is a CXCL12 secreted from podocytes into Bowman´s space, which prevents RPCs activation and proliferation (Figure 48). This mechanism can be described as a security feedback loop of podocytes on RPCs to prevent the activation and over-proliferation of RPCs. Previous data have shown that CXCL12 expression can be further increased by podocytes during glomerulonephritis (116). This deregulation of CXCL12 production seems to be related to the development of nephritis (116). The CXCL12/CXCR-4 axis is involved in such excessive epithelial hyperplasia, which is presented as crescentic glomerulonephritis (35, 117). Recently, studies demonstrated that in diseases with massive loss of podocytes and loss of GBM, e.g. Alport syndrome and crescentic glomerulonephritis , committed PECs along the Bowman´s capsue trying to reduce crescent formation and FSGS (30, 31, 51). The homeostatic control of the RPCs is still not fully

understood (35). The pharmacological use of controlling RPCs is now under evaluation in the context of AN (27).

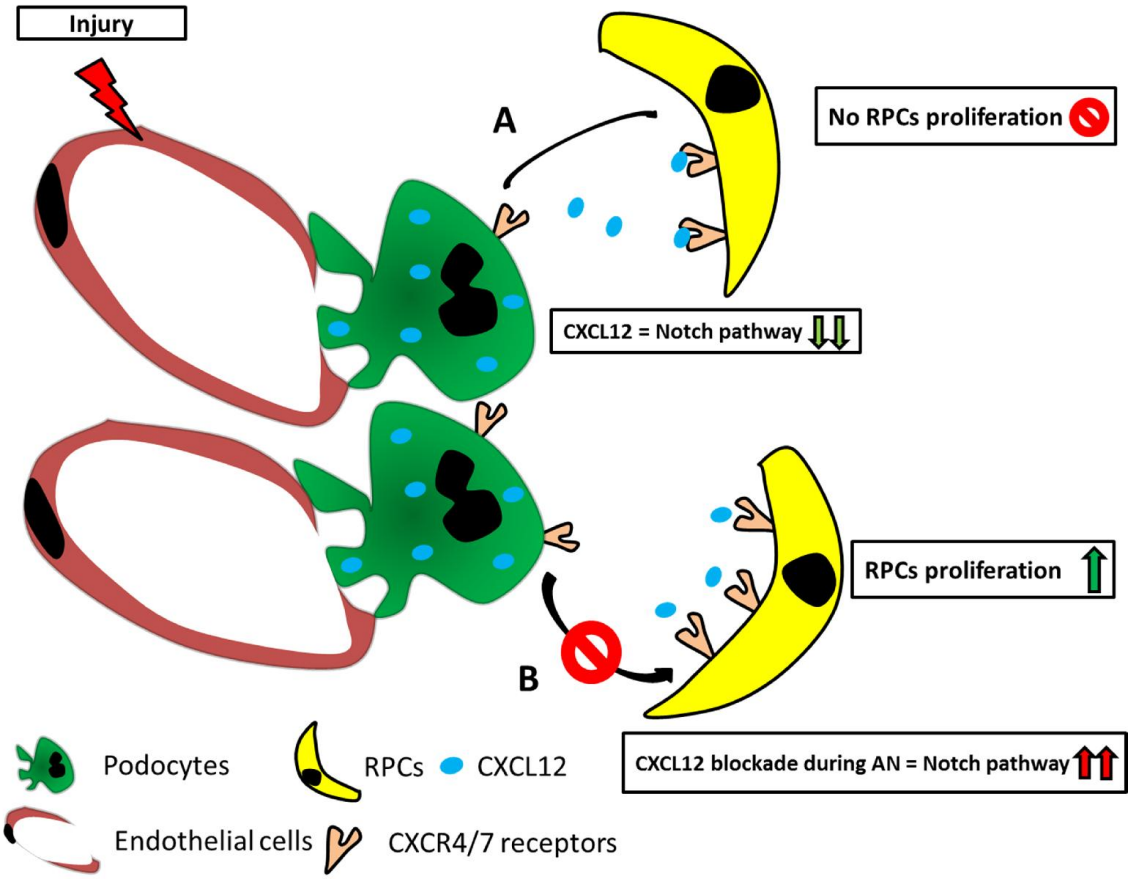

Figure 48. Diagram representing podocyte-derived CXCL12 controls local renal progenitor cell quiescence. (**A**) During glomerular injury, podocyte-derived CXCL12 acts as proliferation suppressor for RPCs, stops RPCs from overproliferation and starts to make crescents formations. (**B**) CXCL12 blockade during glomerular injury in the late phase of the disease leads RPCs to proliferate along the BC and RPCs can differentiate into *de-novo* podocytes.

Therapeutic CXCL12 blockade can enhance the regeneration of podocyte loss during glomerular injury from a local podocyte progenitor source

The course of CKD can be extremely variable. Commonly CKD originates from the glomerulus, where podocytes, the major components of the GBM, are lost or detached in a significant quantity with an estimation of more than 40% (26, 147). Certain renal diseases quickly lead to irreversible ESRD. In daily clinic practice, unluckily, the evidence for ERSD can be detected by UACR, BUN and creatinine, also using kidney biopsies when the disease is already manifested. There are no clinical methods available to repair podocyte damage. However, if the injury exceeds a certain threshold, podocyte hypertrophy reveals itself to be an unfit strategy over time, as the loss of podocytes and segmental sclerosis leads to podocyte detachment and a decreased ultrafiltration capacity (29). Since the RPCs were isolated and characterized, many studies had been performed to evaluate the regeneration capability of these RPCs in kidney diseases context. *Sagrinati, et al*. showed that during AKI induced by glycerol-rhabdomyolysis, the injection of human RPCs ameliorates the disease markers (135). Afterward, *Ronconi, et al.* showed in an AN model in SCID mice that injections of human RPCs ameliorate UACR, BUN and PAS score (28). These data was further confirmed by the work of *Peti-Peterdi, et al*. where they demonstrated by using multi-photon microscopy, that RPCs replaced the lost podocytes in a rat model of PAN-nephritis (glomerulonephritis, arteriolitis, and tubulointerstitial nephritis) (148). Further on, *Angelotti, et al*. confirmed that RPCs can differentiate into tubular lineage. Also, mice treated with human RPCs that were labeled with IF-cell marker, that RPCs were well engrafted in the mouse tubuli after one week and that RPCs showed proliferation activity to restore the damaged tubular cells in the injured nephrons and this was associated with amelioration on AKI disease markers (46). Later on, *Peired, et al*. unravel the mechanisms of RPCs activation and podocyte regeneration in AN. They investigated the impact of UACR on the regeneration of podocytes during AN, and found that RPCs differentiate into podocyte when retinol present in the urine was converted into retinoic acid in the Bowman´s space by the PECs RARE enzyme to become podocytes. When UACR is present in high levels, the lack of albumin in the Bowman´s space is binding the retinol and blocking the differentiation of RPCs into podocytes, which leads activated PECs to make crescent formations (56). *Wanner, et al*. data revealed that podocyte generation is mainly confined to glomerular development and may occur after acute glomerular injury, but this does not relate to podocytes in aging kidneys or in response to nephron loss (132). *Lasagni, et al.* partially unraveled the role of the Notch pathway during AN. They showed that different phases of AN require differential activation of the Notch pathway. Notch pathway activation during the injury phase of AN induces podocyte catastrophic mitosis and consequently aggravation of the AN. During the recovery phase of AN activation of the Notch

pathway leads to RPCs proliferation and differentiation into podocyte lineage followed by an amelioration of UACR and other disease markers (64). The inhibition of Notch via pharmaceutical modulation with DAPT was one of the first studies were the authors tried to modulate the behavior of RPCs during AN (64). In a follow-up study, the outcome of AN was modulated by boosting podocyte regeneration via enhancing the capabilities of RPCs to differentiate in the presence of the inhibitor Glycogen synthase kinase 3, also known as BIO (glycogen synthase inhibitor 6-Bromo-Indirubin-3´-Oxime) (27). Glycogen synthase kinase 3 treatment *in-vivo* using a lineage-tracing *Pax2*-mT/mG reporter system significantly increased disease remission by enhancing the sensitivity of renal progenitors to endogenous retinoic acid. This data emphasized the possibility to pharmacological enhance the differentiation of RPCs by using Glycogen synthase kinase 3 (27). Interestingly, our previous data on CXCL12 blockade during diabetic nephropathy showed that NOX-A12 treatment prevented the progression of glomerulosclerosis in uninephrectomized diabetic mice without involving glomerular leukocyte recruitment but increasing numbers of podocytes (83). Also *Darisipudi, et al*. demonstrated that CXCL12 blockade maintained podocyte numbers and renal *Nephrin* and *Podocin* mRNA expression during diabetic nephropathy of uninephrectomized mice. Consistently, CXCL12 blockade suppressed nephrin mRNA up-regulation in RPCs induced to differentiate toward the podocyte lineage (82). Moreover, CXCL12 blockade suppressed UACR and was associated with the highest levels of glomerular filtration rate (82). However, the findings on diabetic nephropathy seem to be consistent, whereas the authors of the previous studies did not investigate whether the beneficial effects of CXCL12 blockade on podocyte numbers relates to a protective effect on podocyte death/detachment or from enhanced podocyte regeneration by RPCs. The data within this thesis now showed that extrinsic CXCL12 suppressed the proliferation of RPCs and their differentiation into podocytes as indicated by decreased *Nephrin, Podocin*, and *CD2AP* expression. In contrast, when CXCL12 was blocked using NOX-A12, RPCs were able to proliferate and differentiate into podocytes, highlighting an important regulatory role for CXCL12. The data herein provide evidence that soluble mediators released from necrotic podocytes can stimulate RPCs to proliferate, which was further enhanced following CXCL12 inhibition. This indicated that the mitogenic capacity of necrotic cell components can be dampened via intrinsic CXCL12. This was consistent with previous reports showing that Notch signaling is a well-characterized mitogenic stimulus for RPCs and podocytes (64, 149). IF staining illustrated localized expression of NICD-3 in podocytes and parietal epithelial cells within injured glomeruli, which markedly increased upon CXCL12 inhibition. This indicates that podocyte-derived CXCL12 suppresses Notch signaling, which further leads to the inhibition of RPCs to proliferate and to differentiate into podocytes. The healing phase after an acute podocyte injury was initiated can either lead to regeneration of the glomerular

structures and proteinuria remission or to scar formation and persistent renal dysfunction (50, 150). The data showed that unlike treatment with the CXCL12 inhibitor during the early onset of AN, CXCL12 blockade subsequently increased podocyte numbers and attenuated albuminuria, glomerular lesions, and renal dysfunction when AN has already been established. It is important to mention that the number of podocytes had further declined from week one to two in mice treated with the inactive CXCL12 inhibitor, whereas during the same period of time CXCL12 blockade had significantly increased the number of podocytes after AN has been established. This was consistent with a significant increase in renal *Nephrin* and *WT-1* mRNA expression following CXCL12 blockade. These data suggested that CXCL12 has a dual role in acute glomerular injury and acts as a podocyte survival factor during the acute injury phase but promotes glomerular regeneration during the healing phase. The *in-vitro* results suggest that podocyte-derived CXCL12 enforces the quiescent state of podocyte progenitor cells within the PECs layer along the BC and that therapeutic CXCL12 inhibition can enhance their differentiation into podocytes. In an *in-vivo* model of AN using *Pax2.rtTA; TetO.Cre; mT/mG* mice for lineage tracing of RPCs (27), CXCL12 inhibition significantly reduced UACR after four weeks compared to the control inhibitor, which was associated with a significant increase in the number of Pax2+ cells within the glomerular tuft that were also double positive for the podocyte marker synaptopodin. Finally, the therapeutic blockade of CXCL12 during the healing phase resulted in an enhancement of RPC-related podocyte regeneration and improved the functional outcomes of glomerular injury.

Taken together, the data within this thesis demonstrate that the constitutive expression of CXCL12 by podocytes has a homeostatic effect on local stem cells conceptually similar to its role in the bone marrow and in other stem cell niches (Figure 49A) (151). The differential effect of CXCL12 influences terminally differentiated podocytes and local podocyte progenitor cells during homeostasis, injury, and repair. Podocyte-derived CXCL12 serves as a podocyte survival factor by blocking the activation of the Notch signaling pathway. It is possible that CXCL12 released from podocytes might block the mitotic process under homeostatic conditions preventing mitotic catastrophe and podocyte loss during a glomerular injury (Figure 49C). Podocyte-derived CXCL12 is also responsible for maintaining quiescence of Pax2+ podocyte progenitor cells within the PECs layer along the Bowman´s capsule via suppressing Notch signaling. Although, CXCL12 is an important driver during homeostasis, it can limit progenitor cells to regenerate lost podocytes during a glomerular injury (Figure 49B).

The data presented in this thesis also need to be interpreted under the light of our technical limitations. I started this research based on a previous observation within our group, that was

confirmed through animal models and special techniques by Romagnani and colleagues. Many questions have been raised but not all of them have been answered yet. I investigated the connection between CXCL12 and the Notch pathway using different approaches, including human cells and mouse models. These approaches were quite obligated considering the lack of knowledge and surface antibodies to identify RPCs in mice. Currently, there are no such antibodies available to stain for CD24 in rodent kidneys. RPCs have been characterized first in the human context due to the possibility using well-known surface markers like CD24 and CD133. They were used to isolate RPCs from fresh human kidney material and for staining them on human kidney disease biopsies (45, 135). The results obtained from *in-vitro* RPCs cell culture models are indicative. Cell culture, and in particular stem cell culture is a powerful method to unravel molecular mechanisms and proprieties of RPCs. However, one has to keep in mind that cell culture is an artificial system, where many variables can influence cells, e.g. medium composition, time of exposure to grow factors, percentage of FBS concentration, the missing microenvironment, and cell-cell contacts. These factors can influence the proliferation and differentiation of stem cells. So far, I have used the best known approaches to induce RPCs to differentiate into podocyte lineage. It is clear that *in-vitro* experiments are indispensable for the basic research, compounds first screening effects or pre-clinical drugs toxicity tests. However, promising drug *in-vitro* tests can not always predict what will happen in animal models or humans .

For expanding our scientific knowledge about human diseases human clinical trials would be the best approach. However, this is not always possible, especially in kidney science. Even for well-characterized and solid new experimental drugs, the way to reach the human experimentation is very restricted to ethical guidelines. Previously, a few cases, have been reported, where drugs were tested in preclinical studies that immediately got approved by the FDA without carrying out human trials, e.g. the immunotherapy Ab-based for B cell leukemia. Normally, the immediate solution for testing biological and toxic variabilities of compounds/drugs will be carried out in primates, like monkeys. Experiments on primate monkeys are also not available for daily basic research work due to ethical and moral matters, the animal number, infrastructures and the high cost involved. An exception are worldwide health emergencies, like the recent Ebola outbreak in West Africa and the HIV disease. Hence, the mouse model is predominantly the best animal model available for small laboratory needs. Mice have fast reproduction cycle with a lot of offspring, limited needs for space and relatively easy environmental life conditions. Also the mouse genetic modification opened many possibilities: knock-out/-in gene technology, antibiotic gene promoter inducible protein expression system-CRE recombinase and the cell lineage specific tracing-system, are now essential tools for basic researchers. However, one should always pay attention, which animal model would be

appropriate in terms of efficiency, reproducibility, reliability and model contextualization. The recent past is full of promising models that did not fully achieve the expectations in mimicking the actual disease setting. In our hands, using the lineage tracing system based on the *Podocin* promotor (*Pax2*-mT/mG system), we were able to fully characterize and trace renal stem cells in mice that are based on embryonic kidney observations. Currently, it is the only model available; however this might be replaced by a more precise technic for adult stem cell tracing in the future. We are still lacking a clear pattern of mouse surface markers to characterize RPCs like available for identifying human RPCs.

Another experimental limitation in this thesis is the kidney disease model used. Adriamycin nephropathy is only one of the pathological causes inducing FSGS. Also in human FSGS does not represent the predominant human form of kidney disease. However, the AN mouse model is a reliable, fast and quite predictable model, unlike other animal models of kidney disease that are based on chemical induction, e.g. aristolochic acid or cisplatin tubular injury models. Furthermore, within this thesis we have shown that for identifying the mechanisms connecting the Notch pathway and CXCL12, the timing of the treatment was essential. These differential effects of CXCL12 blockade could be an obstacle to perform efficient therapeutic regimes in long-term kidney diseases, e.g. kidney diabetes disease, kidney compliances of systemic lupus erythematosus or GBM disruption like the Alport syndrome .

In conclusion, despite all these scientific limitation of this experimental work, I conclude that CXCL12 inhibition could be a good candidate for a novel therapeutic strategy to promote podocyte regeneration upon injury and to prevent progressive glomerulosclerosis, one of the most common causes for end-stage renal disease.

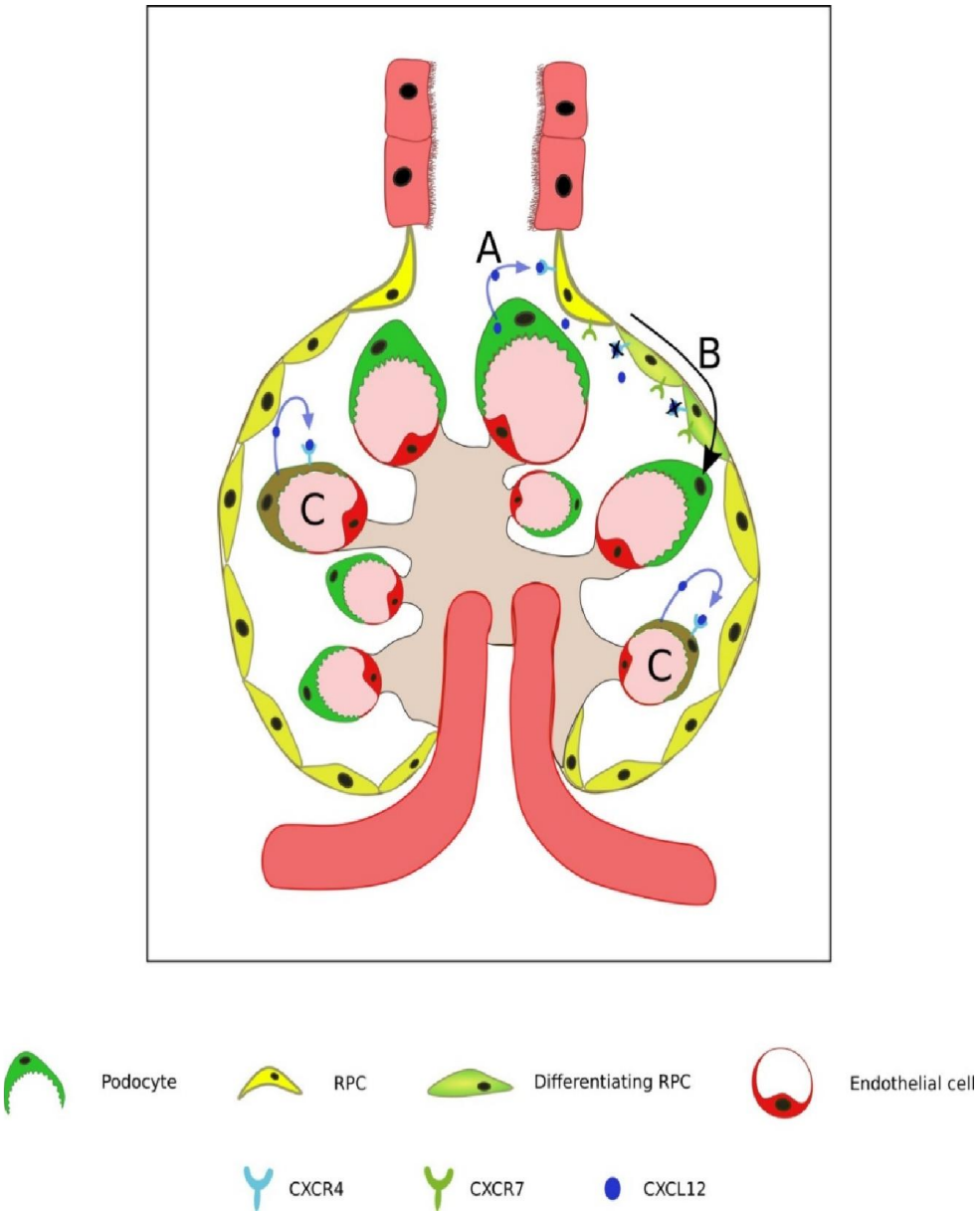

Figure 49. Diagram representing the renal progenitor regeneration during kidney injury. Glomerular compartment: The parietal epithelial cells along the Bowman´s capsule harbor RPCs. Podocytes produce CXCL12, which keeps the RPCs largely in an immobile and quiescent state (**A**). Loss of CXCL12-producing podocytes or therapeutic blockade of CXCL12 activates RPCs proliferation and their differentiation into podocytes (**B**). Furthermore, podocyte-derived CXCL12 also acts as a survival factor in an autocrine fashion (**C**).

6. Conclusion

The research presented within this thesis focused on the functional role of CXCL12 and glomerular regeneration during the pathogenesis of AN, and provides new insights into a potential pro-regenerative therapy in targeting CXCL12 to ameliorates CKD.

The findings of the current study have multiple implications that are listed as followed

- Podocyte secrete CXCL12
- CXCL12 blockade can attenuate progressive glomerulosclerosis
- *In-vitro* CXCL12 protected human podocytes from toxic injury
- *In-vivo* early blockade of intrinsic CXCL12 aggravated proteinuria
- Continued blockade of intrinsic CXCL12 during the course of ADR nephropathy significantly attenuated podocyte loss, proteinuria, and glomerulosclerosis.
- CXCL12 suppressed progenitor growth
- CXCL12 blockade significantly increased podocytes via Pax2+ mouse podocyte progenitor-mediated podocyte regeneration

Taken together, the findings highlight the importance of podocyte-derived CXCL12 as a crucial mediator of RPC regeneration during FSGS.

7. Future Directions

Podocyte-derived CXCL12 has been shown to serve as a podocyte survival factor during podocyte injury and can promote podocyte progenitor quiescence. Future investigations are needed to unravel the molecular mechanisms associated with podocyte mitotic catastrophe. Miotic catastrophe is an ongoing process during AN, which has been proven by the group of Romagnani. Within this thesis, CXCL12 can act as a survival factor for podocytes by preventing Notch-mediated mitotic catastrophe of podocytes highlighting a link between CXCL12 and the Notch pathway during the process of mitotic catastrophe.

One way to investigate this is to perform an experimental model of AN based on a *Podocin*-lineage-tracing system. Similar to the previously used Pax2 mouse model, the induction of a specific podocyte tomato red/green report system would be very useful. Following induction of AN, mice will be treated with the CXCL12 inhibitor NOX-A12 and control revNOX-A12 for two weeks. To test the consequent impact of Notch signaling on CM and regeneration of podocytes, mice will be treated with the Notch inhibitor DAPT at the same time like the NOX-A12 during AN (Figure 46). The final readout in this model will be to quantify the remaining number of green-EGFP-podocin podocytes after the induction of CM compared to the control. This will provide further insight into the mechanisms by which CXCL12 regulates podocyte mitotic catastrophe and regeneration of podocytes.

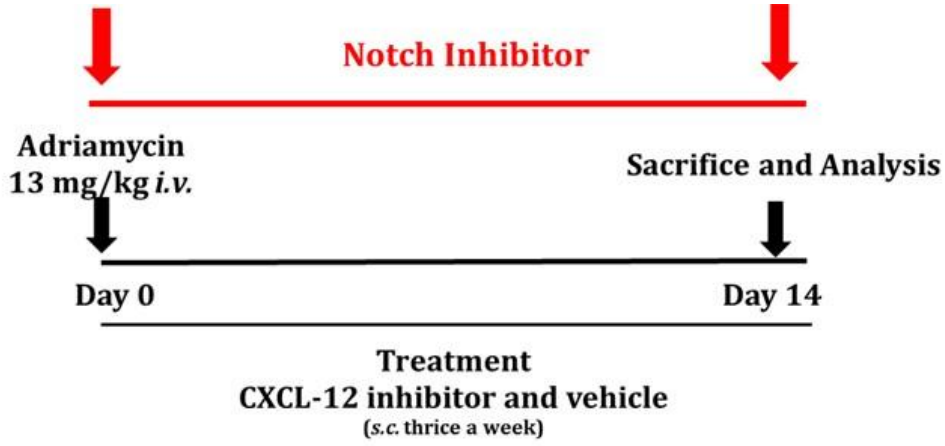

Figure 50. Adriamycin nephropathy model in Balb/c using CXCL12 and Notch inhibitors

8. References

1. Eckardt KU, Coresh J, Devuyst O, Johnson RJ, Kottgen A, Levey AS, et al. Evolving importance of kidney disease: from subspecialty to global health burden. Lancet. 2013;382(9887):158-69. Epub 2013/06/04.
2. Schieppati A, Remuzzi G. Chronic renal diseases as a public health problem: epidemiology, social, and economic implications. Kidney international Supplement. 2005(98):S7-S10. Epub 2005/08/20.
3. Reiser J, Sever S. Podocyte biology and pathogenesis of kidney disease. Annual review of medicine. 2013;64:357-66.
4. Kriz W, Lemley KV. A potential role for mechanical forces in the detachment of podocytes and the progression of CKD. Journal of the American Society of Nephrology : JASN. 2015;26(2):258-69. Epub 2014/07/26.
5. Miner JH. The glomerular basement membrane. Experimental cell research. 2012;318(9):973-8.
6. Menon MC, Chuang PY, He CJ. The glomerular filtration barrier: components and crosstalk. International journal of nephrology. 2012;2012:749010.
7. Pavenstadt H, Kriz W, Kretzler M. Cell biology of the glomerular podocyte. Physiological reviews. 2003;83(1):253-307.
8. Jefferson JA, Nelson PJ, Najafian B, Shankland SJ. Podocyte disorders: Core Curriculum 2011. American journal of kidney diseases : the official journal of the National Kidney Foundation. 2011;58(4):666-77.
9. Greka A, Mundel P. Cell biology and pathology of podocytes. Annual review of physiology. 2012;74:299-323.
10. Patrie KM, Drescher AJ, Welihinda A, Mundel P, Margolis B. Interaction of two actin-binding proteins, synaptopodin and alpha-actinin-4, with the tight junction protein MAGI-1. The Journal of biological chemistry. 2002;277(33):30183-90.
11. Lombardi D, Lasagni L. Transgenic Strategies to Study Podocyte Loss and Regeneration. Stem cells international. 2015;2015:678347. Epub 2015/06/20.
12. D'Agati VD, Kaskel FJ, Falk RJ. Focal segmental glomerulosclerosis. The New England journal of medicine. 2011;365(25):2398-411.
13. Smeets B, Dijkman HB, Wetzels JF, Steenbergen EJ. Lessons from studies on focal segmental glomerulosclerosis: an important role for parietal epithelial cells? The Journal of pathology. 2006;210(3):263-72.
14. Hinkes BG, Mucha B, Vlangos CN, Gbadegesin R, Liu J, Hasselbacher K, et al. Nephrotic syndrome in the first year of life: two thirds of cases are caused by mutations in 4 genes (NPHS1, NPHS2, WT1, and LAMB2). Pediatrics. 2007;119(4):e907-19.
15. Santin S, Garcia-Maset R, Ruiz P, Gimenez I, Zamora I, Pena A, et al. Nephrin mutations cause childhood- and adult-onset focal segmental glomerulosclerosis. Kidney international. 2009;76(12):1268-76.
16. Kim JM, Wu H, Green G, Winkler CA, Kopp JB, Miner JH, et al. CD2-associated protein haploinsufficiency is linked to glomerular disease susceptibility. Science. 2003;300(5623):1298-300.
17. Boute N, Gribouval O, Roselli S, Benessy F, Lee H, Fuchshuber A, et al. NPHS2, encoding the glomerular protein podocin, is mutated in autosomal recessive steroid-resistant nephrotic syndrome. Nature genetics. 2000;24(4):349-54.
18. Iijima K, Someya T, Ito S, Nozu K, Nakanishi K, Matsuoka K, et al. Focal segmental glomerulosclerosis in patients with complete deletion of one WT1 allele. Pediatrics. 2012;129(6):e1621-5.
19. Benetti E, Caridi G, Malaventura C, Dagnino M, Leonardi E, Artifoni L, et al. A novel WT1 gene mutation in a three-generation family with progressive isolated focal segmental glomerulosclerosis. Clinical journal of the American Society of Nephrology : CJASN. 2010;5(4):698-702.
20. Mundel P, Kriz W. Structure and function of podocytes: an update. Anatomy and embryology. 1995;192(5):385-97.

21. LeHir M, Kriz W. New insights into structural patterns encountered in glomerulosclerosis. Current opinion in nephrology and hypertension. 2007;16(3):184-91.
22. Steffes MW, Schmidt D, McCrery R, Basgen JM, International Diabetic Nephropathy Study G. Glomerular cell number in normal subjects and in type 1 diabetic patients. Kidney international. 2001;59(6):2104-13.
23. Kriz W, Kretzler M, Nagata M, Provoost AP, Shirato I, Uiker S, et al. A frequent pathway to glomerulosclerosis: deterioration of tuft architecture-podocyte damage-segmental sclerosis. Kidney & blood pressure research. 1996;19(5):245-53.
24. Shankland SJ. The podocyte's response to injury: role in proteinuria and glomerulosclerosis. Kidney international. 2006;69(12):2131-47.
25. Nagata M, Nakayama K, Terada Y, Hoshi S, Watanabe T. Cell cycle regulation and differentiation in the human podocyte lineage. The American journal of pathology. 1998;153(5):1511-20.
26. Kriz W. Podocyte is the major culprit accounting for the progression of chronic renal disease. Microscopy research and technique. 2002;57(4):189-95.
27. Lasagni L, Angelotti ML, Ronconi E, Lombardi D, Nardi S, Peired A, et al. Podocyte Regeneration Driven by Renal Progenitors Determines Glomerular Disease Remission and Can Be Pharmacologically Enhanced. Stem cell reports. 2015;5(2):248-63. Epub 2015/08/04.
28. Ronconi E, Sagrinati C, Angelotti ML, Lazzeri E, Mazzinghi B, Ballerini L, et al. Regeneration of glomerular podocytes by human renal progenitors. Journal of the American Society of Nephrology : JASN. 2009;20(2):322-32. Epub 2008/12/19.
29. Wiggins RC. The spectrum of podocytopathies: a unifying view of glomerular diseases. Kidney international. 2007;71(12):1205-14.
30. Ryu M, Migliorini A, Miosge N, Gross O, Shankland S, Brinkkoetter PT, et al. Plasma leakage through glomerular basement membrane ruptures triggers the proliferation of parietal epithelial cells and crescent formation in non-inflammatory glomerular injury. The Journal of pathology. 2012. Epub 2012/05/04.
31. Smeets B, Uhlig S, Fuss A, Mooren F, Wetzels JF, Floege J, et al. Tracing the origin of glomerular extracapillary lesions from parietal epithelial cells. Journal of the American Society of Nephrology : JASN. 2009;20(12):2604-15.
32. Kriz W, Lemley KV. The role of the podocyte in glomerulosclerosis. Current opinion in nephrology and hypertension. 1999;8(4):489-97.
33. Matsusaka T, Xin J, Niwa S, Kobayashi K, Akatsuka A, Hashizume H, et al. Genetic engineering of glomerular sclerosis in the mouse via control of onset and severity of podocyte-specific injury. Journal of the American Society of Nephrology : JASN. 2005;16(4):1013-23.
34. Wharram BL, Goyal M, Wiggins JE, Sanden SK, Hussain S, Filipiak WE, et al. Podocyte depletion causes glomerulosclerosis: diphtheria toxin-induced podocyte depletion in rats expressing human diphtheria toxin receptor transgene. Journal of the American Society of Nephrology : JASN. 2005;16(10):2941-52.
35. Lasagni L, Romagnani P. Glomerular epithelial stem cells: the good, the bad, and the ugly. Journal of the American Society of Nephrology : JASN. 2010;21(10):1612-9. Epub 2010/09/11.
36. Wang Y, Wang YP, Tay YC, Harris DC. Progressive adriamycin nephropathy in mice: sequence of histologic and immunohistochemical events. Kidney international. 2000;58(4):1797-804.
37. Lee VW, Harris DC. Adriamycin nephropathy: a model of focal segmental glomerulosclerosis. Nephrology. 2011;16(1):30-8.
38. Gewirtz DA. A critical evaluation of the mechanisms of action proposed for the antitumor effects of the anthracycline antibiotics adriamycin and daunorubicin. Biochemical pharmacology. 1999;57(7):727-41.
39. Otaki Y, Miyauchi N, Higa M, Takada A, Kuroda T, Gejyo F, et al. Dissociation of NEPH1 from nephrin is involved in development of a rat model of focal segmental glomerulosclerosis. American journal of physiology Renal physiology. 2008;295(5):F1376-87.

40. Lee VW, Wang Y, Qin X, Wang Y, Zheng G, Mahajan D, et al. Adriamycin nephropathy in severe combined immunodeficient (SCID) mice. Nephrology, dialysis, transplantation : official publication of the European Dialysis and Transplant Association - European Renal Association. 2006;21(11):3293-8.
41. Kriz W. Progressive renal failure--inability of podocytes to replicate and the consequences for development of glomerulosclerosis. Nephrology, dialysis, transplantation : official publication of the European Dialysis and Transplant Association - European Renal Association. 1996;11(9):1738-42.
42. Lasagni L, Lazzeri E, Shankland SJ, Anders HJ, Romagnani P. Podocyte mitosis - a catastrophe. Current molecular medicine. 2013;13(1):13-23.
43. Romagnani P. Toward the identification of a "renopoietic system"? Stem Cells. 2009;27(9):2247-53. Epub 2009/09/10.
44. Sagrinati C, Ronconi E, Lazzeri E, Lasagni L, Romagnani P. Stem-cell approaches for kidney repair: choosing the right cells. Trends in molecular medicine. 2008;14(7):277-85.
45. Lazzeri E, Crescioli C, Ronconi E, Mazzinghi B, Sagrinati C, Netti GS, et al. Regenerative potential of embryonic renal multipotent progenitors in acute renal failure. Journal of the American Society of Nephrology : JASN. 2007;18(12):3128-38. Epub 2007/11/06.
46. Angelotti ML, Ronconi E, Ballerini L, Peired A, Mazzinghi B, Sagrinati C, et al. Characterization of renal progenitors committed toward tubular lineage and their regenerative potential in renal tubular injury. Stem Cells. 2012;30(8):1714-25.
47. Fogo AB. Mechanisms of progression of chronic kidney disease. Pediatr Nephrol. 2007;22(12):2011-22. Epub 2007/07/25.
48. Romagnani P, Kalluri R. Possible mechanisms of kidney repair. Fibrogenesis & tissue repair. 2009;2(1):3.
49. Moeller MJ, Smeets B. Role of parietal epithelial cells in kidney injury: the case of rapidly progressing glomerulonephritis and focal and segmental glomerulosclerosis. Nephron Exp Nephrol. 2014;126(2):97.
50. Shankland SJ, Smeets B, Pippin JW, Moeller MJ. The emergence of the glomerular parietal epithelial cell. Nature reviews Nephrology. 2014;10(3):158-73. Epub 2014/01/29.
51. Smeets B, Kuppe C, Sicking EM, Fuss A, Jirak P, van Kuppevelt TH, et al. Parietal epithelial cells participate in the formation of sclerotic lesions in focal segmental glomerulosclerosis. Journal of the American Society of Nephrology : JASN. 2011;22(7):1262-74. Epub 2011/07/02.
52. Smeets B, Angelotti ML, Rizzo P, Dijkman H, Lazzeri E, Mooren F, et al. Renal progenitor cells contribute to hyperplastic lesions of podocytopathies and crescentic glomerulonephritis. Journal of the American Society of Nephrology : JASN. 2009;20(12):2593-603. Epub 2009/10/31.
53. Romagnani P, Lasagni L, Remuzzi G. Renal progenitors: an evolutionary conserved strategy for kidney regeneration. Nature reviews Nephrology. 2013;9(3):137-46. Epub 2013/01/23.
54. Chambers SM, Shaw CA, Gatza C, Fisk CJ, Donehower LA, Goodell MA. Aging hematopoietic stem cells decline in function and exhibit epigenetic dysregulation. PLoS biology. 2007;5(8):e201.
55. Conboy IM, Conboy MJ, Wagers AJ, Girma ER, Weissman IL, Rando TA. Rejuvenation of aged progenitor cells by exposure to a young systemic environment. Nature. 2005;433(7027):760-4.
56. Peired A, Angelotti ML, Ronconi E, la Marca G, Mazzinghi B, Sisti A, et al. Proteinuria impairs podocyte regeneration by sequestering retinoic acid. Journal of the American Society of Nephrology : JASN. 2013;24(11):1756-68. Epub 2013/08/21.
57. Morgan TH. The Theory of the Gene. The American Naturalist 1917;51(609):31.
58. Wharton KA, Johansen KM, Xu T, Artavanis-Tsakonas S. Nucleotide sequence from the neurogenic locus notch implies a gene product that shares homology with proteins containing EGF-like repeats. Cell. 1985;43(3 Pt 2):567-81. Epub 1985/12/01.
59. Borggrefe T, Oswald F. The Notch signaling pathway: transcriptional regulation at Notch target genes. Cellular and molecular life sciences : CMLS. 2009;66(10):1631-46. Epub 2009/01/24.
60. Bray SJ. Notch signalling: a simple pathway becomes complex. Nature reviews Molecular cell biology. 2006;7(9):678-89. Epub 2006/08/22.
61. Iso T, Kedes L, Hamamori Y. HES and HERP families: multiple effectors of the Notch signaling pathway. Journal of cellular physiology. 2003;194(3):237-55. Epub 2003/01/28.

62. Fischer A, Gessler M. Delta-Notch--and then? Protein interactions and proposed modes of repression by Hes and Hey bHLH factors. Nucleic acids research. 2007;35(14):4583-96. Epub 2007/06/26.
63. Kageyama R, Ohtsuka T. The Notch-Hes pathway in mammalian neural development. Cell research. 1999;9(3):179-88. Epub 1999/10/16.
64. Lasagni L, Ballerini L, Angelotti ML, Parente E, Sagrinati C, Mazzinghi B, et al. Notch activation differentially regulates renal progenitors proliferation and differentiation toward the podocyte lineage in glomerular disorders. Stem Cells. 2010;28(9):1674-85.
65. Wilson A, Radtke F. Multiple functions of Notch signaling in self-renewing organs and cancer. FEBS letters. 2006;580(12):2860-8. Epub 2006/04/01.
66. Okuyama R, Tagami H, Aiba S. Notch signaling: its role in epidermal homeostasis and in the pathogenesis of skin diseases. Journal of dermatological science. 2008;49(3):187-94. Epub 2007/07/13.
67. Dormoy V, Jacqmin D, Lang H, Massfelder T. From development to cancer: lessons from the kidney to uncover new therapeutic targets. Anticancer research. 2012;32(9):3609-17. Epub 2012/09/21.
68. Glotzer M. The molecular requirements for cytokinesis. Science. 2005;307(5716):1735-9. Epub 2005/03/19.
69. Faul C, Asanuma K, Yanagida-Asanuma E, Kim K, Mundel P. Actin up: regulation of podocyte structure and function by components of the actin cytoskeleton. Trends in cell biology. 2007;17(9):428-37. Epub 2007/09/07.
70. Lasagni L, Lazzeri E, Shankland SJ, Anders HJ, Romagnani P. Podocyte mitosis - a catastrophe. Current molecular medicine. 2012.
71. Neef R, Klein UR, Kopajtich R, Barr FA. Cooperation between mitotic kinesins controls the late stages of cytokinesis. Current biology : CB. 2006;16(3):301-7.
72. Nagasawa T, Hirota S, Tachibana K, Takakura N, Nishikawa S, Kitamura Y, et al. Defects of B-cell lymphopoiesis and bone-marrow myelopoiesis in mice lacking the CXC chemokine PBSF/SDF-1. Nature. 1996;382(6592):635-8. Epub 1996/08/15.
73. Nagasawa T, Kikutani H, Kishimoto T. Molecular cloning and structure of a pre-B-cell growth-stimulating factor. Proceedings of the National Academy of Sciences of the United States of America. 1994;91(6):2305-9. Epub 1994/03/15.
74. Shahnazari M, Chu V, Wronski TJ, Nissenson RA, Halloran BP. CXCL12/CXCR4 signaling in the osteoblast regulates the mesenchymal stem cell and osteoclast lineage populations. FASEB journal : official publication of the Federation of American Societies for Experimental Biology. 2013;27(9):3505-13. Epub 2013/05/25.
75. Yang S, Edman LC, Sanchez-Alcaniz JA, Fritz N, Bonilla S, Hecht J, et al. Cxcl12/Cxcr4 signaling controls the migration and process orientation of A9-A10 dopaminergic neurons. Development. 2013;140(22):4554-64. Epub 2013/10/25.
76. Baggiolini M. Chemokines and leukocyte traffic. Nature. 1998;392(6676):565-8. Epub 1998/04/29.
77. Anders HJ. Immune system modulation of kidney regeneration--mechanisms and implications. Nature reviews Nephrology. 2014;10(6):347-58. Epub 2014/04/30.
78. Hamed S, Egozi D, Dawood H, Keren A, Kruchevsky D, Ben-Nun O, et al. The chemokine stromal cell-derived factor-1alpha promotes endothelial progenitor cell-mediated neovascularization of human transplanted fat tissue in diabetic immunocompromised mice. Plastic and reconstructive surgery. 2013;132(2):239e-50e. Epub 2013/07/31.
79. Ho CY, Sanghani A, Hua J, Coathup MJP, Kalia P, Blunn G. Mesenchymal stem cells with increased SDF-1 expression enhanced fracture healing. Tissue engineering Part A. 2014. Epub 2014/09/25.
80. Peled A, Petit I, Kollet O, Magid M, Ponomaryov T, Byk T, et al. Dependence of human stem cell engraftment and repopulation of NOD/SCID mice on CXCR4. Science. 1999;283(5403):845-8. Epub 1999/02/05.

81. Michineau S, Franck G, Wagner-Ballon O, Dai J, Allaire E, Gervais M. Chemokine (C-X-C motif) receptor 4 blockade by AMD3100 inhibits experimental abdominal aortic aneurysm expansion through anti-inflammatory effects. Arteriosclerosis, thrombosis, and vascular biology. 2014;34(8):1747-55. Epub 2014/05/31.
82. Darisipudi MN, Kulkarni OP, Sayyed SG, Ryu M, Migliorini A, Sagrinati C, et al. Dual blockade of the homeostatic chemokine CXCL12 and the proinflammatory chemokine CCL2 has additive protective effects on diabetic kidney disease. The American journal of pathology. 2011;179(1):116-24. Epub 2011/06/28.
83. Sayyed SG, Hagele H, Kulkarni OP, Endlich K, Segerer S, Eulberg D, et al. Podocytes produce homeostatic chemokine stromal cell-derived factor-1/CXCL12, which contributes to glomerulosclerosis, podocyte loss and albuminuria in a mouse model of type 2 diabetes. Diabetologia. 2009;52(11):2445-54. Epub 2009/08/27.
84. Liu Y, Carson-Walter E, Walter KA. Chemokine receptor CXCR7 is a functional receptor for CXCL12 in brain endothelial cells. PloS one. 2014;9(8):e103938. Epub 2014/08/02.
85. Ding YL, Fu QY, Tang SF, Zhang JL, Li ZY, Li ZT. [Effect of stromal cell-derived factor-1 and its receptor CXCR4 on liver metastasis of human colon cancer]. Zhonghua wai ke za zhi [Chinese journal of surgery]. 2009;47(3):210-3. Epub 2009/07/01.
86. Vater A, Klussmann S. Turning mirror-image oligonucleotides into drugs: the evolution of Spiegelmer therapeutics. Drug discovery today. 2014. Epub 2014/09/23.
87. Wang Y, Liang WC, Pan WL, Law WK, Hu JS, Ip DT, et al. Silibinin, a novel chemokine receptor type 4 antagonist, inhibits chemokine ligand 12-induced migration in breast cancer cells. Phytomedicine : international journal of phytotherapy and phytopharmacology. 2014;21(11):1310-7. Epub 2014/08/31.
88. Mazzinghi B, Ronconi E, Lazzeri E, Sagrinati C, Ballerini L, Angelotti ML, et al. Essential but differential role for CXCR4 and CXCR7 in the therapeutic homing of human renal progenitor cells. The Journal of experimental medicine. 2008;205(2):479-90. Epub 2008/02/13.
89. Liu H, Liu S, Li Y, Wang X, Xue W, Ge G, et al. The role of SDF-1-CXCR4/CXCR7 axis in the therapeutic effects of hypoxia-preconditioned mesenchymal stem cells for renal ischemia/reperfusion injury. PloS one. 2012;7(4):e34608. Epub 2012/04/19.
90. Moll NM, Ransohoff RM. CXCL12 and CXCR4 in bone marrow physiology. Expert review of hematology. 2010;3(3):315-22. Epub 2010/11/19.
91. Jung Y, Shiozawa Y, Wang J, Patel LR, Havens AM, Song J, et al. Annexin-2 is a regulator of stromal cell-derived factor-1/CXCL12 function in the hematopoietic stem cell endosteal niche. Experimental hematology. 2011;39(2):151-66 e1. Epub 2010/11/27.
92. Liu N, Tian J, Cheng J, Zhang J. Migration of CXCR4 gene-modified bone marrow-derived mesenchymal stem cells to the acute injured kidney. Journal of cellular biochemistry. 2013;114(12):2677-89. Epub 2013/06/25.
93. Ma M, Ye JY, Deng R, Dee CM, Chan GC. Mesenchymal stromal cells may enhance metastasis of neuroblastoma via SDF-1/CXCR4 and SDF-1/CXCR7 signaling. Cancer letters. 2011;312(1):1-10. Epub 2011/09/13.
94. Martin C, Burdon PC, Bridger G, Gutierrez-Ramos JC, Williams TJ, Rankin SM. Chemokines acting via CXCR2 and CXCR4 control the release of neutrophils from the bone marrow and their return following senescence. Immunity. 2003;19(4):583-93. Epub 2003/10/18.
95. Zhang Z, Zhong W, Hall MJ, Kurre P, Spencer D, Skinner A, et al. CXCR4 but not CXCR7 is mainly implicated in ocular leukocyte trafficking during ovalbumin-induced acute uveitis. Experimental eye research. 2009;89(4):522-31. Epub 2009/06/16.
96. de Vivar Chevez AR, Finke J, Bukowski R. The role of inflammation in kidney cancer. Advances in experimental medicine and biology. 2014;816:197-234. Epub 2014/05/14.
97. Gahan JC, Gosalbez M, Yates T, Young EE, Escudero DO, Chi A, et al. Chemokine and chemokine receptor expression in kidney tumors: molecular profiling of histological subtypes and association with metastasis. The Journal of urology. 2012;187(3):827-33. Epub 2012/01/17.

98. Kawakami Y, Ii M, Matsumoto T, Kuroda R, Kuroda T, Kwon SM, et al. SDF-1/CXCR4 Axis in Tie2-lineage Cells Including Endothelial Progenitor Cells Contributes to Bone Fracture Healing. Journal of bone and mineral research : the official journal of the American Society for Bone and Mineral Research. 2014. Epub 2014/08/19.
99. Zhang XY, Su C, Cao Z, Xu SY, Xia WH, Xie WL, et al. CXCR7 upregulation is required for early endothelial progenitor cell-mediated endothelial repair in patients with hypertension. Hypertension. 2014;63(2):383-9. Epub 2013/11/06.
100. Ochoa-Espinosa A, Affolter M. Branching morphogenesis: from cells to organs and back. Cold Spring Harbor perspectives in biology. 2012;4(10). Epub 2012/07/17.
101. Gerrits H, van Ingen Schenau DS, Bakker NE, van Disseldorp AJ, Strik A, Hermens LS, et al. Early postnatal lethality and cardiovascular defects in CXCR7-deficient mice. Genesis. 2008;46(5):235-45. Epub 2008/04/30.
102. Ara T, Tokoyoda K, Okamoto R, Koni PA, Nagasawa T. The role of CXCL12 in the organ-specific process of artery formation. Blood. 2005;105(8):3155-61. Epub 2005/01/01.
103. Haege S, Einer C, Thiele S, Mueller W, Nietzsche S, Lupp A, et al. CXC chemokine receptor 7 (CXCR7) regulates CXCR4 protein expression and capillary tuft development in mouse kidney. PloS one. 2012;7(8):e42814. Epub 2012/08/11.
104. Dona E, Barry JD, Valentin G, Quirin C, Khmelinskii A, Kunze A, et al. Directional tissue migration through a self-generated chemokine gradient. Nature. 2013;503(7475):285-9. Epub 2013/09/27.
105. Grone HJ, Cohen CD, Grone E, Schmidt C, Kretzler M, Schlondorff D, et al. Spatial and temporally restricted expression of chemokines and chemokine receptors in the developing human kidney. Journal of the American Society of Nephrology : JASN. 2002;13(4):957-67. Epub 2002/03/26.
106. Takabatake Y, Sugiyama T, Kohara H, Matsusaka T, Kurihara H, Koni PA, et al. The CXCL12 (SDF-1)/CXCR4 axis is essential for the development of renal vasculature. Journal of the American Society of Nephrology : JASN. 2009;20(8):1714-23. Epub 2009/05/16.
107. Floege J, Smeets B, Moeller MJ. The SDF-1/CXCR4 axis is a novel driver of vascular development of the glomerulus. Journal of the American Society of Nephrology : JASN. 2009;20(8):1659-61. Epub 2009/07/18.
108. Rankin SM. Chemokines and adult bone marrow stem cells. Immunology letters. 2012;145(1-2):47-54. Epub 2012/06/16.
109. Anders HJ, Romagnani P, Mantovani A. Pathomechanisms: homeostatic chemokines in health, tissue regeneration, and progressive diseases. Trends in molecular medicine. 2014;20(3):154-65. Epub 2014/01/21.
110. Hernandez PA, Gorlin RJ, Lukens JN, Taniuchi S, Bohinjec J, Francois F, et al. Mutations in the chemokine receptor gene CXCR4 are associated with WHIM syndrome, a combined immunodeficiency disease. Nature genetics. 2003;34(1):70-4. Epub 2003/04/15.
111. Ma Q, Jones D, Borghesani PR, Segal RA, Nagasawa T, Kishimoto T, et al. Impaired B-lymphopoiesis, myelopoiesis, and derailed cerebellar neuron migration in CXCR4- and SDF-1-deficient mice. Proceedings of the National Academy of Sciences of the United States of America. 1998;95(16):9448-53. Epub 1998/08/05.
112. Broxmeyer HE, Orschell CM, Clapp DW, Hangoc G, Cooper S, Plett PA, et al. Rapid mobilization of murine and human hematopoietic stem and progenitor cells with AMD3100, a CXCR4 antagonist. The Journal of experimental medicine. 2005;201(8):1307-18. Epub 2005/04/20.
113. Vater A, Sahlmann J, Kroger N, Zollner S, Lioznov M, Maasch C, et al. Hematopoietic stem and progenitor cell mobilization in mice and humans by a first-in-class mirror-image oligonucleotide inhibitor of CXCL12. Clinical pharmacology and therapeutics. 2013;94(1):150-7. Epub 2013/04/17.
114. Ostendorf T, Kunter U, Eitner F, Loos A, Regele H, Kerjaschki D, et al. VEGF(165) mediates glomerular endothelial repair. The Journal of clinical investigation. 1999;104(7):913-23. Epub 1999/10/08.

115. Rizzo P, Perico N, Gagliardini E, Novelli R, Alison MR, Remuzzi G, et al. Nature and mediators of parietal epithelial cell activation in glomerulonephritides of human and rat. The American journal of pathology. 2013;183(6):1769-78. Epub 2013/10/08.
116. Balabanian K, Couderc J, Bouchet-Delbos L, Amara A, Berrebi D, Foussat A, et al. Role of the chemokine stromal cell-derived factor 1 in autoantibody production and nephritis in murine lupus. J Immunol. 2003;170(6):3392-400. Epub 2003/03/11.
117. Sicking EM, Fuss A, Uhlig S, Jirak P, Dijkman H, Wetzels J, et al. Subtotal ablation of parietal epithelial cells induces crescent formation. Journal of the American Society of Nephrology : JASN. 2012;23(4):629-40. Epub 2012/01/28.
118. Barisoni L, Nelson PJ. Collapsing glomerulopathy: an inflammatory podocytopathy? Current opinion in nephrology and hypertension. 2007;16(3):192-5. Epub 2007/04/11.
119. Neusser MA, Lindenmeyer MT, Moll AG, Segerer S, Edenhofer I, Sen K, et al. Human nephrosclerosis triggers a hypoxia-related glomerulopathy. The American journal of pathology. 2010;176(2):594-607. Epub 2009/12/19.
120. Reichel RR. Acute kidney injury: quoi de neuf? The Ochsner journal. 2014;14(3):359-68. Epub 2014/09/25.
121. Lotan D, Sheinberg N, Kopolovic J, Dekel B. Expression of SDF-1/CXCR4 in injured human kidneys. Pediatr Nephrol. 2008;23(1):71-7. Epub 2007/11/01.
122. Lameire N, Van Biesen W, Vanholder R. The changing epidemiology of acute renal failure. Nature clinical practice Nephrology. 2006;2(7):364-77. Epub 2006/08/26.
123. Stokman G, Stroo I, Claessen N, Teske GJ, Florquin S, Leemans JC. SDF-1 provides morphological and functional protection against renal ischaemia/reperfusion injury. Nephrology, dialysis, transplantation : official publication of the European Dialysis and Transplant Association - European Renal Association. 2010;25(12):3852-9. Epub 2010/06/04.
124. Blanpain C, Horsley V, Fuchs E. Epithelial stem cells: turning over new leaves. Cell. 2007;128(3):445-58. Epub 2007/02/10.
125. Remuzzi G, Benigni A, Remuzzi A. Mechanisms of progression and regression of renal lesions of chronic nephropathies and diabetes. The Journal of clinical investigation. 2006;116(2):288-96. Epub 2006/02/03.
126. Bo CJ, Chen B, Jia RP, Zhu JG, Cao P, Liu H, et al. Effects of ischemic preconditioning in the late phase on homing of endothelial progenitor cells in renal ischemia/reperfusion injury. Transplantation proceedings. 2013;45(2):511-6. Epub 2013/03/19.
127. Klussmann S, Nolte A, Bald R, Erdmann VA, Furste JP. Mirror-image RNA that binds D-adenosine. Nature biotechnology. 1996;14(9):1112-5. Epub 1996/09/01.
128. Liu SC, Alomran R, Chernikova SB, Lartey F, Stafford J, Jang T, et al. Blockade of SDF-1 after irradiation inhibits tumor recurrences of autochthonous brain tumors in rats. Neuro-oncology. 2014;16(1):21-8. Epub 2013/12/18.
129. Roccaro AM, Sacco A, Purschke WG, Moschetta M, Buchner K, Maasch C, et al. SDF-1 Inhibition Targets the Bone Marrow Niche for Cancer Therapy. Cell reports. 2014;9(1):118-28. Epub 2014/09/30.
130. Thomas MN, Kalnins A, Andrassy M, Wagner A, Klussmann S, Rentsch M, et al. SDF-1/CXCR4/CXCR7 is pivotal for vascular smooth muscle cell proliferation and chronic allograft vasculopathy. Transplant international : official journal of the European Society for Organ Transplantation. 2015. Epub 2015/08/13.
131. Hoellenriegel J, Zboralski D, Maasch C, Rosin NY, Wierda WG, Keating MJ, et al. The Spiegelmer NOX-A12, a novel CXCL12 inhibitor, interferes with chronic lymphocytic leukemia cell motility and causes chemosensitization. Blood. 2014;123(7):1032-9. Epub 2013/11/28.
132. Wanner N, Hartleben B, Herbach N, Goedel M, Stickel N, Zeiser R, et al. Unraveling the role of podocyte turnover in glomerular aging and injury. Journal of the American Society of Nephrology : JASN. 2014;25(4):707-16. Epub 2014/01/11.

133. Buch T, Heppner FL, Tertilt C, Heinen TJ, Kremer M, Wunderlich FT, et al. A Cre-inducible diphtheria toxin receptor mediates cell lineage ablation after toxin administration. Nature methods. 2005;2(6):419-26. Epub 2005/05/24.
134. Mulay SR, Thomasova D, Ryu M, Anders HJ. MDM2 (murine double minute-2) links inflammation and tubular cell healing during acute kidney injury in mice. Kidney international. 2012. Epub 2012/02/03.
135. Sagrinati C, Netti GS, Mazzinghi B, Lazzeri E, Liotta F, Frosali F, et al. Isolation and characterization of multipotent progenitor cells from the Bowman's capsule of adult human kidneys. Journal of the American Society of Nephrology : JASN. 2006;17(9):2443-56. Epub 2006/08/04.
136. Mulay SR, Thomasova D, Ryu M, Kulkarni OP, Migliorini A, Bruns H, et al. Podocyte loss involves MDM2-driven mitotic catastrophe. The Journal of pathology. 2013;230(3):322-35. Epub 2013/06/12.
137. Dressler GR. Epigenetics, development, and the kidney. Journal of the American Society of Nephrology : JASN. 2008;19(11):2060-7. Epub 2008/08/22.
138. Ye Y, Wang B, Jiang X, Hu W, Feng J, Li H, et al. Proliferative capacity of stem/progenitor-like cells in the kidney may associate with the outcome of patients with acute tubular necrosis. Human pathology. 2011;42(8):1132-41. Epub 2011/02/15.
139. Liu Y, Wu BQ, Geng H, Xu ML, Zhong HH. Association of chemokine and chemokine receptor expression with the invasion and metastasis of lung carcinoma. Oncology letters. 2015;10(3):1315-22. Epub 2015/12/02.
140. Moser B, Wolf M, Walz A, Loetscher P. Chemokines: multiple levels of leukocyte migration control. Trends in immunology. 2004;25(2):75-84. Epub 2004/04/23.
141. Migliorini A, Angelotti ML, Mulay SR, Kulkarni OO, Demleitner J, Dietrich A, et al. The antiviral cytokines IFN-alpha and IFN-beta modulate parietal epithelial cells and promote podocyte loss: implications for IFN toxicity, viral glomerulonephritis, and glomerular regeneration. The American journal of pathology. 2013;183(2):431-40. Epub 2013/06/12.
142. Mirandola L, Apicella L, Colombo M, Yu Y, Berta DG, Platonova N, et al. Anti-Notch treatment prevents multiple myeloma cells localization to the bone marrow via the chemokine system CXCR4/SDF-1. Leukemia. 2013;27(7):1558-66. Epub 2013/01/29.
143. Xie J, Wang W, Si JW, Miao XY, Li JC, Wang YC, et al. Notch signaling regulates CXCR4 expression and the migration of mesenchymal stem cells. Cellular immunology. 2013;281(1):68-75. Epub 2013/03/12.
144. Romagnani P, Lasagni L, Mazzinghi B, Lazzeri E, Romagnani S. Pharmacological modulation of stem cell function. Current medicinal chemistry. 2007;14(10):1129-39. Epub 2007/04/26.
145. Kortesidis A, Zannettino A, Isenmann S, Shi S, Lapidot T, Gronthos S. Stromal-derived factor-1 promotes the growth, survival, and development of human bone marrow stromal stem cells. Blood. 2005;105(10):3793-801. Epub 2005/01/29.
146. Broxmeyer HE, Cooper S, Kohli L, Hangoc G, Lee Y, Mantel C, et al. Transgenic expression of stromal cell-derived factor-1/CXC chemokine ligand 12 enhances myeloid progenitor cell survival/antiapoptosis in vitro in response to growth factor withdrawal and enhances myelopoiesis in vivo. J Immunol. 2003;170(1):421-9. Epub 2002/12/24.
147. Kriz W, LeHir M. Pathways to nephron loss starting from glomerular diseases-insights from animal models. Kidney international. 2005;67(2):404-19. Epub 2005/01/28.
148. Peti-Peterdi J, Sipos A. A high-powered view of the filtration barrier. Journal of the American Society of Nephrology : JASN. 2010;21(11):1835-41. Epub 2010/06/26.
149. El Machhour F, Keuylian Z, Kavvadas P, Dussaule JC, Chatziantoniou C. Activation of Notch3 in Glomeruli Promotes the Development of Rapidly Progressive Renal Disease. J Am Soc Nephrol. 2015;26(7):1561-75.
150. Peired A, Lazzeri E, Lasagni L, Romagnani P. Glomerular regeneration: when can the kidney regenerate from injury and what turns failure into success? Nephron Exp Nephrol. 2014;126(2):70.

151. Sugiyama T, Kohara H, Noda M, Nagasawa T. Maintenance of the hematopoietic stem cell pool by CXCL12-CXCR4 chemokine signaling in bone marrow stromal cell niches. Immunity. 2006;25(6):977-88.

9. Abbreviations

AN	ADR-induced nephropathy
ATN	Acute Tubular Necrosis
ATRA	All-Trans Retinoic Acid
AKI	Acute Kidney Injury
UACR	Urinary Albumin to Creatinine Ratio
ADR	Adriamycin
BUN	Blood Urea Nitrogen
CD24	Cluster of Differentiation-24
CD133	Prominin-1
CKD	Chronic Kidney Disease
CXCL12/SDF-1	Stromal Derived Factor- 1
CD2AP	CD2-Associated Protein
CXCR	Chemokine C-X-C motif Receptor
DAPT	N-[N-(3,5-Difluorophenacetyl)-L-alanyl]-S-phenylglycine t-butyl ester
Dll-1	Delta-like protein 1
DMEM-F12	Dulbecco Eagle Modified Medium Ham F-12
DT	Diphtheria Toxin
EBM	Endothelial Cell Basal Medium
ERSD	End Renal Stage Disease
EGM-MV	Endothelial Cell Growth Medium
FSGS	Focal Segmental Glomerulosclerosis
GBM	Glomerular Basement Membrane
GN	Glomerulonephritis
BIO	Glycogen synthase inhibitor 6-bromo-indirubin-3´-oxime
Hey-1	Hairy/enhancer-of-split related with YRPW motif protein 1
Hes-1	Hairy and enhancer of split-1
HEK	Human embryonic Kidney cells
IF	Immunofluorescent staining

IHC	Immunohistochemistry staining
Jag-1	Jagged-1
Jag-2	Jagged-2
KDIGO	Kidney Disease Improving Global Outcomes
MPGN	Membrano-proliferative glomerulonephritis
NPHS1	Nephrin
NPHS2	Podocin
Notch-1	Notch homolog 1, translocation-associated
Notch-2	Notch homolog 2, translocation-associated
Notch-3	Notch homolog 3, translocation-associated
NICD-1	Notch Intracellular Domain-1
NICD-3	Notch Intracellular Domain-3
NS	Podocyte's derived necrotic Supernatant
PAS	Periodic acid–Schiff staining
PECs	Parietal epithelial cells
RA	Retinoic Acid
RPCs	Human renal progenitor cells
TLRs	Toll-like Receptors
TECs	Tubular epithelial cells
SCID	Severe Combined Immunodeficiency
FSGS	Focal segmental glomerulosclerosis
VEGF	Vascular Endothelial Growth Factor
WT-1	Wilm´s tumor 1

10. Appendix

Composition of buffers used

FACS Buffer:	BSA 3%, NaN3 0.05% and PBS1x (see below)-1
IF Buffers:	PBS1x, BSA3%,PBS1x, 0.5% Saponin
RIPA Buffer:	50 mM Tris-HCl (pH 8);150 mM NaCl, 1% NP-40; 0,05%sodium deoxycholate, 0.1% SDS
For 1000 ml	Tris-HCL 6.057 g, NaCl 8.772 g, NP-40 10mL, Sodium deoxycholate 0.5mL, SDS 1mL
EDTA 2mM:	EDTA 7.44 mg in 10 ml HBSS (without Ca, Mg) To be preheated in 37 $^{\circ}$C water bath before use
PBS:	2.74 M NaCl, 54mM KCl, 30mM KH_2PO_4, 130mM Na_2HPO_4, in ddH_20, adjust to pH 7.5 with HCl
Gel Running Buffer 10x:	Tris-NaCl 30g, Glycine 144g, SDS 5g make up volume 1000mL with pH 8.3
Transfer Buffer 1x:	Tris-Nacl 1.5g, Glycine 7.2 make up to 500mL
TBS 10x:	Tris 24.23g, NaCl 80.06g, HCl circa 17.5mL and make up volume 1000mL (pH7.6)
TBS-T 1x:	TBS (1x) 1000mL and Tween 20 1mL
Sample Buffer:	Millipore water 3.8mL , 0.5 M Tris-NaCl pH6.8 1mL, Glycerol 0.8mL, 10%SDS 1.6mL, 2-mercaptoethanol 0.4mL and 1% Bromophenol 0.4mL
Separating Buffer:	Tris (1.5mM), SDS 400mg muke up volume to 100mL (pH8.8)
Stacking Buffer:	Tris (0.5M), SDS 400mg make up volume to 100mL (pH6.8)
Staining Solution:	Methanol 500mL, Acetic acid 100mL, Water 400mL, Coomasie Brilliant Blue R 2.5g (0.25%)
Destaining solution:	Methanol 150mL, Acetic Acid, 100mL, Water 750mL

UNIVERSITÀ
DEGLI STUDI
FIRENZE

DIPARTIMENTO DI
MEDICINA SPERIMENTALE
E CLINICA

Florence, 1 November 2015

Duccio Lombardi and Laura Lasagni, we declared that Simone Romoli, from the University of Munich-LMU, got the permission to include inside his Ph.D thesis, our figures from the article "Transgenic Strategies to Study Podocyte Loss and Regeneration". Accordantly with the international copyright rules of Creative Commons Attribution License, which permits unrestricted use, distribution, and reproduction in any medium, provided the original work is properly cited.

Laura Lasagni

Duccio Lombardi

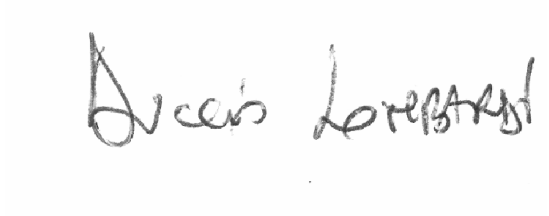

Acknowledgement

It's time to say thank you for these wonderful and full four years of life in Bavaria.

There are not enough words to express my gratitude to my mother, my sister, my father and to all my grandmothers, for their constant love and encouragement through my abroad adventure. Grazie di cuore.

I would like to thanks and to express my gratitude to my mentor and supervisor Prof. Dr. Hans-Joachim Anders. He provided me guidance and advice during my research work. I appreciated his trust in my scientific skills and support which contribute to my progress as a scientist.

Many thanks to all my "German" colleagues and friends, from Munich: Julian, Alexander, Jyaysi, Mohsen, Marc, Dana, Khader, Kirstin, Henny, Maciej, Mi, Onkar, Tomo, Daigo, Mary, Jenny, Bea, Anais, Andrei, Melissa, Martin, Jhon, Jhonny, Nico, Anja and all medical students for all your help and for the delightful time we had together.

Many thanks are necessary for Dr. Bruno Luckow, Dr. Volker Vielhauer and Dr. Peter Nelson and their respective teams for their support and suggestions during my research work throughout my stay in the Nephrology Center.

Special and super thanks to Katharina Witte. I will miss you "mama".

Many thanks to my Garching Italian friends: Nicola, "Parente" and Michele. Grazie di tutto!

It is my pleasure to thank Prof. Dr. Stefan Endres, Leader of GRAKO1202, LMU, for allowing me to become a member of graduate students network during my Ph.D. and for the incredible experience of the Immunofest.

I would like to acknowledge Prof. Paola Romagnani (University of Florence, Italy) for giving me the opportunity to perform part of my work on their laboratory and providing me outstanding experimental supports for my research work.

Many thanks to all the lab colleagues and friends, from Florence; Anna, Elena, Laura, Marialucia, Francesca. Benedetta, Duccio, Sara, for all your help and for the delightful time we had together.

I would like to express my gratitude to Ewa, Dan, and Jana for providing skillful technical assistance to carry out the research work successfully.

Especially to Shrikant and Santhosh, thank you, you have helped me and have been my friend since the first day of my adventure in Munich. Thank you for sharing your knowledge and for listening me every time, and for all your precious help and support as colleague, but moreover as incredible friends. India it will be always in my heart.

Special gratitude to all my friends all over the word, who always gave me support and encouragement: Arianna, Francesco, Marta e Alessandro.

Grazie a tutti i miei amici di Firenze per tutto il supporto in questi anni.

A billion of thanks goes to Adriana, for all.

Steffy, I want say, thank you from my heart, to be such an incredible person, impressive scientist and outstanding friend, without you, this work and my future would not be the same. Guida sempre veloce!

I am grateful to everybody who has been part of my life but I failed to mention their names. Thank you all Folks!